AD-A103 148 PENNSYLVANIA STATE UNIV UNIVERSITY PARK APPLIED RESE--ETC F/G 20/1
A NUMERICAL SOLUTION OF THE SECOND-ORDER-NONLINEAR ACOUSTIC WAV--ETC(U)
JAN 81 F S MCKENDREE N00024-79-C-6043
UNCLASSIFIED ARL/PSU/TM-81-44 NL

1 OF 2
AD A
103148

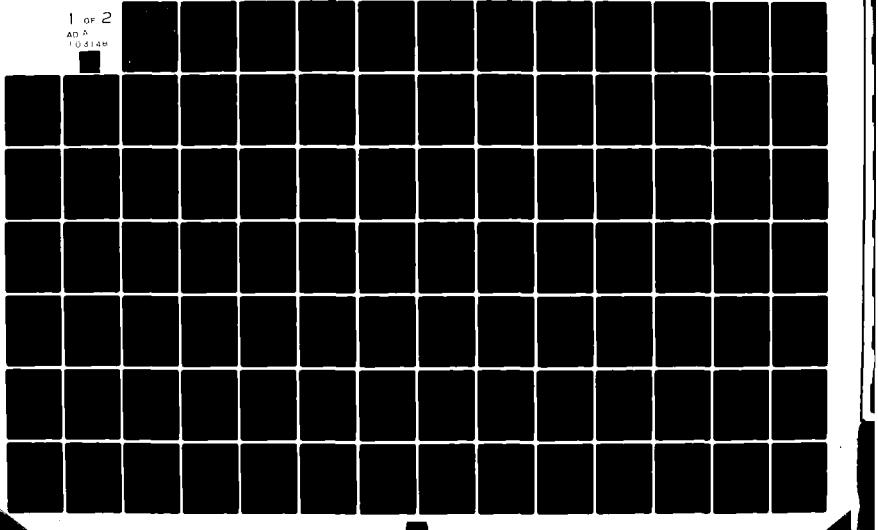

(6)

A NUMERICAL SOLUTION OF THE SECOND-ORDER-NONLINEAR ACOUSTIC WAVE EQUATION IN ONE AND IN THREE DIMENSIONS

Francis Speed McKendree

Technical Memorandum
File No. TM 81-44
January 8, 1981
Contract No. N00024-79-C-6043

Copy No. 5

The Pennsylvania State University
Intercollege Research Programs and Facilities
APPLIED RESEARCH LABORATORY
Post Office Box 30
State College, PA 16801

NAVY DEPARTMENT

NAVAL SEA SYSTEMS COMMAND

UNCLASSIFIED

SECURITY CLASSIFICATION OF THIS PAGE (When Data Entered)

REPORT DOCUMENTATION PAGE		READ INSTRUCTIONS BEFORE COMPLETING FORM
1. REPORT NUMBER TM-81-44	2. GOVT ACCESSION NO. AD-A103 148	3. RECIPIENT'S CATALOG NUMBER
4. TITLE (and Subtitle) A NUMERICAL SOLUTION OF THE SECOND-ORDER-NONLINEAR ACOUSTIC WAVE EQUATION IN ONE AND IN THREE DIMENSIONS.		5. TYPE OF REPORT & PERIOD COVERED Ph.D, Thesis, August 1981 6. PERFORMING ORG. REPORT NUMBER TM-81-44
7. AUTHOR(s) Francis Speed McKendree		8. CONTRACT OR GRANT NUMBER(s) N00024-79-C-6043
9. PERFORMING ORGANIZATION NAME AND ADDRESS The Pennsylvania State University Applied Research Laboratory, P.O. Box 30 State College, PA 16801		10. PROGRAM ELEMENT, PROJECT, TASK AREA & WORK UNIT NUMBERS
11. CONTROLLING OFFICE NAME AND ADDRESS Naval Sea Systems Command Department of the Navy Washington, DC 20362		12. REPORT DATE January 8, 1981 13. NUMBER OF PAGES 145 pages & figures
14. MONITORING AGENCY NAME & ADDRESS(if different from Controlling Office)		15. SECURITY CLASS. (of this report) Unclassified, Unlimited 15a. DECLASSIFICATION/DOWNGRADING SCHEDULE

16. DISTRIBUTION STATEMENT (of this Report)

Approved for Public release, distribution unlimited,
per NSSC (Naval Sea Systems Command), February 17, 1981

17. DISTRIBUTION STATEMENT (of the abstract entered in Block 20, if different from Report)

18. SUPPLEMENTARY NOTES

19. KEY WORDS (Continue on reverse side if necessary and identify by block number)

acoustic, wave, equation, thesis

20. ABSTRACT (Continue on reverse side if necessary and identify by block number)

The effects of moderate nonlinearity on the propagation of sound are appreciable, and become dominant at very high amplitudes. These effects and the phenomena of linear acoustics are described by the second-order-nonlinear wave equation, which is derived in this thesis and solved by numerical means. The validity of the solution is demonstrated by its agreement with various approximations in their domains of applicability, and by its reproduction of results derived from experiments. Using the numerical solution in simulation

DD FORM 1 JAN 73 1473 EDITION OF 1 NOV 65 IS OBSOLETE
S/N 0102-LF-014-6601

UNCLASSIFIED

SECURITY CLASSIFICATION OF THIS PAGE (When Data Entered)

of the operation of acoustic transducers at finite amplitudes, conclusions are presented concerning the amount of energy that may be transmitted to the far field by various types of signals.

ABSTRACT

The effects of moderate nonlinearity on the propagation of sound are appreciable, and become dominant at very high amplitudes. These effects and the phenomena of linear acoustics are described by the second-order-nonlinear wave equation, which is derived in this thesis and solved by numerical means. The validity of the solution is demonstrated by its agreement with various approximations in their domains of applicability, and by its reproduction of results derived from experiments. Using the numerical solution in simulation of the operation of acoustic transducers at finite amplitudes, conclusions are presented concerning the amount of energy that may be transmitted to the far field by various types of signals.

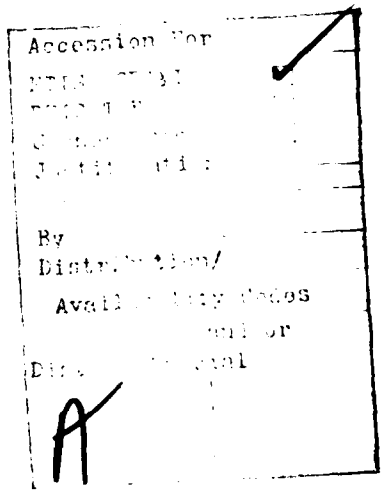

TABLE OF CONTENTS

TABLE OF CONTENTS (continued)

LIST OF TABLES

LIST OF FIGURES

LIST OF FIGURES (continued)

LIST OF FIGURES (continued)

LIST OF FIGURES (continued)

CONVENTIONS OF SYMBOLS AND NOTATION

This thesis uses a notation for nonlinear acoustics derived from the classic papers of Beyer, Zabusky, Fenlon, Blackstock, and Westervelt, which are cited in the text. Subscripts are used to qualify the meanings of symbols according to the following convention:

* : asterisk, used to denote a reference quantity;

o : denotes a nominal quantity, or one referred to a mean-carrier frequency;

1 : denotes the higher carrier of a bifrequency pair;

2 : denotes the lower carrier of a bifrequency pair;

- : denotes the difference frequency of a bifrequency pair;

n : denotes the n-th component, e. g., of a spectrum.

For example, the variable u is a particle velocity, u_* a reference velocity, u_o a nominal or mean-carrier particle velocity, and so on. In certain instances a subscripted symbol has a different meaning; such symbols are given explicitly in the list of symbols which follows.

The superscript prime (′) is used to denote an excess quantity above the nominal or equilibrium value, unless otherwise defined. For example, the excess acoustic pressure is denoted $p'=p-p_o$.

LIST OF SYMBOLS AND NOTATION

a : amount of absorption within the Rayleigh distance, $a=\alpha r_o$

a_T : combined-primary-wave absorption within the Rayleigh distance, $a_T = a_1 + a_2 - a_- = \alpha_T r_o$

c : velocity of wave propagation

c_o : small-signal velocity of wave propagation

d : simple dispersion parameter, $d=2\beta\epsilon/m(w_* \tau_R)^2$

f : frequency in Hertz

k : wave number

m : dispersion number,

p : local pressure in an element of fluid

p^{WFA} : pressure amplitude deduced from the weak-finite-amplitude solution of Fenlon (1979) and McKendree

p^W : pressure amplitude of a parametric array as given by Westervelt (1963)

r : physical range variable along the direction of propagation in spherical coordinates

r_o : Rayleigh distance of a plane piston projector, $r_o=A/\lambda_o$

r_c : plane-wave shock formation distance, $r_c=1/\beta\epsilon k$

s : condensation of a fluid, $s=(p-p_o)/p_o$

t : time

t' : retarded time, $t'=t-z/c_o$

u : local particle velocity in an element of fluid

z : physical range variable in Cartesian coordinates along the direction of propagation

LIST OF SYMBOLS AND NOTATION (continued)

A : area of a plane piston projector

A, B : measured parameters in the equation of state of a liquid, after Beyer (1960)

B_n : amplitude of the n-th Fourier component of a signal relative to the amplitude at the source

C_p : specific heat of a fluid at constant pressure

G_o : parametric gain function of Fenlon and McKendree (1979)

I_n : modified Bessel function of the first kind and order n

J_n : Bessel function of the first kind and order n

K : thermal conductivity of a fluid

P : normalized excess acoustic pressure, $P=p'/p_o$

R : physical range divided by the Rayleigh distance, $R=r/r_o$

N : arbitrary integer constant

α : attenuation per unit distance in a fluid, defined at frequency f as $\alpha=\delta f^2$

β : parameter of nonlinearity, defined as $\gamma-1$ in an ideal gas, and as $1+\frac{B}{2A}$ in a fluid after Beyer (1960)

γ_o : frequency downshift ratio of a bifrequency pair $f_1>f_2$, $\gamma_o = \frac{1}{2}\frac{f_1+f_2}{f_1-f_2}$

δ : thermoviscous attenuation parameter of a fluid, $\delta = \frac{1}{2\rho_o c_o^2}[2\eta+\eta'+K(\gamma-1)/C_p]$

LIST OF SYMBOLS AND NOTATION (continued)

ε : (1) Mach number,

(2) normalized radial distance, measured perpendicular to the direction of propagation

σ : range scaled with respect to the plane-wave shock formation distance, $\sigma = \beta\varepsilon kz = z/r_c$

σ_o : Rayleigh distance divided by the plane-wave shock formation distance, $\sigma_o = \beta\varepsilon kr_o$

λ : Wavelength

η : shear coefficient of viscosity

η' : dilatational coefficient of viscosity

τ : scaled retarded time,

τ_R : relaxation time of a polyatomic fluid

ω : angular frequency

Γ : acoustic Reynold's number,

Λ : scaled dispersion number,

∇^2 : Laplacian operator

∇^2_L : transverse Laplacian operator in physical coordinates, excluding the derivative in the direction of propagation

$\nabla^2_{L'}$: transverse Laplacian operator in scaled coordinates

$*$: convolution operator

ACKNOWLEDGEMENTS

The author of this thesis is very grateful for the help and cooperation of Drs. William Thompson, Jr., Robert Farwell, and Carter Ackerman, the members of his doctoral committee. The patience and understanding of Dr. Francis Fenlon, his thesis advisor, is beyond thanks.

The author wishes particularly to thank Dr. Gilbert Hoffman of The Pennsylvania State University for aid in the numerical solution of the diffusion-in-frequency equation.

This research was supported under the Exploratory and Foundational Research Program directed by Dr. M. T. Pigott of the Applied Research Laboratory at The Pennsylvania State University, under contract with the U. S. Naval Sea Systems Command.

Chapter 1

INTRODUCTION

Acoustical signals may easily exceed those levels for which the linear lossy wave equation provides an adequate model. Even if the amplitude is small, distortion products will accumulate unless they are removed by absorption in the medium. The wave equation may be taken to second order to include the effects of moderate nonlinearity.

Numerous solutions exist for particular forms of the second-order-nonlinear wave equation, for example, Burger's equation (1948). Analytic solutions have been obtained only for restricted cases, such as for particular regions of the field or for plane-wave propagation.

The purpose of this thesis is to present an original numerical solution of the second-order-nonlinear acoustic wave equation, applicable to plane-wave propagation and to propagation from an axisymmetric source of finite extent having an arbitrary amplitude and phase profile. As the solution is a numerical procedure, no approximations are made in the second-order-nonlinear acoustic wave equation as it is solved. This represents an advance on the prior art, in which solutions were obtained for simpler forms of the equation solved in this thesis. The numerical solution presented in this thesis is valid within an unbounded medium which is either lossless or has any desired attenuation character-

istic as a function of frequency, and is either non-dispersive, or has any desired phase velocity as a function of frequency. The useful conditions of a thermoviscous or a monorelaxing medium are special cases which may be handled with ease.

The first chapter of this thesis introduces the fundamental concepts of nonlinear systems and presents a review of the prior art in solutions. A brief derivation of the second-order-nonlinear wave equation is presented in Chapter 2 and a numerical solution of this equation in Chapter 3. The results of the solution under various conditions are discussed in Chapter 4, and some of its implications are presented in Chapter 5.

Nonlinear Systems and Equations

A nonlinear system is one for which the principle of linear superposition fails. That is, if $f(x)$ is the output of the system in response to the input x, then

$$f(ax+by) \neq af(x)+bf(y) \tag{1.1}$$

The functional relationship between two variables--for example, the pressure on and condensation of an element of fluid--may be expressed as a power series. If p' is the excess acoustic pressure and s the condensation, then the series in Beyer's notation (1960) truncated at the second term may be written

$$p' = As+(B/2)s^2, \qquad (1.2)$$

which is called second-order as the first missing term is proportional to the third power of s, a number much less than unity. The dependence of pressure on the specific entropy has been omitted from Equation (1.2), as the latter is intended to apply for values of the Mach number ε less than 1/10. The Mach number is the ratio of the peak particle velocity to the small-signal speed of sound. Whitham (1974) has shown that the change in entropy across a shock front is of the order of the Mach number cubed, and is therefore negligible in a second-order analysis.

The subject of this thesis is a numerical solution of the second-order-nonlinear wave equation in several systems of coordinates. A numerical solution is a procedure that, given the values of the dependent variables at one set of values of the independent variables, specifies how the former may be computed at another set of the latter. Numerical solutions generally involve a degree of error due to approximation, which may be reduced as far as is desired by appropriate numerical techniques.

Previous Solutions to Nonlinear Wave Equations

This section reviews previous solutions to nonlinear wave equations. Beginning with Euler's equations, Earnshaw

(1860) obtained a result valid for inviscid progressive plane-wave propagation and determined that the velocity of propagation is a function of amplitude:

$$c = c_o + \beta u, \tag{1.3}$$

where β is the parameter of nonlinearity of the fluid after Beyer's notation, u is the particle velocity, and c_o is the small signal speed of sound. Riemann (1860) independently obtained a solution which includes plane waves traveling in two opposite directions.

If a sinusoidal signal of small amplitude (compared with the equilibrium pressure) is followed as it propagates through an inviscid fluid, the compressions, whose particle velocities are positive, will travel faster than the rarefactions, whose particle velocities are negative. Thus adjacent compressions and rarefactions will approach one another, and a discontinuity in the pressure will be formed. If a numerical procedure based directly on Equation (1.3) is used, at the point at which a discontinuity is formed it will fail, as the compressions and rarefactions continue to travel past one another, and the predicted pressure will have several distinct values at each point in the vicinity of the discontinuity. This method is capable of giving good results out to the critical range, as reported by Pestorius and Blackstock (1973). Beyond the critical range the authors average across the shock front, thus suppressing the multivalued waveform.

The Fubini (1935) and inviscid Fay (1931) solutions for initially monofrequency waves give analytic solutions for the near and the far fields of the lossless Burger's equation. In the near field, i.e. for $\sigma<1$, Fubini's expression for the n-th harmonic of the pressure is

$$p_n(\sigma) = \frac{2}{n\sigma} J_n(n\sigma), \tag{1.4}$$

and in the far field, for $\sigma>3$, Fay's result is

$$P_n(\sigma)=\frac{2}{n(1+\sigma)} \tag{1.5}$$

where $\sigma=\beta\varepsilon kz$ is the distance relative to the plane-wave shock formation distance

$$r_c= 1/\beta\varepsilon k. \tag{1.6}$$

The Fubini-Fay solution for the near field and the asymptotic far-field spectrum of a decaying shock wave were combined by Blackstock (1966). His formulation uses a polynomial in σ to match the values and derivatives of the near- and far-field solutions. This formula gives excellent agreement with comparatively lossless plane-wave experimental data throughout the field.

The limits of classical theory lie in its neglect of dissipation. Fox and Wallace (1954) obtained a perturbation solution for plane waves in a lossy medium. This solution perturbs the rates of harmonic generation and decay of the lossless plane-wave solution. Their paper discusses the usefulness of scaled coordinates such as will be used in

this thesis (though their notation is different), and also considers the impossibility of generating acoustic signals of arbitrarily large amplitude due to saturation of the medium. Their paper also reports on comparison between numerical simulation and experiments in air, water, and carbon tetrachloride. The agreement between simulation and experimental results is excellent.

Cook (1962) described an iterative numerical procedure for the calculation of the distortion of plane finite-amplitude waves in a lossy medium. This procedure is similar to that used in this thesis for nondispersive plane-wave propagation, but is somewhat different in its details and motivation. The model is based on two assumptions: that the distortion mechanism may be described by a change in phase velocity which is directly proportional to the particle velocity, and that the absorption of each frequency component is proportional to its amplitude times the square of its frequency. The procedure is to distort the waveform as it propagates over a small interval, and then to correct for absorption.

Another nonlinear wave equation of great interest is the Korteweg-DeVries equation; as given by Lamb (1965), it may be written in the following scaled form:

$$\frac{\partial P}{\partial \sigma} - P \frac{\partial P}{\partial \tau} = -K \frac{\partial^3 P}{\partial \tau^3} \qquad (1.7)$$

This equation describes propagation in lossless and dispersive nonlinear media. As Lamb's analysis (1965) of

this equation indicates, the signal

$$P(\tau) = a\,\mathrm{sech}^2(\tau/D), \tag{1.8}$$

where

$$D = (12K/a)^{1/2} \tag{1.9}$$

is a steady-state solution of the K-dV equation. This signal is termed a solitary wave solution, or soliton. It will propagate through the medium at a velocity dependent on its amplitude a. As Zabusky (1967) has shown by means of a numerical analysis of Equation (1.7), several solitons may interact without losing their identities. Any signal propagating in a nonlinear dispersive medium will be resolved into one or more solitons. Under certain conditions these may coalesce at a later time to re-form the initial signal.

Rosen (1966) discussed the computational solution of nonlinear parabolic differential equations by linear programming. This method involves choosing a set of functions of which a linear combination approximates the desired solution. Two sets of conditions need to be satisfied: the boundary conditions and the partial differential equation. One may choose the functions so that each satisfies the boundary conditions and a linear combination satisfies the differential equation, or choose them so that each satisfies the differential equation and a linear combination satisfies the boundary conditions. In either case, it is a linear programming problem to

determine the coefficients of the linear combination which minimize the error in some sense. Of particular interest to the subject of this thesis is that the method is directly applicable to the plane-wave form of Burger's equation. Rosen gives several examples of the error bound which may be expected, showing that with as few as five well-chosen functions an error of less than 1/10 percent may be obtained.

The work discussed above dealt with the propagation of finite-amplitude plane waves only. It is possible to use a stretched coordinate system for Burger's equation which will accommodate plane, cylindrical, or spherical spreading. This approach is used by Fenlon (1971) in a method for computing the interaction between spectral components in progressive finite-amplitude waves. In this method, the spectral representation is truncated at a finite number of terms, and a coupled set of nonlinear differential equations is obtained for the component amplitudes. Given an initial spectrum at $\sigma=o$, the spectrum at $\sigma=\Delta\sigma$ may be obtained; then, at $\sigma=2\Delta\sigma$, and so on until the desired range is reached.

Cary used the transformation of Naugol'nykh (1963) to obtain an equation from which an expression for the "extra decibel loss" due to finite amplitude absorption was obtained (1967). This paper reaches the conclusion that finite-amplitude losses in spherical waves are less than for

plane waves of the same source level, but still are not negligible.

A second paper by Cary (1968) that is of interest in the history of numerical solutions to nonlinear wave equations presents a numerical solution based on Burger's equation in a stretched coordinate system, suitable for plane, cylindrical, and spherical spreading. Following the method of Banta (1965), the normalized particle velocity is represented as a Taylor's series, and enough terms are kept to ensure an adequate model of the distortion process. This method is valid until the effects of absorption have become dominant over nonlinear effects. Reasonably good agreement between experimental data published by Romanenko (1959) and the numerical predictions is shown. Cary notes that this method should be useful in the design of nonlinear acoustic systems.

The pressure field radiated by an acoustic source may be conceptually divided into three zones. Zone I is the region close to the projector in which energy is transferred into harmonic or modulation frequencies by nonlinearity faster than it is removed by viscous losses or reduced by spreading losses. Conversely, zone III is the region far from the projector in which either viscous losses or spreading losses are dominant over the effects of nonlinearity. Between zones I and III, a shock wave may form and, if so, the rates of harmonic generation and loss will be comparable within some region, giving rise to a

quasi-stable waveform. This region, if it exists, is called zone II. Cary (1973) has published an exact zone II solution of Burger's equation for a parametric source.

Sadchev and Seebass (1973) published a study of the decay of spherical and cylindrical shock waves. This article presents a numerical finite-difference solution to a general form of Burger's equation including the effects of viscous absorption in either plane, cylindrical, or spherical geometry. The plane wave form may be transformed into a linear equation by the methods of Hopf (1950) and Cole (1951). The latter equation has been solved by Lighthill (1956), and Sadchev and Seebass use Lightill's analytic results as a test for their numerical method.

The numerical method of Sadchev and Seebass employs a mesh of sample points in two coordinates, which may be considered as along and normal to the direction of propagation. Cylindrical and spherical spreading each have the effect of transferring energy outward from the beam axis. For this reason it is necessary to increase the number of mesh points in the normal direction and the size of the normal mesh-point spacing from time to time, so as to represent the whole of the pulse as it propagates and spreads.

The concept of the parametric array was introduced by Westervelt (1963) and led to considerably increased interest in finite-amplitude acoustics. A parametric array is an end-fire array formed in a nonlinear medium

by the interaction of relatively high-frequency carrier beams of different frequencies, which generate a difference-frequency signal. As the amplitude of the carriers is reduced by absorption and spreading, the parametric array has a built-in amplitude taper. The principal advantages of a parametric array are the relatively narrow beamwidth of the difference-frequency signal, which is comparable with that of the carriers, the virtual absence of side lobes in the difference-frequency beam in many cases, and wide relative bandwidth. The principal disavantage is its low conversion efficiency.

An asymptotic far-field value for the difference frequency level arising from a bifrequency signal has been derived by Fenlon (1972). Let the acoustic Reynold's number be defined by

$$\Gamma = \beta \varepsilon k/\alpha, \tag{1.10}$$

where ε is the Mach number, β is the parameter of nonlinearity, k is the wave number of the reference frequency, in this case the difference frequency, and $\alpha=\delta f^2$ is the attenuation coefficient of the difference frequency. The downshift ratio γ_o is the ratio of the mean carrier frequency to the difference frequency. A scaled acoustic Reynold's number may be defined as

$$\Gamma_{1,2} = \Gamma/2\gamma_o \tag{1.11}$$

provided that $f_1 \cong f_2$, i. e., that γ_o is large, and that

the carrier amplitudes are equal; then, the function

$$p_{-}(\sigma) = \frac{1}{\gamma_o \Gamma_{1,2}} \frac{I_1^2(\Gamma_{1,2}/2)}{I_o^2(\Gamma_{1,2}/2)} e^{-\sigma/\Gamma} \qquad (1.12)$$

expresses the difference-frequency level as a function of σ for $\sigma >> 1$. Here f_1 is the higher of the two carriers and f_2 is the lower, with σ the scaled range as defined previously. Equation (1.12) may be multiplied through by $\exp(\sigma/\Gamma)$ so as to cancel the effect of viscous absorption, and written in the form

$$p_{-}(\sigma/\Gamma)e^{\sigma/\Gamma} = \frac{1}{\gamma_o \Gamma_{1,2}} \frac{I_1^2(\Gamma_{1,2}/2)}{I_o^2(\Gamma_{1,2}/2)} \cong \frac{1}{\gamma_o^2} \frac{(\Gamma_{1,2}/4)}{1+(\Gamma_{1,2}/4)^2}, \qquad (1.13)$$

where the latter approximation, involving the leading terms of the Bessel functions, is accurate to within a few percent. The right side of this equation is a maximum for $\Gamma_{1,2}/4$. Since

$$\Gamma_{1,2} = \Gamma/2\gamma_o, \qquad (1.14)$$

for any downshift ratio, there is a value of Γ that will maximize the efficiency of the parametric conversion. The value of Γ for which maximum efficiency is attained is

$$\Gamma_{max} = 8\gamma_o \ . \qquad (1.15)$$

In Fenlon and Mckendree's (1979) solution for the propagation of a bifrequency signal at weak finite amplitudes, the beam shapes of the carrier waves are

approximated by Gaussian functions, and it is assumed that each carrier propagates linearly. Unlike any of the previous methods, this technique includes the effects of diffraction (spreading losses) via a three-dimensional form of Burger's equation due to Zablotskaya and Kokhlov (1969) and to Kuznetsov (1971). This method allows the difference-frequency level arising from interaction of the carriers to be determined. This solution applies for axisymmetric waves propagating in a viscous fluid and can be evaluated for a wide range of parameters. However, it fails at large source levels due to its neglect of finite-amplitude losses in the carriers, and the amount of the error cannot be determined as a function of the source level. The weak-finite-amplitude solution is compared with the results of the numerical method in Chapter 4.

Bakhvalov, Zhileikin, Zablotskaya, and Kokhlov (1978, 1979) have published papers to date on finite amplitude wave propagation. They employ a direct numerical solution of the second-order nonlinear wave equation, but their method is not explained. The results of the operational solution are compared with the results obtained by these researchers in Chapter 4.

Experiments at Finite Amplitudes

A number of experiments have been conducted using sources driven at finite amplitudes. Shooter, Muir, and Blackstock (1974) used a 454 kHz (kiloHertz) source in fresh water. Muir and Willette (1972) performed experiments with bifrequency signals having carriers in the vicinity of 450 kHz, and Eller (1974) used carriers near 1435 kHz. Each of these experiments has been simulated by the numerical solution, and the agreement between numerical and experimental results is discussed in Chapter 4.

Chapter 2

DERIVATION

This chapter presents a brief derivation of the second-order-nonlinear wave equation in the form in which it will be used subsequently in this thesis. The second section reduces the equation to Burger's form and shows the simplicity of the resulting equation in scaled coordinates. The last section of this chapter introduces attenuation and dispersion into Burger's equation.

The Second-Order-Nonlinear Wave Equation

The inviscid form of the nonlinear wave equation correct to second order as given by Goldstein (1960) is

$$(\nabla^2 - \frac{1}{C_0^2}\frac{\partial^2}{\partial t^2})\phi = \frac{1}{C_o^2}\left[\frac{\partial}{\partial t}(\nabla\phi\cdot\nabla\phi) + \frac{\gamma-1}{C_o^2}\frac{\partial\phi}{\partial t}\nabla^2\phi\right] \qquad (2.1)$$

where ϕ is the velocity potential. The first term within the brackets on the right side of Equation (2.1) represents the nonlinearity introduced by convection of momentum through the element of fluid. The second term represents the nonlinearity of the equation of state to second order. The form shown is for an ideal gas; in a fluid, the coeffi-

cient $\gamma-1$ may be replaced by $1+\frac{B}{2A}$, a measured parameter, as indicated by Beyer (1960).

In the right side of Equation (2.1) the definition of the potential function in the absence of rotation of the fluid may be applied. Also, the linearized wave equation

$$\nabla^2\phi = \frac{1}{C_o^2}\frac{\partial^2\phi}{\partial^2} \tag{2.2}$$

may be substituted, since the inclusion of second-order terms in this substitution would lead to terms of the third order, which are explicitly ignored in this thesis. These substitutions give for the second nonlinear term

$$\frac{\gamma-1}{C_o}\frac{\partial\phi}{\partial}\nabla^2\phi = \frac{\gamma-1}{C_o^4}\frac{\partial^2\phi}{\partial^2} = \frac{\gamma-1}{2C_o}\frac{\partial}{\partial}\left(\frac{\partial\phi}{\partial}\right)^2 . \tag{2.3}$$

By using the plane-wave impedance relationship

$$u = p'/p_o c_o \tag{2.4}$$

and applying the definition of the velocity potential

$$p' = -p_o\frac{\partial\phi}{\partial} , \tag{2.5}$$

the first nonlinear term on the right-hand side of Equation (2.1) becomes

$$\frac{\partial}{\partial\tau}(\nabla\phi\cdot\nabla\phi) = \frac{\partial}{\partial\tau}(p'^2/p_o^2c_o^2), \tag{2.6}$$

so that the inviscid second-order-nonlinear wave equation may be written in terms of the excess acoustic pressure p'

in the form

$$(\nabla^2 - \frac{1}{c_o}\frac{\partial^2}{\partial\tau^2})\ p' = -\frac{\beta}{p_o c_o^4}\ \frac{\partial^2 p'^2}{\partial\tau^2}\ . \qquad (2.7)$$

Scaled Coordinates and Burger's Equation

In nonlinear equations, a system of scaled coordinates is used that emerges naturally from normalization of Equation (2.7). A transformation due to Kokhlov (1961) is applied to Equation (2.7), involving the dummy range variable ξ and substitution of the retarded time τ':

$$\xi = z, \quad \tau' = \tau - z/c_o, \qquad (2.8a,b)$$

where is the direction of propagation. If the definition

$$\nabla^2 = \nabla_\perp^2 + \frac{\partial^2}{\partial z^2} \qquad (2.9)$$

is used, then the Zablotskaya-Kokhlov equation results:

$$\frac{\partial p'}{\partial z} - \frac{c_o}{2}\nabla_\perp^2 \int p'\,d\tau' = \frac{\beta}{2p_o c_o^3}\ \frac{\partial p'^2}{\partial\tau'} \qquad (2.10)$$

whose plane-wave form is Burger's equation:

$$\frac{\partial p'}{\partial z} = \frac{\beta}{2p_o c_o^3}\ \frac{\partial p'^2}{\partial\tau'}\ . \qquad (2.11)$$

To obtain this result, it is assumed that the rate of change of the waveform with respect to distance is very much less than its rate of change with respect to time.

In finite-amplitude propagation in fluids, this assumption is justified as the cumulative effects of nonlinearity occur over many wavelengths of the signal.

Now the retarded time, range, and pressure are normalized with respect to the subscript-star references:

$$\tau = \omega_* t' = \omega_*(t-z/c_o) = \omega_* t - k_* z, \tag{2.12a}$$

$$\sigma = \beta \varepsilon_* k_* z \tag{2.12b}$$

and

$$P = p'/p_* \tag{2.12c}$$

where ω_*, k_*, ε_* , and p_* are the frequency, wavenumber, Mach number, and peak pressure of an arbitrary reference wave. Substitution of the above into Burger's equation leads to the equation in scaled coordinates:

$$\frac{\partial P}{\partial \sigma} = \frac{1}{2} \frac{\partial P^2}{\partial \tau} \tag{2.13}$$

Attenuation and Dispersion

The presence of viscous forces and of dispersivity in the medium introduces additional terms into the forces acting on each element of fluid. These effects are linear and thus do not affect the nonlinear term as represented in Burger's equation.

Attenuation of sound in a fluid is produced by viscous losses and by thermal relaxation. The thermoviscous

attenuation parameter of a fluid, σ, is defined by Landau and Lifshitz (1959) as

$$\delta = \frac{2\eta+\eta'}{2\rho_o c_o^2} + \frac{K(\gamma-1)/Cp}{2\rho_o c_o^2} \qquad (2.14)$$

in which η and $\eta'$are the shear and dilatational coefficients of viscosity, p_o and ρ_o are the equilibrium pressure and density, K is the thermal conductivity, γ is the ratio of specific heats, and Cp is the specific heat at constant pressure. The first part of Equation (2.14) represents viscous absorption, and the second represents thermal relaxation. In all fluids except liquid metals, the thermal relaxation term is several orders of magnitude smaller than the viscous absorption term.

The thermoviscous attenuation coefficient of a fluid at the frequency f is defined:

$$\alpha = \delta f^2 \ , \qquad (2.15)$$

and in progressive plane-wave propagation, the effect of absorption is an exponential decrease in amplitude as a function of the distance traveled:

$$p(z) = p(o)e^{-\alpha z} \qquad (2.16)$$

which applies for the value of α corresponding to each frequency component.

In fluids which contain or are made up of polyatomic molecules, different molecular configurations may have different internal energies. It is possible for acoustic

energy to be stored in a rearrangement of the molecular structure and subsequently restored to the acoustic signal. Each internal relaxation process is characterized by its relaxation time τ_R . A monorelaxing fluid exhibits the property of dispersion--that is, a linear dependence of the velocity of propagation on frequency--at frequencies far removed from its relaxation frequency. The dispersivity of a fluid is defined

$$m = (c_\infty^2 - c_0^2)/c_\infty^2 \cdot \qquad (2.17)$$

The complete derivation of the second-order-nonlinear wave equation including thermoviscous absorption and relaxation terms is outside the scope of this thesis. The interested reader is referred to the derivation by Lamb (1959) for the dispersion term and the wave equation derivation by Kuznetsov (1971).

For a monorelaxing fluid having relaxation time τ_R and attenuation parameter α, the acoustic Reynold's number may be written:

$$\Gamma = \beta\varepsilon_* k_*/\alpha, \qquad (2.18)$$

and the scaled relaxation and dispersion coefficients Λ and d may be written

$$= 2\beta\varepsilon_*/m \qquad (2.19)$$

and

$$d = 2\beta\varepsilon_*/m(\omega_*\tau_R)^2, \tag{2.20}$$

each evaluated at the scaling frequency ω_* and Mach number ε_*. In scaled coordinates, the second-order-nonlinear wave equation including the effects of relaxation, thermoviscous losses, and diffraction takes the form of an equation first derived in slightly different form by Kokhlov (1961). In a non-relaxing fluid, this equation reduces to Kuznetsov's equation (1971) and, in a non-relaxing and lossless fluid, it reduces to the Zablotskaya-Kokhlov equation (1969). The second-order-nonlinear wave equation in scaled coordinates including relaxation, spreading, and losses, takes the form

$$(1+\omega_*\tau_R\frac{\partial}{\partial\tau})\left[\frac{\partial P}{\partial\sigma} - \frac{1}{\Gamma}\frac{\partial^2 P}{\partial\tau^2} - \frac{1}{2}\frac{\partial P^2}{\partial\tau} - \frac{1}{\sigma_o}\int\nabla_\perp'^2 P\,\partial\tau\right] = \frac{\omega_*\tau_R}{\Lambda}\frac{\partial^2 P}{\partial\tau^2} \tag{2.21}$$

where the transverse Laplacian operator is primed to indicate that it is in scaled coordinates. If $\omega_*\tau_R << 1$, then Equation (2.21) takes a simpler form including dispersion rather than relaxation:

$$\frac{\partial P}{\partial\sigma} - \frac{1}{d}\frac{\partial^3 P}{\partial\tau^3} - \frac{1}{\Gamma}\frac{\partial^2 P}{\partial\tau^2} - \frac{1}{\sigma_o}\int\nabla_\perp'^2 P\,d\tau = \frac{1}{2}\frac{\partial P^2}{\partial\tau}. \tag{2.22}$$

In Equation (2.22), the nonlinearity is represented in the same form as Burger's equation. The second term represents dispersion, the third represents thermoviscous absorption, and the fourth represents diffraction. The

plane-wave form of Equation (2.22) is

$$\frac{\partial P}{\partial \sigma} - \frac{1}{d}\frac{\partial^3 P}{\partial \tau^3} - \frac{1}{\Gamma}\frac{\partial^2 P}{\partial \tau^2} = \frac{1}{2}\frac{\partial P^2}{\partial \tau} , \qquad (2.23)$$

which is the limit as σ_o tends to infinity, suppressing the diffraction term. In a lossless fluid, the acoustic Reynold's number tends to infinity, removing the absorption term. In a non-relaxing fluid m is zero, so d becomes infinite and removes the dispersion term.

Equations (2.21), (2.22), and (2.23) were derived using the progressive-wave transformation due to Kokhlov, as was used in the scaling of Equations (2.10) and (2.11); thus, the same restrictions apply. In addition, a paraxial assumption requires that the effects of attenuation and dispersion are significant only along the direction of propagation; the transverse components of attenuation and dispersion are ignored.

Chapter 3

NUMERICAL SOLUTION

This chapter presents each feature of the numerical solution separately. The second-order-nonlinear wave equation, Equation (2.22), is solved in parts: first the lossless Burger's equation; then that part representing loss and dispersion; and last, the diffraction term. It is assumed that each of these effects operates independently of the others over small distances, so that it is possible to consider them one at a time. That is, a sampled wavform is propagated over an incremental range according to the lossless Burger's equation. It is then Fourier transformed, and each frequency component is subjected to that attenuation and dispersion which it would have suffered in propagating over the same distance in a linear manner. For axisymmetric three-dimensional propagation, the procedure outlined above is applied to each of a set of sampled waveforms at various radial distances; then the resulting signal is subjected to linear diffraction over the incremental distance.

The first section of this chapter discusses the numerical solution of the lossless Burger's equation. The next section presents the method by which attenuation and dispersion are introduced in the frequency domain, and

the third section explains the numerical diffraction method. The last section of this chapter discusses features of the computer programs which implement the numerical solution, and reviews the reasons for certain choices made in the methods of implementation.

Lossless Plane-Wave Solution

The lossless plane-wave solution is obtained by direct application of a method due to Bellman et al. (1965). In this method the points on the waveform advance at a velocity that is proportional to their amplitudes. Beginning with the lossless Burger's equation,

$$\frac{\partial P}{\partial \sigma} - P \frac{\partial P}{\partial \tau} = 0 \ , \tag{3.1}$$

the derivative with respect to σ may be approximated as

$$\frac{\partial P}{\partial \sigma} \simeq \frac{1}{\sigma}\left[P(\sigma,\tau) - P\ (0,\tau)\right] \tag{3.2}$$

where σ is used in the sense of an incremental range. Equations (3.1) and (3.2) become, by rearranging terms,

$$P(\sigma,\tau) = P(0,\tau) + \sigma P(\sigma,\tau)\frac{\partial P}{\partial \tau} \cdot \tag{3.3}$$

If the quantity $\sigma P(\sigma,\tau)$ is small, then it is reasonable to relate Equation (3.3) to a Taylor's series expansion. If P is slowly varying then, correct to second-order terms,

$$P(\sigma,\tau) = P\left[0,\tau+\sigma P(0,\tau)\right] \cdot \tag{3.4}$$

This formulation is not subject to failure by prediction of multivalued pressures, as each point of the waveform at the advanced range is related to a definite point at the initial range. Other formulations involving explicit numerical differentiation in a form reminiscent of Equation (3.3) have been found to become unstable in the vicinity of a discontinuity.

The numerical implementation may be enhanced by including an estimate of $P(\sigma,\tau)$in the expression for the incremental time. Using Equation (3.4), an estimate of $P(\sigma,\tau)$, denoted $P_e(\sigma,\tau)$, may be defined as

$$P_e(\sigma,\tau) = P\left[0,\tau+\sigma P(0,\tau)\right] \tag{3.5}$$

and this estimate may be substituted into Equation (3.4) to give

$$P(\sigma,\tau) = P\left[0,\tau+\sigma P_e(\sigma,\tau)\right] \cdot \tag{3.6}$$

Equations (3.4) and (3.6) are implemented in the following manner. A number of samples of the pressure waveform are taken at equal intervals covering the data window. These samples represent $P(0,\tau)$. A second array of samples is prepared, each of whose values is interpolated from among the $P(0,\tau)$at the time specified by Equation (3.4). These are the values of the waveform at the range σ. The values of the waveform at the new range may be used as the origin for a new range step, and the procedure may be repeated

until the desired range is reached. Both equations are based on a Taylor's series and are valid for σ less than 1. For implementation of Equation (3.6), the first estimate is used to obtain a new estimate of the advanced waveform at each range step.

Attenuation and Dispersion in the Frequency Domain

If the normalized pressure waveform P is Fourier transformed, its spectrum will consist of the coefficients P_ω at frequencies which are related by integers. Equation (2.22) expressed in the frequency domain takes the form

$$\frac{\partial P_\omega}{\partial \sigma} + \left(\frac{\dot{\lambda}\omega^3}{d} + \frac{\omega^2}{\Gamma} \right) P_\omega = \frac{\dot{\lambda}\omega}{2} P_\omega * P_\omega \cdot \tag{3.7}$$

Without loss of generality, it may be assumed that ω is an integer multiple of ω_*, the frequency at which the scaling of Equations (2.21) et seq. was performed. Then, the equation in the frequency domain becomes

$$\frac{\partial P_n}{\partial \sigma} + \left(\frac{\dot{\lambda} n^3}{d} + \frac{n^2}{\Gamma} \right) P_n = \frac{\dot{\lambda} n}{2} P_n * P_n , \tag{3.8}$$

with P_n the n-th Fourier harmonic component.

For a mono-relaxing fluid having relaxation time τ_R, additional terms in the scaled frequency $n\omega_*$ are introduced by the derivatives in Equation (2.21). The frequency-domain equation then takes the form

$$\frac{\partial P_n}{\partial \sigma} - \left\{\frac{n^2}{\Gamma}\left[1+\frac{\omega_* \tau_R \Gamma/\Lambda}{1+(n\omega_* \tau_R)^2}\right] + \frac{\dot{\lambda} n^3}{d}\left[\frac{1}{1+(n\omega_* \tau_R)^2}\right]\right\} P$$

$$= \frac{\dot{\lambda} n}{2} P_n * P_n . \qquad (3.9)$$

Since the method of the first section provides a satisfactory solution of the lossless equation, it may be used to propagate the waveform to an incrementally advanced range. The waveform is then Fourier transformed, and each of its spectral components is processed according to the linear equation for attenuation and dispersion:

$$\frac{\partial P_n}{\partial \sigma} + \left(\frac{\dot{\lambda} n^3}{d} + \frac{n^2}{\Gamma}\right) P_n = 0, \qquad (3.10)$$

for which the formal solution is

$$P_n(\sigma,\tau) = P_n(0,\tau) e^{-\left(\frac{\dot{\lambda} n^3}{d} + \frac{n^2}{\Gamma}\right)} . \qquad (3.11)$$

Note that the coefficient of P_n in Equation (3.10) is transferred intact into the exponential in the solution. Thus, the effects of an arbitrary attenuation and dispersion as a function of frequency may be introduced by multiplying the spectrum by a complex function of frequency whose form may be determined from the governing wave equation by inspection.

Diffraction by Diffusion in Frequency

The nonlinear wave equations, Equation (2.21) et seq., contain diffraction terms. If the other terms are taken

into account by the methods of the preceding sections, then the remaining equation takes the form of a diffusion equation in the frequency domain:

$$-\frac{\partial P_n}{\partial \sigma} + \frac{\dot{\lambda}}{n\sigma_o} \nabla_L^2 P_n = 0. \tag{3.12}$$

The effects of diffraction on the propagation of finite amplitude waves in three dimensions is introduced by a finite-difference numerical solution of Equation (3.12); this method is termed "diffusion in frequency".

The incremental range σ may be chosen small enough to render negligible all terms higher than the first order. Under these conditions, Equation (3.12) may be converted to

$$P_n(\sigma) \cong P_n(o) - \frac{\dot{\lambda}\sigma}{n\sigma_o} \nabla_L^2 P_n(o), \tag{3.13}$$

which is easily solved by finite-difference methods. A finite-difference numerical technique must be used as the functional form of P_n is not known.

Comments on the Numerical Solution

The method of numerical solution of the second-order-nonlinear wave equation described in this chapter is implemented by a group of computer programs written in ANSI standard FORTRAN IV and operating on an IBM 370/3033 running under OS/MVT. On this system, data sample arrays of almost unlimited size may be accommodated. The data arrays in the program are restricted to 256 by 40 points so that

the program will fit into a smaller computer, also used during this research. The processing time for simulations which exercise the program most severely is on the order of 300 to 1000 seconds. Plane wave propagation may be modeled with up to 2048 waveform samples. Such simulations require comparable lengths of time for execution.

The evaluation of Equation (3.4) or (3.6) requires interpolation between samples of the waveform. Several methods have been tried, including spline fitting, second- through fifth-order fitted polynomials, and third- through seventh-order Lagrange interpolation. Each of these advanced methods fails in the vicinity of the discontinuity. Accordingly, a linear fit interpolator is used. The advanced time for each new waveform sample falls between two samples of the old waveform, and the interpolated value is assumed to lie on the straight line joining the old samples. This procedure has been found to be sufficiently accurate by comparison with known analytic solutions in their domains of applicability. The method is biased, however, in the following manner. A sinusoidal signal is everywhere concave with respect to the ordinate axis. A linear interpolator will therefore tend to underestimate its values, as the sinusoid lies further from the ordinate axis between nearby samples, than does the straight line joining them. This property of the linear interpolator introduces an error or bias into the numerical results. Other waveforms of practical interest have segments which are convex with

respect to the ordinate axis and are there overestimated. The amount of the error may be reduced by taking more waveform samples. The accuracy of the interpolation is also affected by the number of steps per unit range. If the step size is small, the advanced times at which the interpolated waveform values are desired will be close to the times of the existing waveform samples, and the error of the linear interpolation will be less than if the advanced times lay further from the existing samples.

It is instructive to consider the sample number constraints in the frequency domain. A sequence of N samples spanning a time T can be Fourier transformed into the amplitudes of frequency components which are the harmonics of 1/T. It has been found that acceptable results are obtained in the numerical solution if at least ten harmonics of the highest significant frequency component at the source can be accommodated in the spectrum. A sequence of length N yields a spectrum which covers $N/2+1$ harmonics of 1/T. Thus $N/2+1$ must be chosen greater than or equal to ten times the relative frequency of the highest frequency source component. For a pure tone input, the highest significant source frequency is the input tone. For a bifrequency signal, the sum frequency must have about ten harmonics to ensure reasonably good results from the nonlinear operator.

Certain kinds of signals, for example, trains of solitons, will propagate in an appropriate medium without loss

of energy. For this reason, the numerical solution as implemented in the computer programs includes an optional feature which ensures conservation of energy in the nonlinear operator. This option must be used with discretion, as many kinds of signals are subject to finite-amplitude losses.

For $R \gg 1$, that is, at ranges much greater than the Rayleigh distance, spherical spreading may be assumed. The diffraction by diffusion-in-frequency operator, as implemented in its subroutine, allows the user to select a value of R beyond which spherical spreading is assumed. Since the Rayleigh distance differs for each harmonic, the values of σ at which spherical spreading may be imposed differ in a corresponding way, in direct proportion to their Fourier harmonic numbers.

The effects of diffraction may be taken into account by any of several different techniques. It is possible to represent the beam function at each frequency as a sum of eigenmodes of the geometry in use; then, the diffraction may be interpreted as a phase modulation of the spatial-frequency spectrum. Attempts to implement this method by numerical means were usable but subject to breakdown in the far field. The finite number of samples in the radial direction implies a spatial periodicity of the source function, and interference between the image sources becomes evident in the far field.

Chapter 4

RESULTS

This chapter presents results of the application of the numerical solution to a number of problems. The first section gives examples of the independent operation of certain parts of the numerical solution to demonstrate its degree of stability and accuracy. The second section deals with finite amplitude propagation of plane waves, and discusses the coupled effects of nonlinearity, attenuation, and dispersion as they are introduced in various relative strengths. The third section shows the results of the weak finite amplitude solution and those of the numerical solution for equivalent conditions, including diffraction and spreading. The fourth section presents the results of certain experiments at finite amplitudes and their numerical simulations. The last section presents numerical simulations of various types of modulated signals in axisymmetric propagation in one and in three dimensions at finite amplitudes.

Numerical Solution of the Lossless Burger's Equation and of Linear Diffraction

The number of waveform samples and the number of steps per unit of range may be chosen at the discretion of the

user of the numerical solution. Table 4.1 presents the amplitudes of the first three harmonics of a pure-tone signal at two ranges as a function of the number of waveform samples, with 10 steps per unit range. Table 4.2 presents the amplitudes of the first three harmonics of a pure-tone signal at two ranges as a function of the number of steps per unit range for 64 waveform sample points. For each table, the analytic value according to the Fay solution and the error as a percentage of this value is shown. These results were derived from the use of Equation (3.4) after the method due to Bellman (1965).

If the revised expression given by Equation (3.6) is used, then better results may be obtained with a smaller number of calculations. Table 4.3 shows the amplitudes of the first three harmonics of a pure-tone signal at various ranges, as deduced from the matched-asymptotic solution due to Blackstock (1966) and from the numerical implementation of Equation (3.6). In this case 128 waveform samples were used, with 10 steps per unit σ to $\sigma=1$ and 5 steps per unit σ beyond $\sigma=1$. Errors are shown between the best numerical results and the matched-asymptotic solution values as a percentage of the latter.

Figure 1 shows the level on axis of a Gaussian beam, $\exp(-\epsilon^2)$ at $R=0$, and Figure 2 shows the beam widths to the -3, -6, and -10 dB points, as measured in the numerical solution as a function of range. The discrete points are derived from the implementation of the diffusion-in-fre-

Table 4.1. Harmonic Levels at Two Ranges for an Initially Pure-Tone Signal Propagating in a Lossless Nonlinear Medium, For Various Numbers of Waveform Samples and 10 Steps Per Unit Range, Derived from the Numerical Solution of Equation (3.4).

NUMBER OF WAVEFORM SAMPLES	B (5) 1	B (5) 2	B (5) 3	B (10) 1	B (10) 2	B (10) 3
8	.288	.108	.040	.158	.058	.020
16	.310	.142	.083	.170	.076	.042
32	.317	.153	.096	.174	.082	.050
64	.320	.157	.102	.175	.084	.053
128	.321	.158	.104	.176	.086	.055
256	.321	.159	.104	.176	.086	.056
512	.321	.159	.104	.176	.086	.056
1024	.321	.159	.104	.176	.086	.056
analytic	.333	.167	.111	.182	.091	.061
error, %	-3.6	-4.8	-6.3	-3.3	-5.5	-8.2

Table 4.2. Harmonic Levels at Two Ranges for an Initially Pure-Tone Signal Propagating in a Lossless Nonlinear Medium, For Various Number of Steps Per Unit Range and 64 Waveform Samples, Derived from the Numerical Solution of Equation (3.4).

NUMBER OF RANGE STEPS	B (5) 1	B (5) 2	B (5) 3	B (10) 1	B (10) 2	B (10) 3
5	.311	.153	.099	.172	.083	.052
10	.320	.157	.102	.175	.084	.053
20	.324	.159	.103	.177	.086	.054
40	.326	.160	.103	.178	.086	.054
analytic	.333	.167	.111	.182	.091	.061
error, %	-2.1	-4.2	-6.3	-2.2	-5.5	-11.5

Table 4.3. Levels of the First Three Harmonics of a Pure Tone Signal in Lossless Nonlinear Plane-Wave Propagation as Derived from the Matched-Asymptotic Solution due to Blackstock (1966) and from the Numerical Solution of Equation (3.6), with Errors Expressed as a Percentage of the Former.

SIGMA	MATCHED-ASYMPTOTIC	NUMERICAL EQUATION (3.6)	ERROR, PERCENT
	$B_1(\sigma)$	$B_1(\sigma)$	
0.1	0.9988	0.9986	-0.02
0.2	0.9950	0.9948	-0.02
0.5	0.9691	0.9685	-0.06
1.0	0.8801	0.8820	0.22
2.0	0.6484	0.6518	0.52
5.0	0.3333	0.3349	0.48
10.0	0.1818	0.1816	-0.11
	$B_2(\sigma)$	$B_2(\sigma)$	
0.1	0.0498	0.0496	-0.40
0.2	0.0987	0.0981	-0.61
0.5	0.2298	0.2284	-0.61
1.0	0.3528	0.3482	-1.3
2.0	0.3134	0.3113	-0.67
5.0	0.1667	0.1679	0.72
10.0	0.0909	0.0932	2.5
	$B_3(\sigma)$	$B_3(\sigma)$	
0.1	0.0037	0.0037	0.0
0.2	0.0147	0.0144	2.0
0.5	0.0802	0.0803	0.12
1.0	0.2060	0.2023	-1.8
2.0	0.2070	0.2047	-1.1
5.0	0.1111	0.1117	0.54
10.0	0.0606	0.0584	-3.6

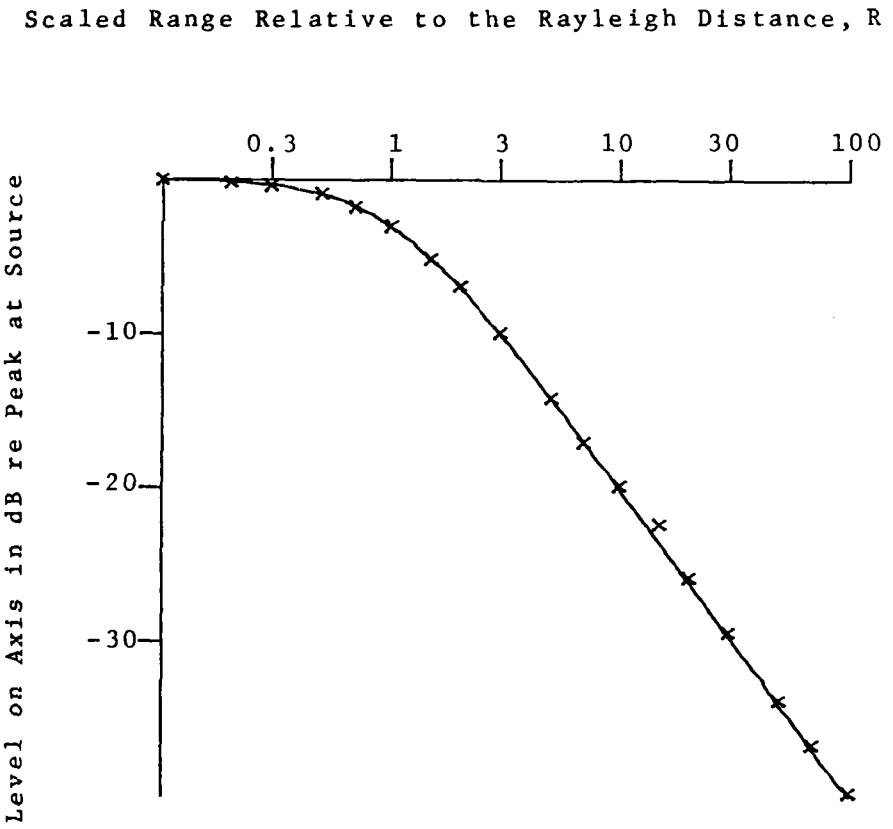

Figure 1. Level On Axis of a Gaussian Beam as a Function of Range, Under the Influence of Linear Diffraction.

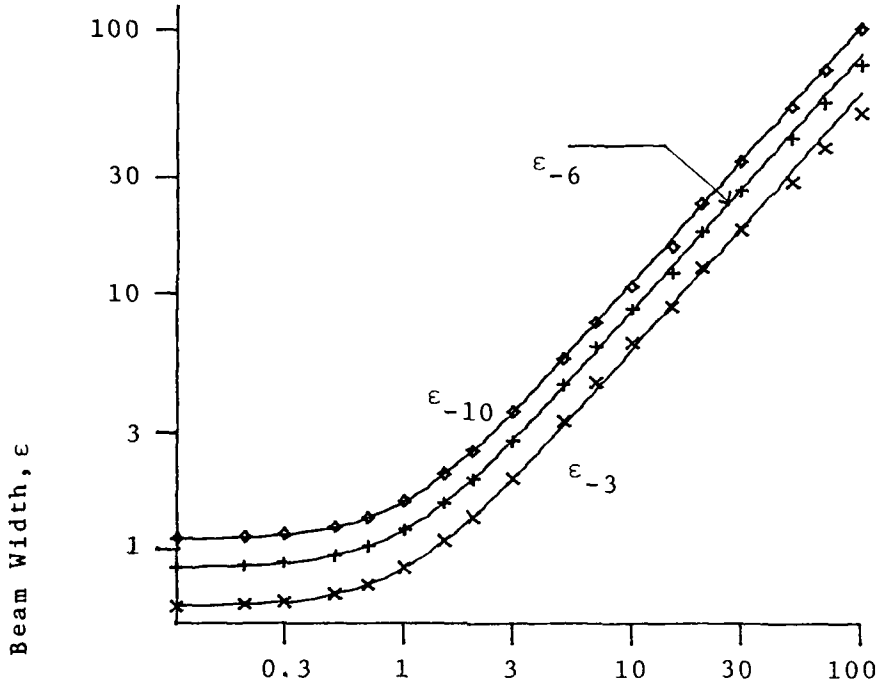

Figure 2. Beam Widths to the 3, 6, and 10 dB Down Points as a Function of Range, for a Gaussian Beam Under the Influence of Linear Diffraction.

quency technique which is used in the numerical solution. The known analytic values for the diffraction of a Gaussian beam are shwon in these figures as solid curves. The accuracy with which the numerical solution matches the analytic values indicates that the numerical solution of the diffraction term by diffusion-in-frequency is satisfactory. The remaining difficulty with the diffusion-in-frequency technique will be discussed in Chapter 5.

Finite-Amplitude Propagation of Plane Waves

The finite-amplitude propagation of plane waves in a thermoviscous mono-relaxing fluid is governed by three effects: nonlinearity, attenuation, and dispersion. This section demonstrates the operation of the numerical solution of Equation (2.22) in each of these effects, taken separately and in combination.

The nonlinear operator may be tested by comparison with Blackstock's matched asymptotic solution to the lossless Burger's equation. Figure 3 shows the harmonic amplitudes which are predicted by Blackstock's formula; Figure 4 shows the same function as predicted by the plane-wave lossless numerical solution. The difference between the matched-asymptotic and the numerical solution is nowhere greater than a few percent; this indicates the accuracy of the numerical solution in lossless plane-wave propagation.

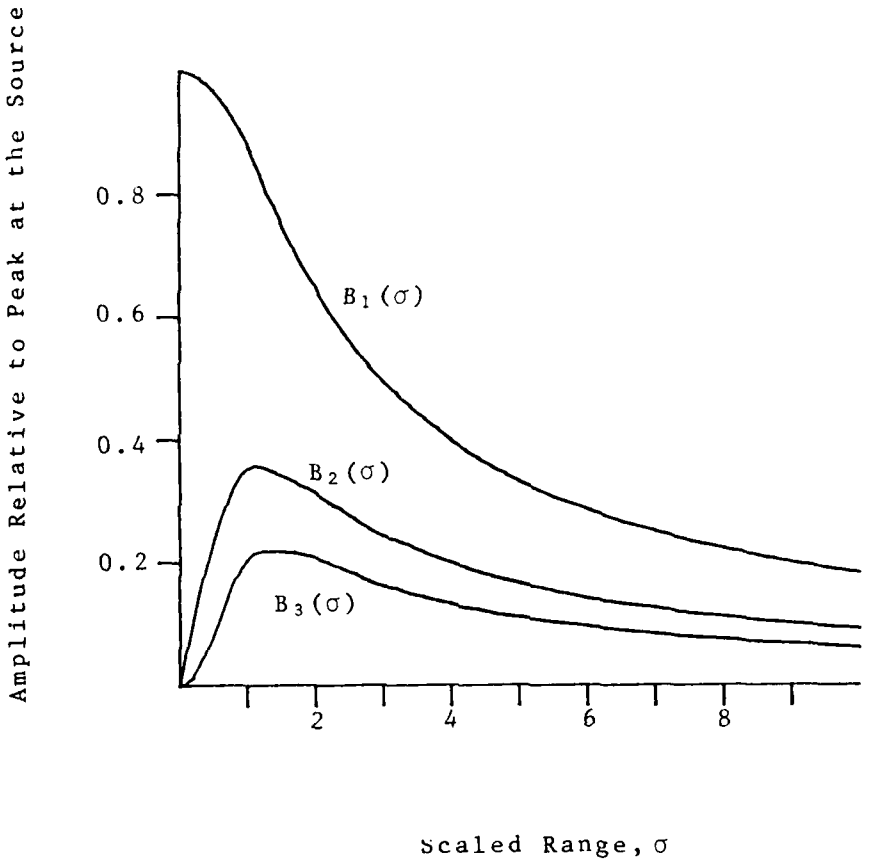

Figure 3. Lossless Plane-Wave Harmonic Coefficients from the Matched Asymptotic Expression Derived by Blackstock.

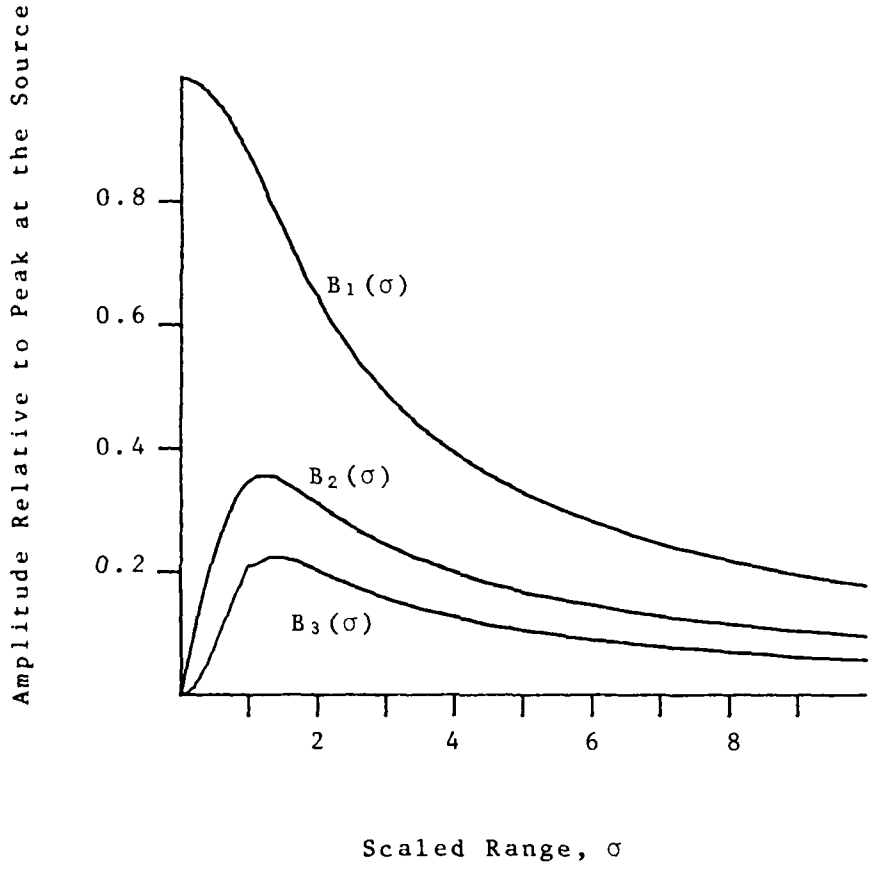

Figure 4. Lossless Plane-Wave Harmonic Coefficients Derived from the Numerical Solution.

Viscous losses introduce an exponential decay of signal level with range. With P_n the n-th harmonic amplitude, σ the range, and Γ the attenuation parameter,

$$P_n(\sigma) = P_n(0)e^{-n^2\sigma/\Gamma}, \tag{4.1}$$

is an obvious consequence of Equation (3.10) with respect to viscous losses.

Figure 5 shows the waveform of a monofrequency signal at σ =1, 2, and 3, as it propagates in a lossless medium. The waveform steepens until a shock is formed, and the shock wave decays due to finite amplitude loss without changing its shape. In Figure 6, attenuation has been introduced with an acoustic Reynold's number of 10. The amplitude of the wave is reduced by finite-amplitude losses, and in addition each harmonic is attenuated by thermoviscous effects. Figure 7 shows the waveforms with very high attenuation, corresponding to Γ =3. At σ =3, the waveform is nearly restored to a sinusoid. Table 4.4 lists the levels of the first three harmonics of each of the waveforms at each range. These results show the profound effect on the waveform and spectrum which is produced by viscous absorption. As the rate of thermoviscous absorption is usually proportional to the square of the frequency, the effect on higher-frequency components is even more marked.

Modulated waveforms are also subject to shock formation. Figures 8 through 10 show a bifrequency signal propagating in a lossless medium. The large amplitude

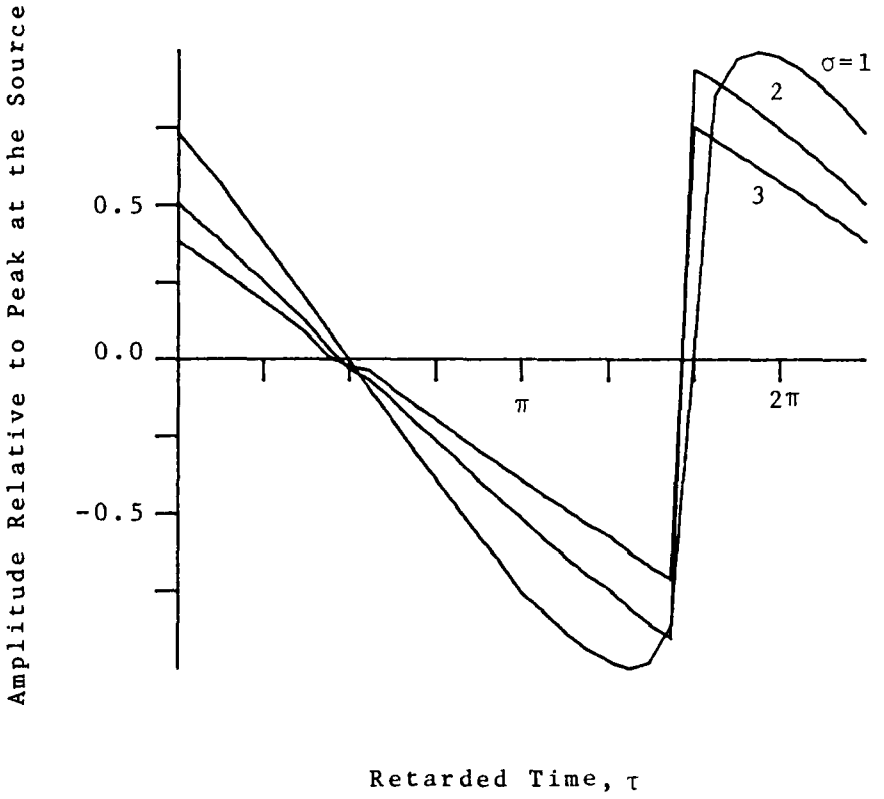

Figure 5. Waveforms in Lossless Monofrequency Propagation at Selected Ranges.

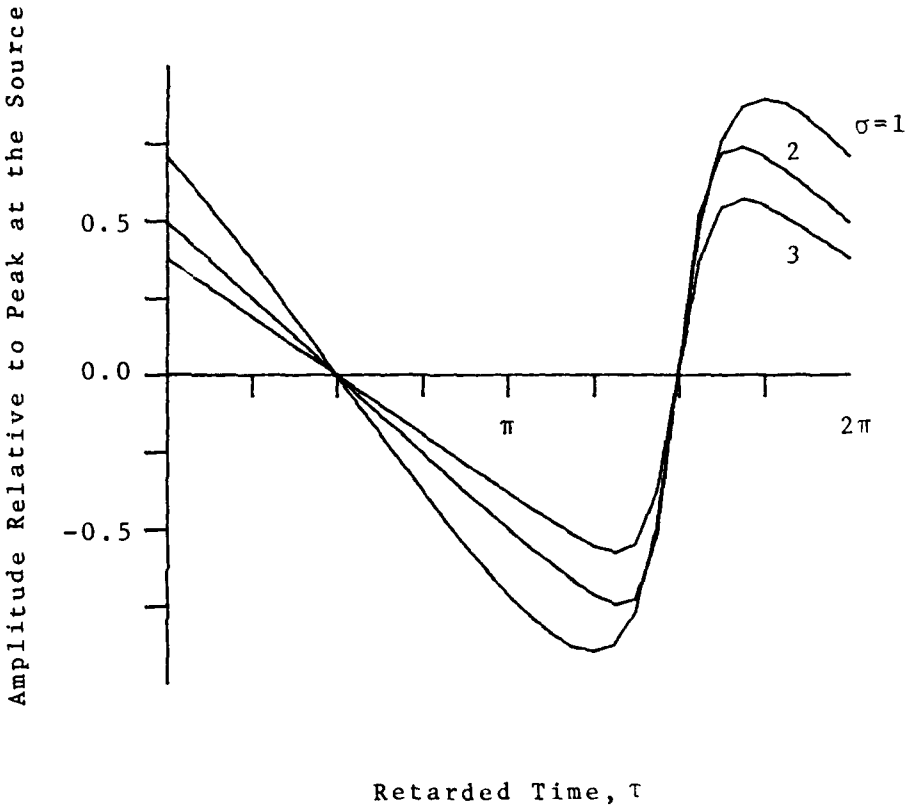

Figure 6. Waveforms in Lossy Monofrequency Propagation with $\Gamma = 10$, at Selected Ranges.

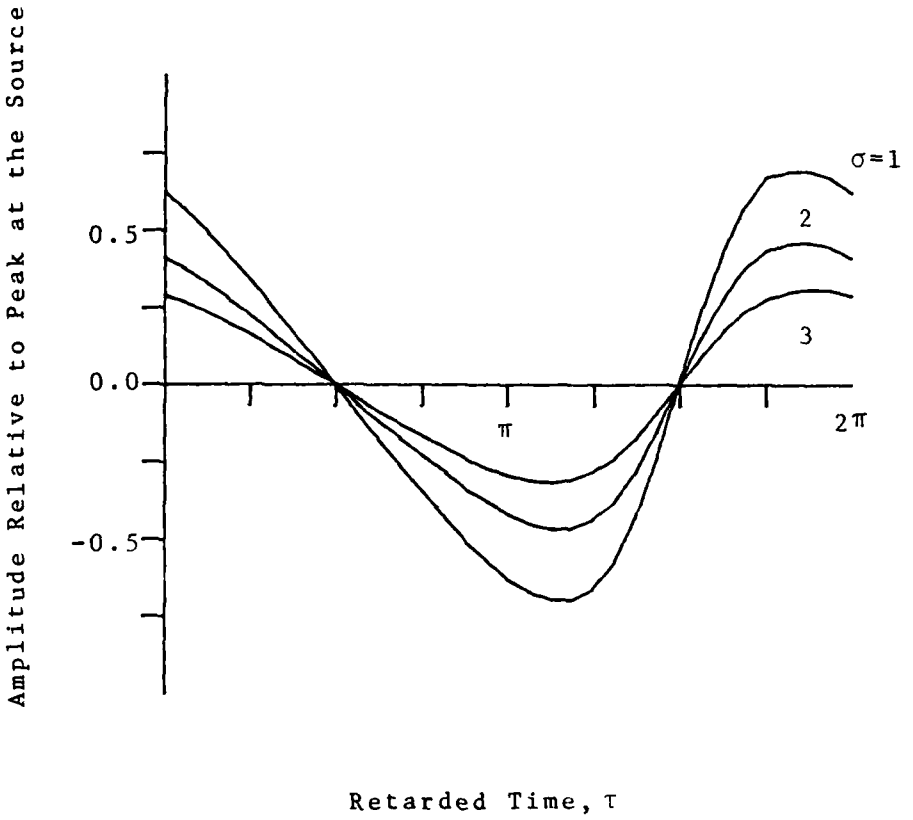

Figure 7. Waveforms in Lossy Monofrequency Propagation with Γ=3, at Selected Ranges.

Table 4.4. Amplitudes of the First Three Harmonics of a Monofrequency Signal in Plane Wave Propagation, with Selected Amounts of Absorption, at Selected Ranges.

SIGMA	B (σ) 1	B (σ) 2	B (σ) 3
	(lossless)		
0.5	.9662	.2292	.0786
1.0	.8760	.3525	.2045
2.0	.6427	.3097	.2038
3.0	.4906	.2421	.1605
5.0	.3300	.1648	.1097
10.0	.1805	.0907	.0598
	(GAMMA=10)		
0.5	.9219	.1988	.0600
1.0	.8133	.2837	.1362
2.0	.6042	.2635	.1514
3.0	.4619	.2042	.1152
5.0	.3055	.1248	.0621
	(GAMMA=3)		
0.5	.8253	.1423	.0320
1.0	.6684	.1585	.0462
2.0	.4439	.1055	.0281
3.0	.3043	.0586	.0120
5.0	.1508	.0162	.0018

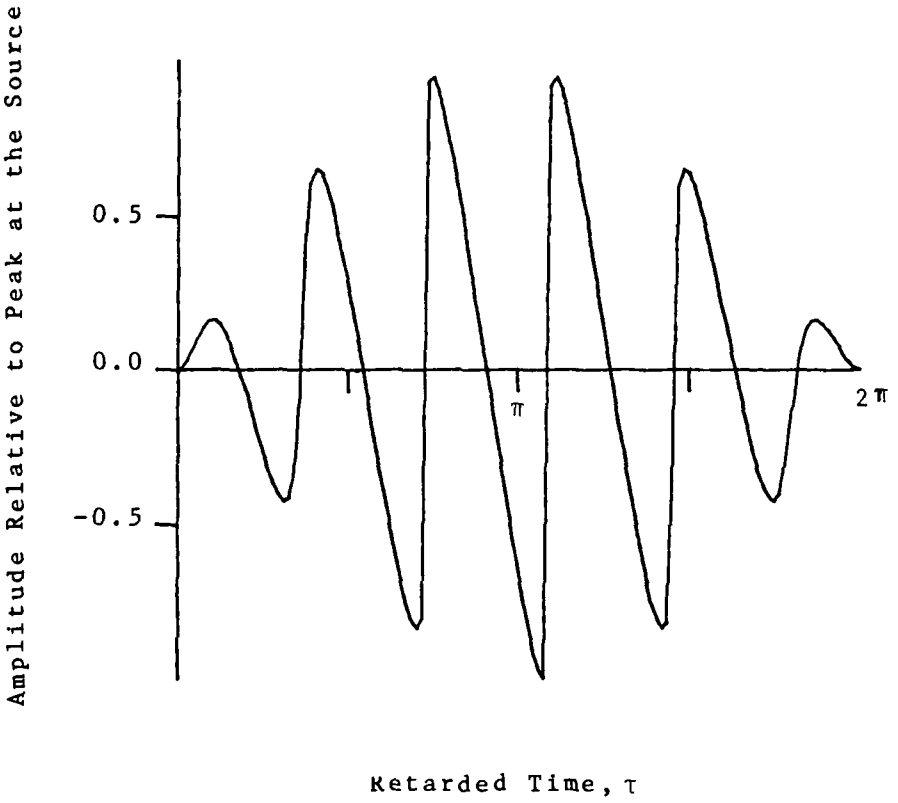

Figure 8. Lossless Bifrequency Waveform at $\sigma = 0.25$.

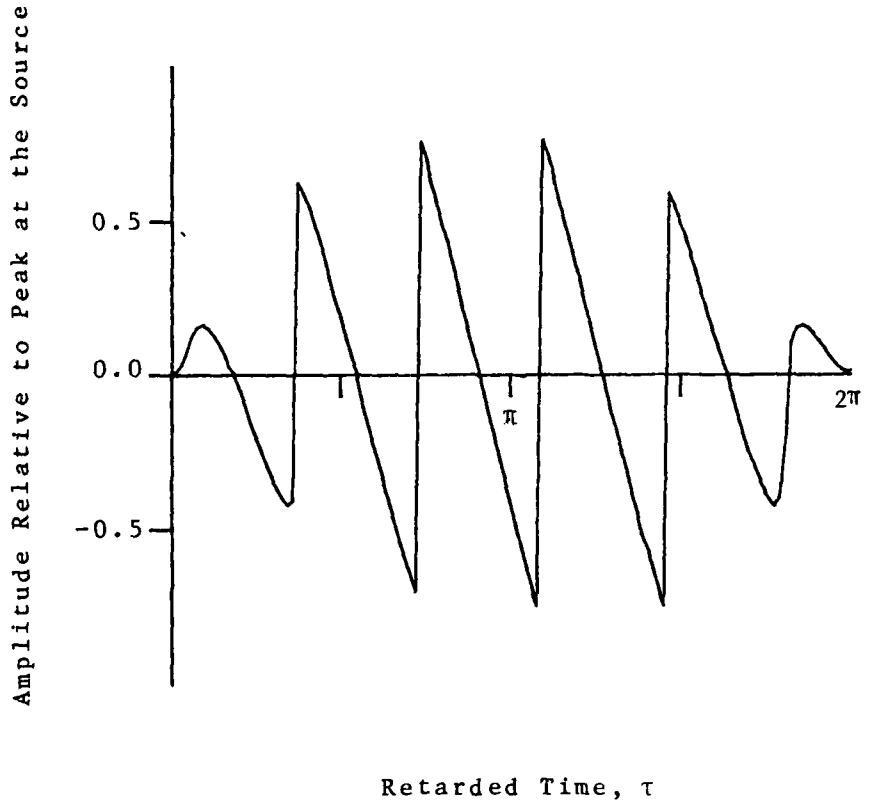

Figure 9. Lossless Bifrequency Waveform at $\sigma = 0.5$.

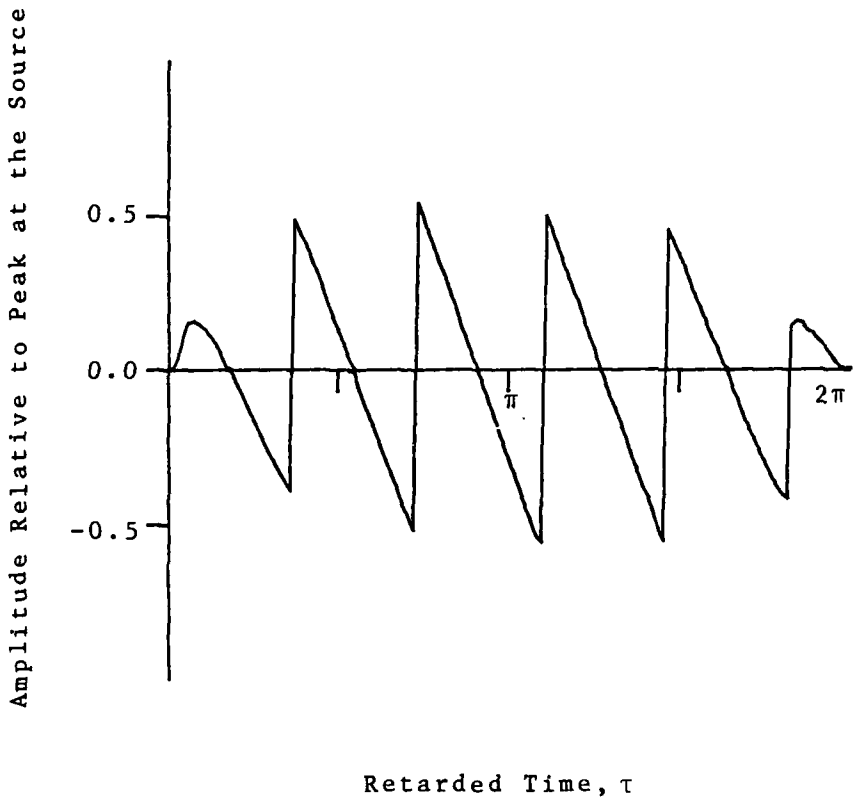

Figure 10. Lossless Bifrequency Waveform at $\sigma = 0.8$.

cycles go into shock quickly and are reduced by finite amplitude effects more rapidly than the small amplitude cycles. The result is distortion of the envelope function. Figure 11 shows an envelope function constructed by connecting the peaks of the cycles of the modulated waveform. As the wave propagates, the distortion of the envelope becomes more evident. Figure 12 shows modulation envelopes for a larger downshift ratio.

Bifrequency signals propagating in a nonlinear medium give rise to combination frequencies due to the self-convolution of the signal. If the two carriers are denoted f_1 and f_2, the lowest frequency in the nonlinearly generated spectrum is the difference frequency $f=f_1-f_2$. Figure 13 shows the difference-frequency level as a function of σ generated by a bifrequency signal for each of several values of Γ. After all finite-amplitude effects have ended, the plane-wave difference-frequency signal will continue to propagate subject only to thermoviscous losses. Figure 14 shows the difference-frequency level multiplied by $\exp(\sigma/\Gamma)$. Each of the curves is tending towards a limiting value. Figure 15 shows the far-field difference-frequency level times $\exp(\sigma/\Gamma)$ as a function of Γ for three downshift ratios. The discrete points are derived from the numerical solution, and the solid curves are from the asymptotic far-field solution due to Fenlon (1972). The results derived from the numerical solution are very similar to the exact analytic results as either the acoustic Reynold's

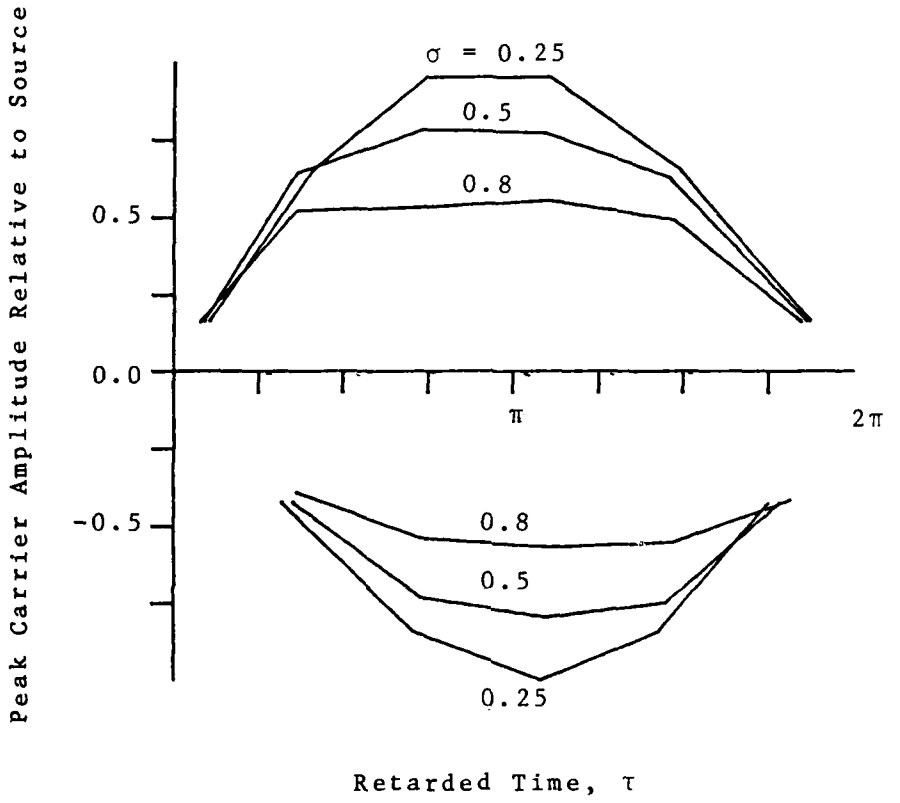

Figure 11. Modulation Envelopes of a Bifrequency Signal Having a Frequency Downshift Ratio of 5.5, at Selected Ranges.

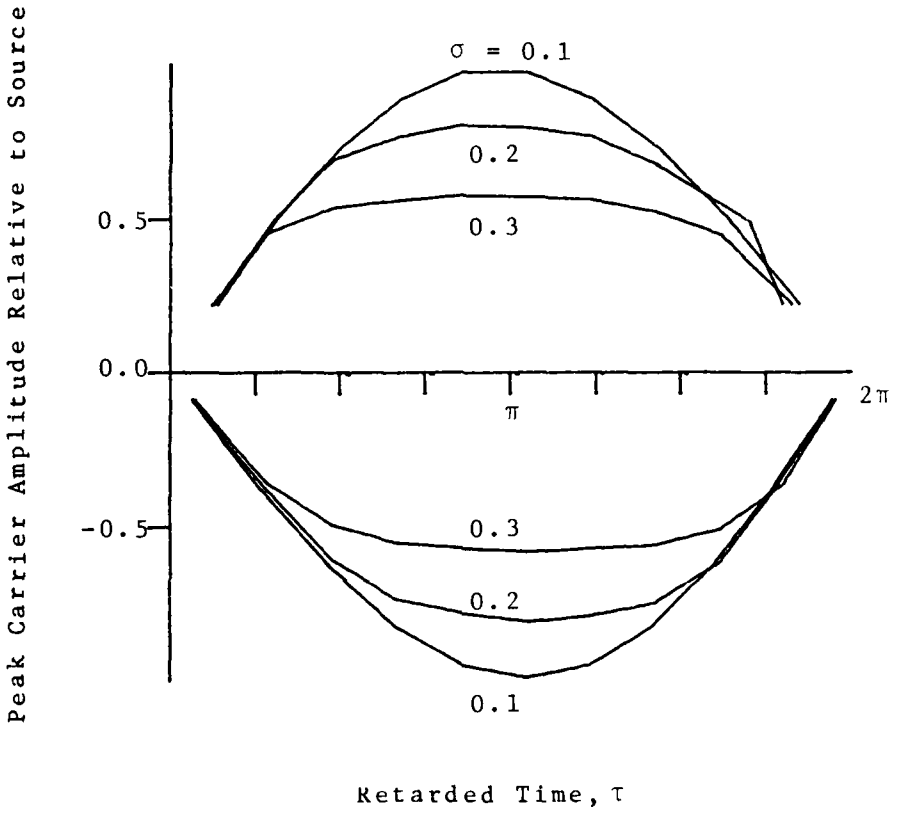

Figure 12. Modulation Envelopes of a Bifrequency Signal Having a Frequency Downshift Ratio of 10.5, at Selected Ranges.

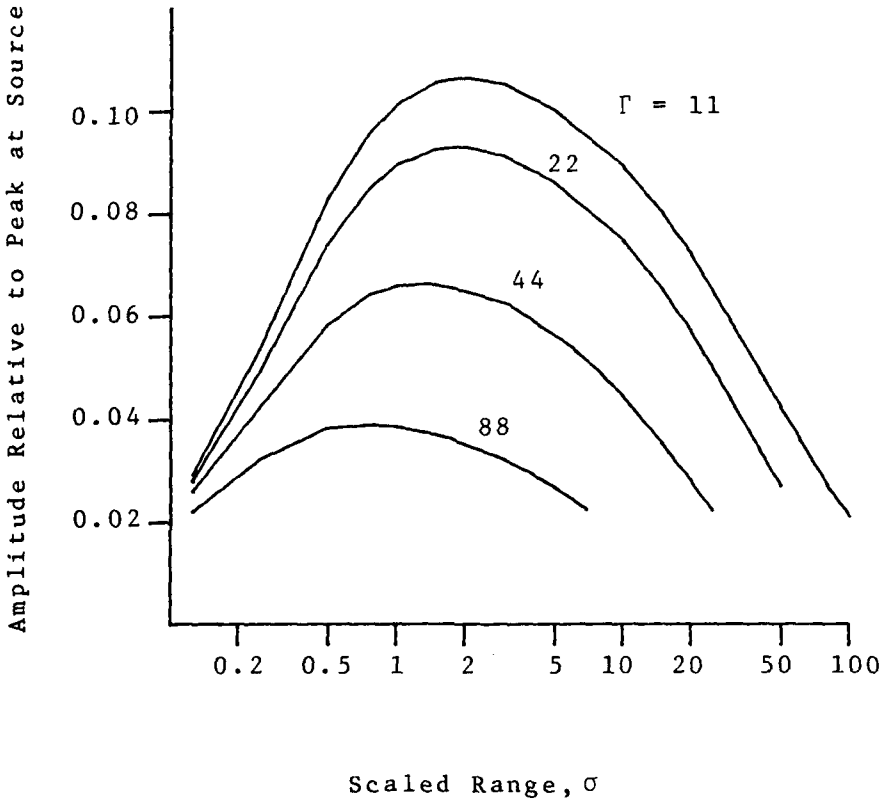

Figure 13. Difference-Frequency Level as a Function of Range, for Selected Values of Γ .

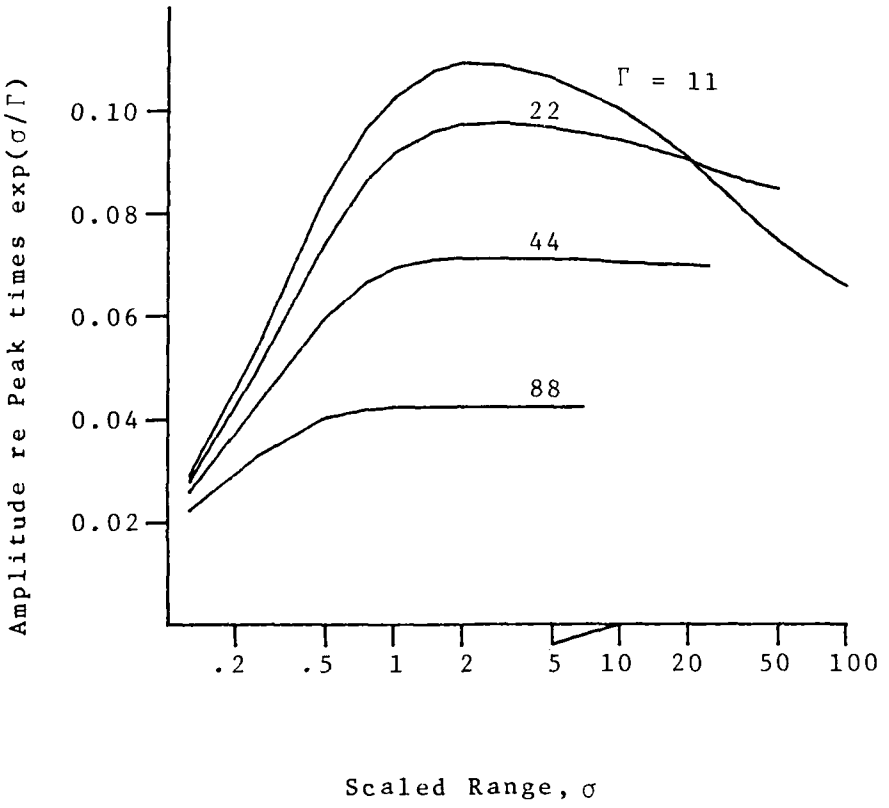

Figure 14. Difference-Frequency Level Times exp(σ/Γ), as a Function of Range, for Selected Values of Γ .

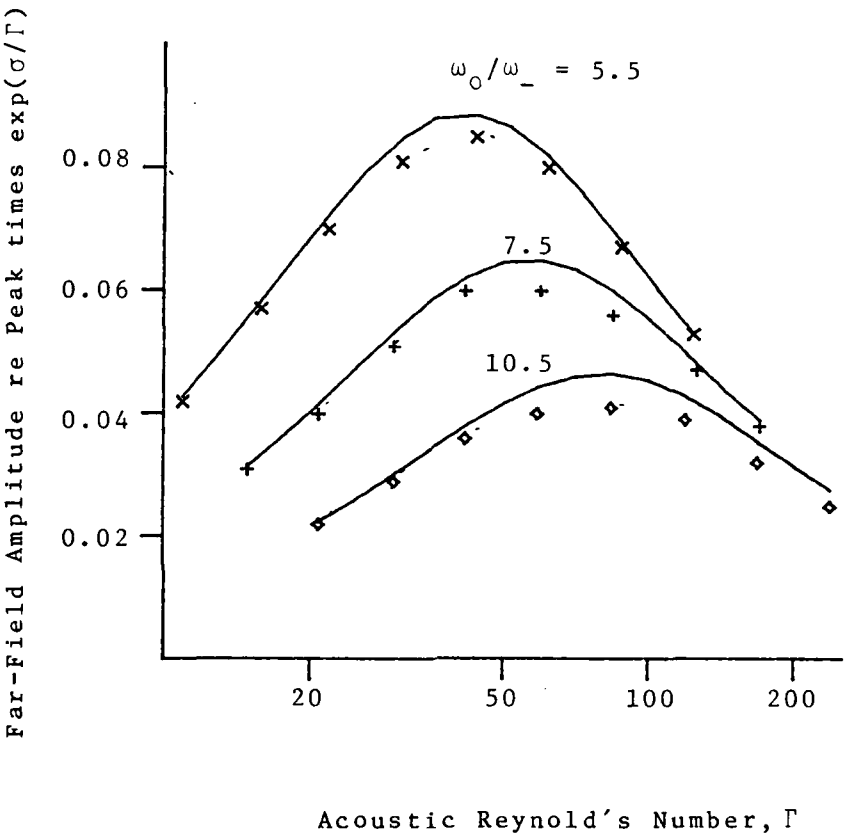

Figure 15. Far-Field Difference-Frequency Level Times $\exp(\sigma/\Gamma)$, as a Function of Γ, for Selected Frequency Downshift Ratios.

number or the frequency downshift ratio, or both, are varied. That correct results are obtained as either is varied implies that both the scaling of the nonlinear operator with respect to frequency, and the effects of thermoviscous absorption, are correctly modeled.

The presence of nonlinearity in a lossless dispersive medium gives rise to the formation of solitons. Figure 16 shows the numerical simulation of the interaction of two solitons as they propagate past one another. The solitons interact and pass through each other without change. By contrast, a sinusoidal input signal in a nonlinear and dispersive medium will be resolved into a set of solitons. Each of these will propagate at its own speed. If a continuous wave signal is thus resolved into a soliton train, it is possible for the solitons to coalesce at later times and to regenerate the initial waveform. This behavior has been deduced on analytic grounds by Zabusky and Kruskal (1965), and is illustrated in the following two figures.

Figure 17 shows the history of an initially sinusoidal signal as it propagates through a lossless, nonlinear, and dispersive medium. This figure is a series of snapshots of the waveform at the ranges indicated on the margin of the figure. At $\sigma=6.45$, and again at $\sigma=14.3$, the fundamental is nearly completely regenerated. Figure 18 presents the amplitudes of the first three harmonics as a function of range; it is apparent that most of the energy has been returned to the fundamental at the recurrence distances,

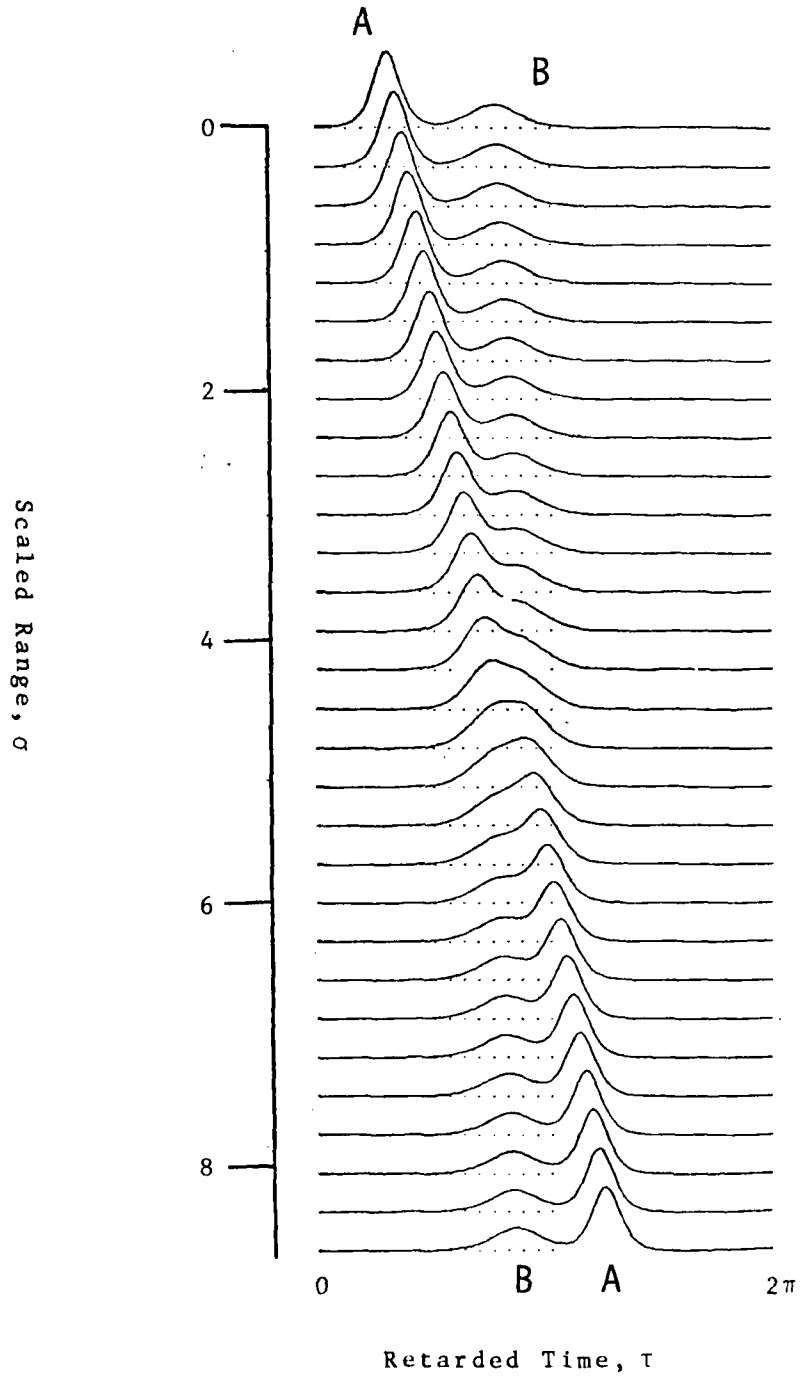

Figure 16. Interaction of Two Solitons, A and B, in a Lossless, Nonlinear, and Dispersive Medium.

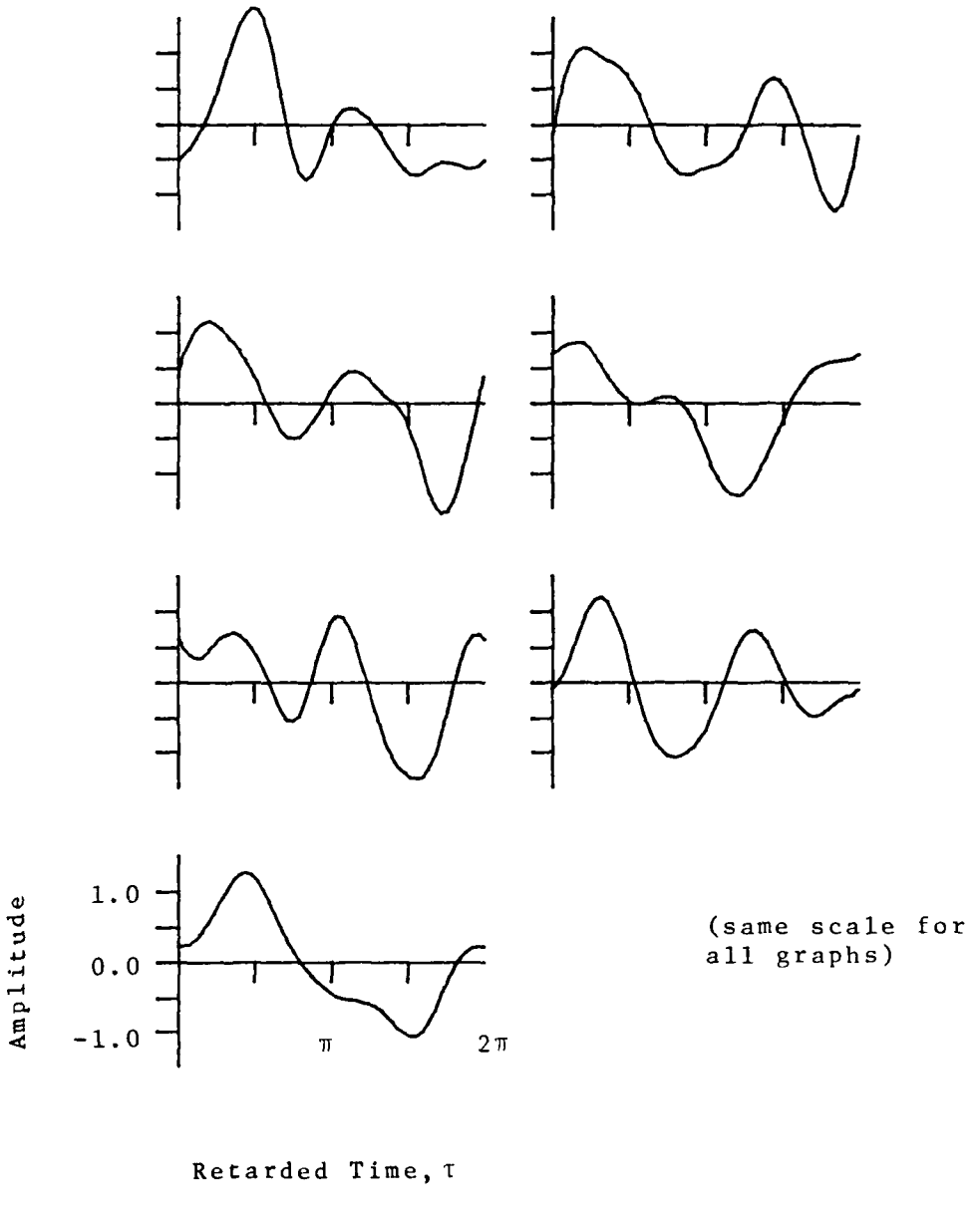

Figure 17. Waveforms of a Monofrequency Signal Propagating in a Lossless, Nonlinear, and Dispersive Medium, at Selected Ranges.

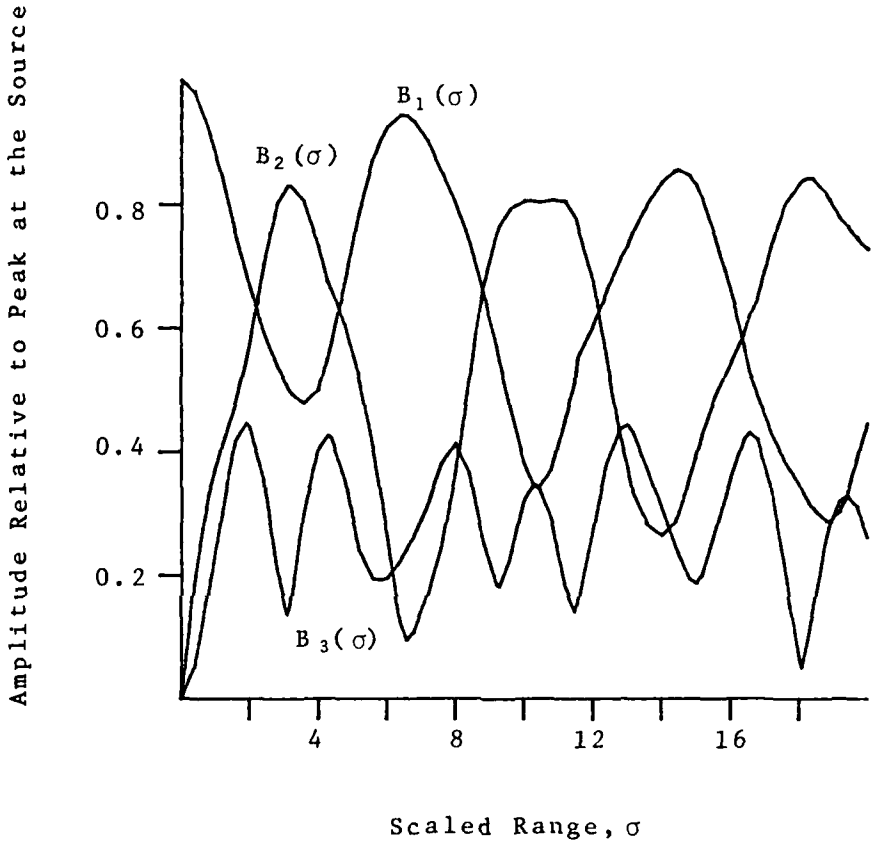

Figure 18. Harmonic Amplitudes as a Function of Range for a Monofrequency Signal Propagating in a Lossless, Nonlinear, and Dispersive Medium.

by the coupled effects of nonlinearity and dispersion.

Weak-Finite-Amplitude Propagation of Waves from Finite Sources

The numerical method is capable of simulating weak-finite-amplitude propagation from finite sources, by an appropriate choice of parameters. If the Rayleigh distance (or plane-wave collimation distance) is given by

$$r_o = A/\lambda_o, \tag{4.2}$$

then the scaled Rayleigh distance is

$$\sigma_o = \beta\varepsilon k r_o. \tag{4.3}$$

This quantity is also called the scaled source level; as the quantity kr_o is an indication of the prominence of spherical spreading, a large value of σ_o implies that the nonlinear interaction will be quasi-planar, and a small value of σ_o implies that the nonlinear interaction will extend into the spherical spreading region, at least if the signal level is not reduced too far by spreading or viscous losses. Weak-finite-amplitude propagation thus may be modeled by using small values of σ_o.

The scaled Rayleigh distance is used to define a new scaled range R. If r is the physical range and σ is the scaled range as previously defined, then $R = r/r_o = \sigma/\sigma_o$.

The acoustic Reynold's number Γ and the attenuation

parameter α of the fluid, are related to a new parameter a_o, which is used in three-dimensional finite amplitude propagation modeling, by the following equations:

$$a_o = \alpha r_o \tag{4.4}$$

and

$$\alpha r = \sigma/\Gamma, \tag{4.5}$$

so that

$$\Gamma = \sigma_o/a_o. \tag{4.6}$$

The parameter a_o defines the amount of absorption which occurs within the Rayleigh distance.

The combined-primary-wave attenuation coefficient is defined

$$\alpha_T = \alpha_1 + \alpha_2 - \alpha_- \tag{4.7}$$

so that the absorption within the Rayleigh distance is

$$a_T = a_1 + a_2 - a_- \ . \tag{4.8}$$

The results published by Fenlon and McKendree (1979) are normalized with respect to the parametric array response given by Westervelt (1963), which may be written

$$P_-^W(R) = (p_*/2\gamma_o^2 a_T R)e^{-a_- R}, \tag{4.9}$$

where R is the mean-carrier-frequency range, p_* is a reference pressure, γ_o is the frequency downshift ratio, a_T

is the combined-primary-wave attenuation coefficient, and a_- is the difference-frequency attenuation coefficient within the carrier's Rayleigh distance. Thus, to convert the parametric gain function values of Fenlon and McKendree to pressure, it is necessary to multiply the parametric gain functions by $2a_T\gamma_o^2 R$, bearing in mind that the numerical solution uses R to denote the reference-frequency range. An additional factor of 4 is introduced by a difference in the definition of the reference pressure

$$p_* = \beta p_1 p_2 k_o r_o / \rho_o C_o^2, \tag{4.10}$$

as the numerical solution contains the implicit assumption that the peak scaled pressure is unity, so that $p_1 p_2 = \frac{1}{4}$ for a bifrequency signal. The factor $k_o r_o$ is inversely proportional to the square of the frequency; thus, the actual pressure level predicted by the weak-finite-amplitude gain function is

$$p_-^{WFA}(R) = G_o(R) - 20 \log_{10}\left[p_-^W(R)\right] - 20 \log_{10}\left[\gamma_o^2/4\right] \tag{4.11}$$

Other beam shapes than Bessel beams from a plane piston projector require different definitions of the Rayleigh distance, and corresponding differences in the parameters of the numerical solution; for example, in the case of a Gaussian beam, the ranges are one-half those for a plane piston projector, and the required attenuation coefficients are doubled.

Figures 19, 20, and 21 show the difference-frequency levels as a function of range, as predicted by the weak-finite-amplitude solution in solid curves, and as predicted by the numerical solution as discrete points. Each graph is for a particular frequency downshift ratio and shows two curves for two different amounts of absorption. Figure 22 shows the difference-frequency level on axis as a function of range for a frequency downshift ratio of 5.5 and a normalized primary-wave attenuation coefficient of 1.0, which represents very high attenuation. These figures indicate that large amounts of thermoviscous absorption reduce the difference-frequency level in the far field. The numerical solution predicts somewhat higher values in the far field than does the weak-finite-amplitude solution; however, the latter has been found to underestimate the difference-frequency level slightly when it is used to simulate experimental results, as shown by Fenlon and McKendree (1979).

Simulations of Experiments at Finite Amplitudes

The experiment performed by Shooter, Muir, and Blackstock (1974) used a projector 0.0762 m in diameter operating at a frequency of 454 kHz in fresh water. The maximum peak source level attained was 235 dB re 1 μPa at 1 meter, corresponding to 1 kiloWatt peak input power. The following paragraph gives an example of the procedure for conversion from physical to scaled parameters.

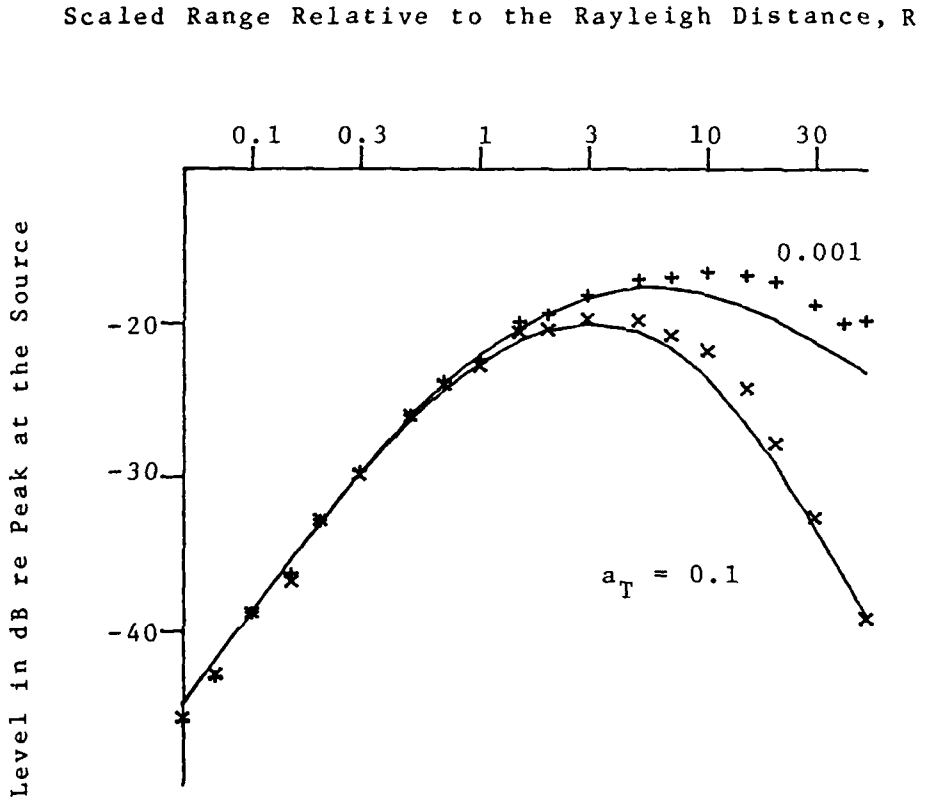

Figure 19. Difference-Frequency Level On Axis as a Function of Range for a Bifrequency Signal Having a Frequency Downshift Ratio of 5.5, for Selected Values of a_T .

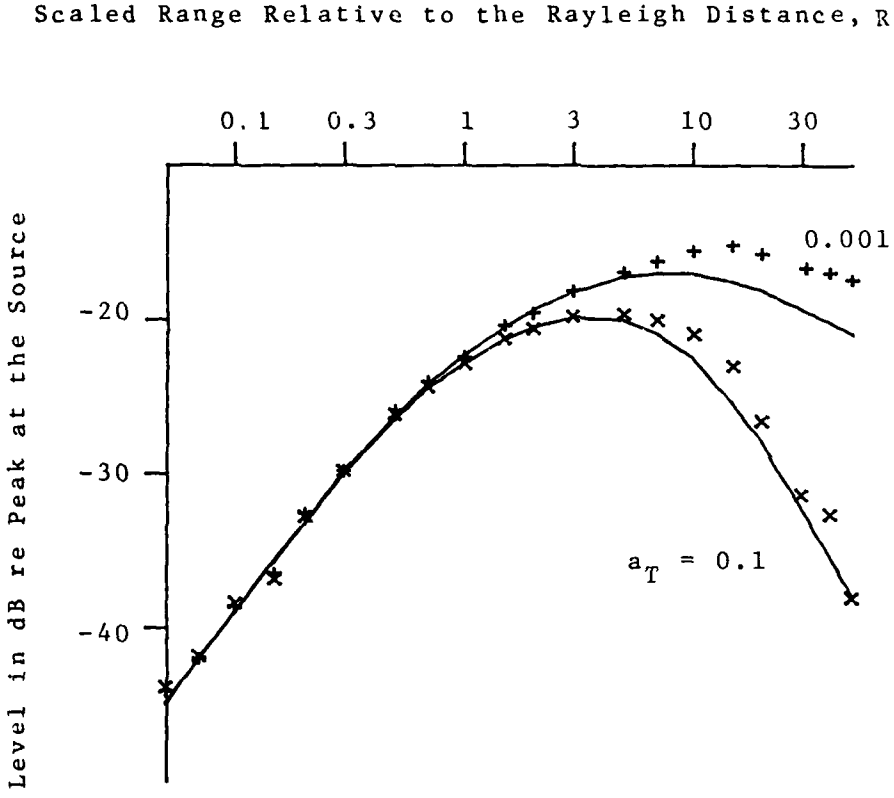

Figure 20. Difference-Frequency Level On Axis as a Function of Range for a Bifrequency Signal Having a Frequency Downshift Ratio of 7.5, for Selected Values of a_T.

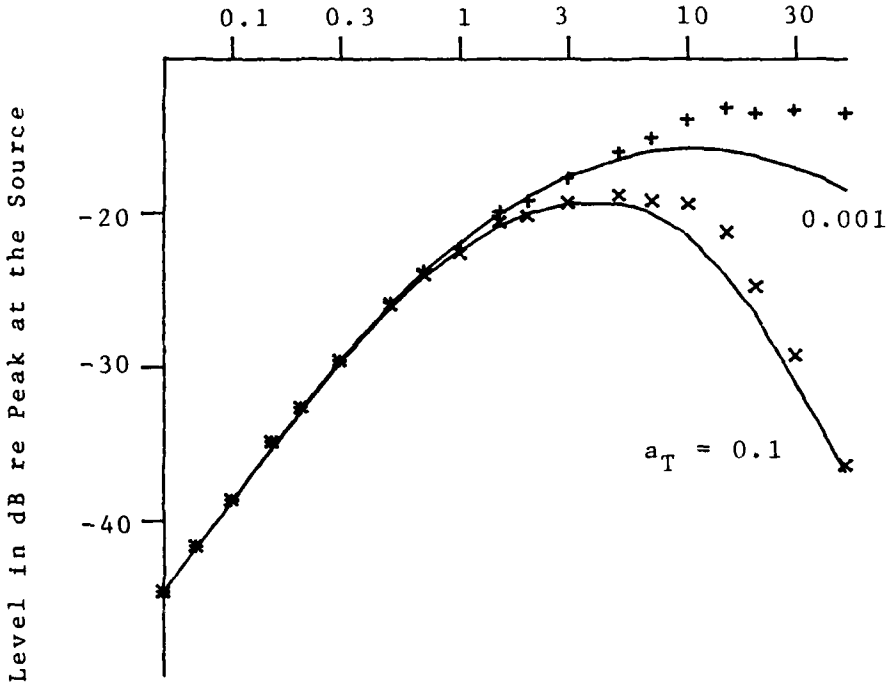

Figure 21. Difference-Frequency Level On Axis as a Function of Range for a Bifrequency Signal Having a Frequency Downshift Ratio of 10.5, for Selected Values of a_T.

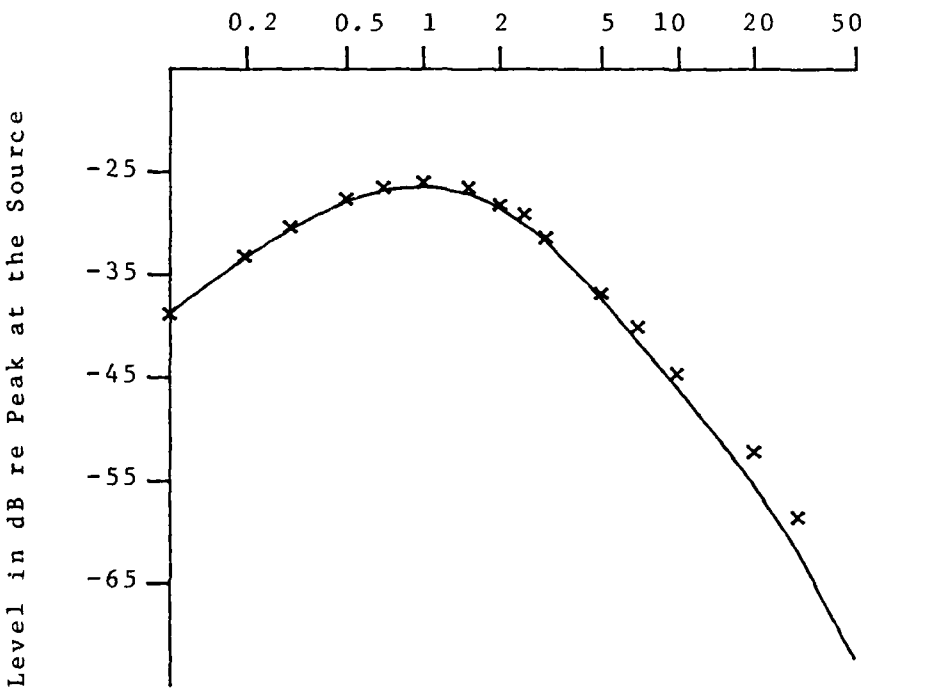

Figure 22. Difference-Frequency Level On Axis as a Function of Range for a Bifrequency Signal Having a Frequency Downshift Ratio of 5.5 and a_T =1.0.

For a 454-kHz signal radiating from a projector 0.0762 m in diameter, the wave number is

$$k_o = \omega_o / c_o = 2.852 \cdot 10^6 / 1480 = 1927.0, \tag{4.12}$$

and the Rayleigh distance is

$$r_o = A/\lambda_o = 1.398\text{m} . \tag{4.13}$$

The source level is defined

$$SL_o = 20 \log_{10} (r_o p_o), \tag{4.14}$$

hence, the peak signal pressure is

$$p_o = r_o^{-1} \, 10^{SL_o/20} \tag{4.15}$$

so that, for a peak source level of 235 dB re 1 μPa at 1 meter the peak acoustic pressure has the value

$$p_o = 1.398^{-1} \, 10^{235/20} = 4.02 \cdot 10^{11} \ \mu\text{Pa} = 4.02 \cdot 10^6 \ \mu\text{Bar}, \tag{4.16}$$

and the Mach number has the value

$$\varepsilon_o = p_o / \rho_o c_o^2 = 4.02 \cdot 10^6 / 2.25 \cdot 10^{14} = 1.84 \cdot 10^{-4}. \tag{4.17}$$

For fresh water, the scaled source level corresponding to SL_o =235 dB in this experiment thus is

$$\sigma_o = 3\varepsilon_o k_o r_o = 1.74 . \tag{4.18}$$

The scaled attenuation parameter, a_o , is the amount of absorption which is suffered by the reference frequency in traveling over the Rayleigh distance. As the thermo-

viscous attenuation at 454 kHz in fresh water is given by

$$\alpha = \delta f^2 = 4.91 \cdot 10^{-3} , \tag{4.19}$$

the scaled attenuation parameter has the value

$$a_o = \alpha r_o = 6.86 \cdot 10^{-3} . \tag{4.20}$$

The experiment performed by Shooter, Muir, and Blackstock has been simulated by means of the numerical solution with Gaussian beam input. For this reason, the results shown in the following figures indicate scaled source levels twice those for a plane piston projector. Figure 23 shows the level of the fundamental on axis as a function of range, in solid curves for the numerical results and as discrete points for those ranges at which experimental data were taken. The numerical solution is slightly low at small ranges and slightly high at large ranges, as a Gaussian beam was used to approximate the uniform source excitation. The incipient saturation of the medium is evident, as the 10 dB increase in source level from 215 to 225 dB re 1 μ Pa has a considerably larger effect on the far-field sound pressure level than the similar increase from 225 to 235 dB. Further increases in source level would raise the level in the near field, i.e. $R < 1$, but would have a minimal effect in the far field, $R > 10$.

Figure 24 presents the beam widths of the fundamental to the -10 dB point as a function of range, for several scaled source levels. Finite-amplitude losses at the center

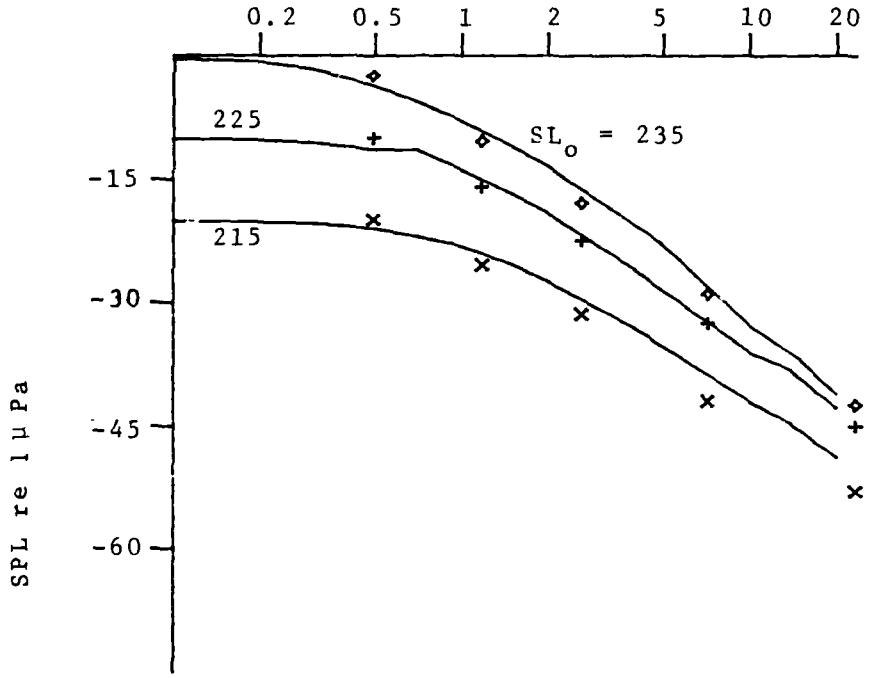

Figure 23. Numerical Simulation of the Experiment of Shooter, Muir, and Blackstock: Level On Axis of the 454-kHz Fundamental as a Function of Range. Source Levels 235, 225, and 215 dB.
Numerical Results are Shown as Solid Curves, and Experimental Results as Discrete Points.

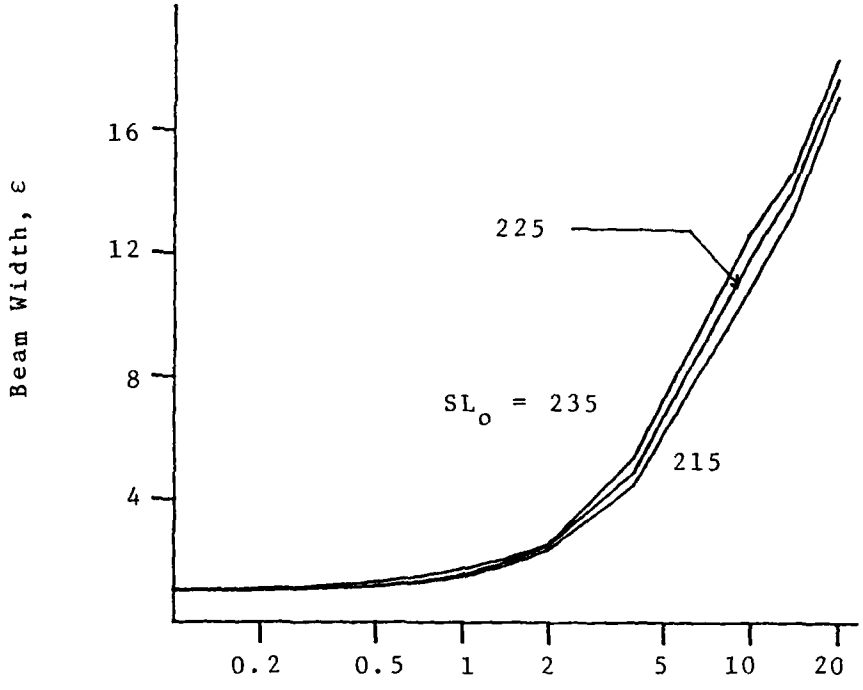

Figure 24. Numerical Simulation of the Experiment of Shooter, Muir, and Blackstock: Beam Width of the 454-kHz Fundamental to the -10 dB Point as a Function of Range for Selected Source Levels.

of the beam lower its level relative to the edges, thus progressively broadening the beam as the scaled source level increases.

Figure 25 shows the levels of the second harmonic as a function of range for selected scaled source levels, on axis and at a radial distance equal to the effective spot size of the Gaussian beam, that is, to the original 1/e width at $\varepsilon=0$. Figure 26 shows the 10-dB beam widths of the second harmonic as a function of range for several scaled source levels.

Bifrequency experiments may be simulated using the numerical method by choosing the reference frequency, to which the equations are normalized, so that each carrier and the difference frequency lie at one of the Fourier eigenfrequencies; that is, so that each carrier and the difference frequency are periodic within the set of waveform samples. The scaled source level and other parameters are determined in the manner outlined previously, but all must be specified in terms of the reference frequency. Thus, if N_1, N_2, and N_- are the Fourier eigenfrequency numbers which correspond to the carriers and the difference frequency, then the nominal attenuation coefficient a_T as used by Fenlon and McKendree (1979) is converted to the reference coefficient a_o by the expression

$$a_o = a_T/(N_1^2 + N_2^2 - N_-^2) \quad . \tag{4.21}$$

The scaled source level is influenced by the frequency

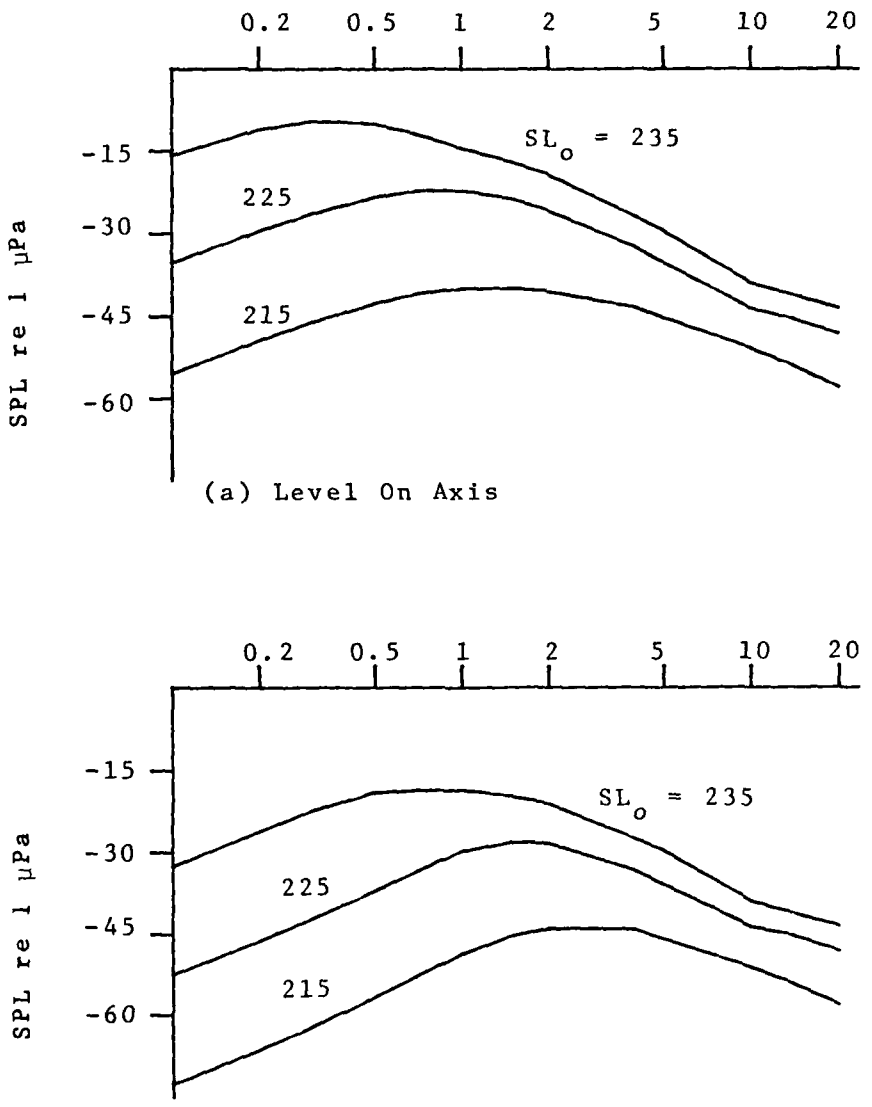

Figure 25. Numerical Simulation of the Experiment of Shooter, Muir, and Blackstock: Level of the 908-kHz Second Harmonic as a Function of Range.

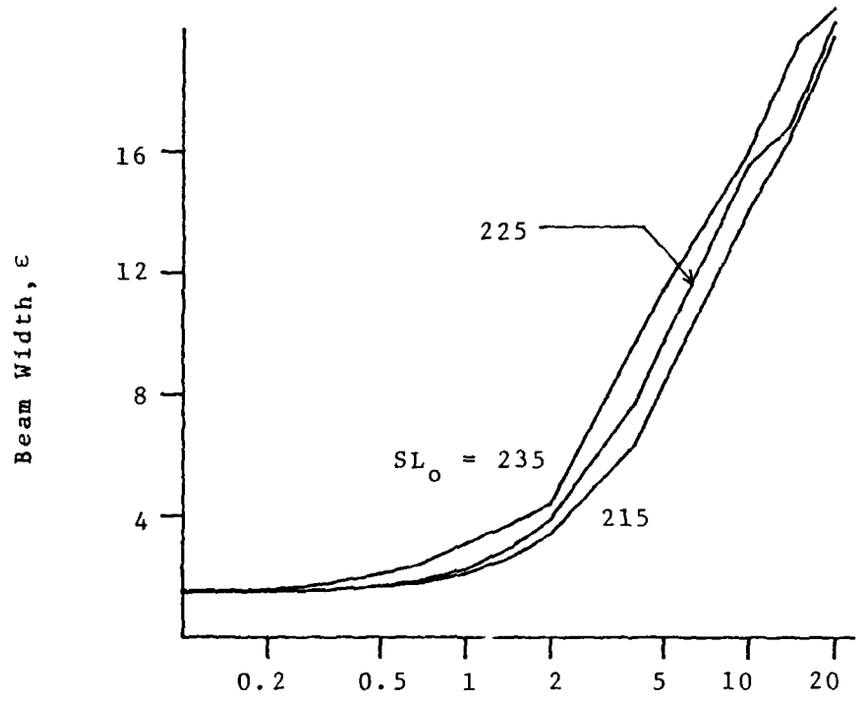

Figure 26. Numerical Simulation of the Experiment of Shooter, Muir, and Blackstock: Beam Width of the 908-kHz Second Harmonic to the -10 dB Point as a Function of Range, for Selected Source Levels.

dependence of the Rayleigh distance and the wave number. If σ_o is the scaled source level of the nominal carrier frequency and peak signal amplitude, then the reference scaled source level is given by

$$\sigma_* = \sigma_o\{\left[2N_-/(N_1 + N_2)\right]^2\} \quad . \tag{4.22}$$

In the experiment performed by Muir and Willette, the reference scaled source level is σ_*=0.00076 and the normalized thermoviscous attenuation coefficient is a_o=0.0003. This experiment used a projector 0.02 m in diameter, operating at 418 and 482 kHz to generate a 64-kHz difference frequency. For the numerical solution, N_- was chosen as 2 and the reference frequency as 32 kHz. The carriers of 480 and 416 kHz corresponding to N_1=15 and N_2=13 are a good approximation of the actual values. Figure 27 shows the level of the difference frequency on axis as a function of range. The numerical solution is shown as a solid curve and the values measured in the experiment are shown as discrete points. Values derived from the weak-finite-amplitude solution are also shown for purposes of comparison. Figure 28 presents the beam widths of the difference frequency as a function of range as measured and as predicted by the solutions. The numerical results are fairly close to the experimental values. Cases such as this, involving large frequency downshift ratios, very small scaled source levels, and large ranges, are relatively difficult for the numerical solution to simulate. For such cases, the weak-finite-ampli-

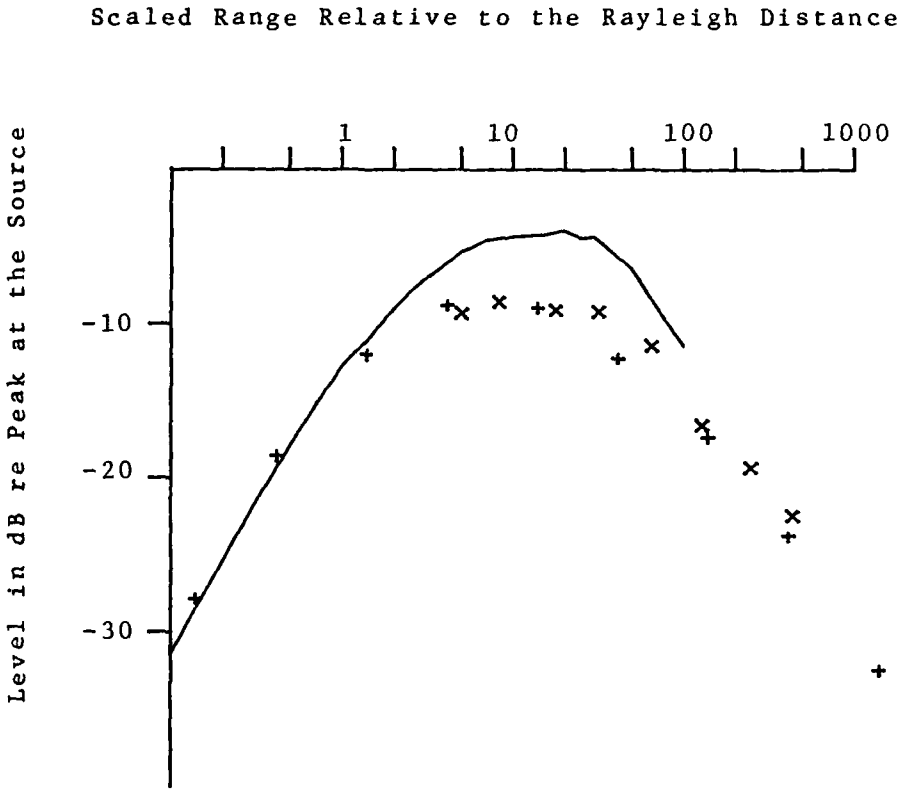

Figure 27. *Numerical Simulation of the Experiment of* Muir and Willette: Difference-Frequency Level On Axis as a Function of Range. Numerical Results are Shown as a Solid Curve; Experimental Data as 'x'; and Weak-Finite-Amplitude Theory as '+'.

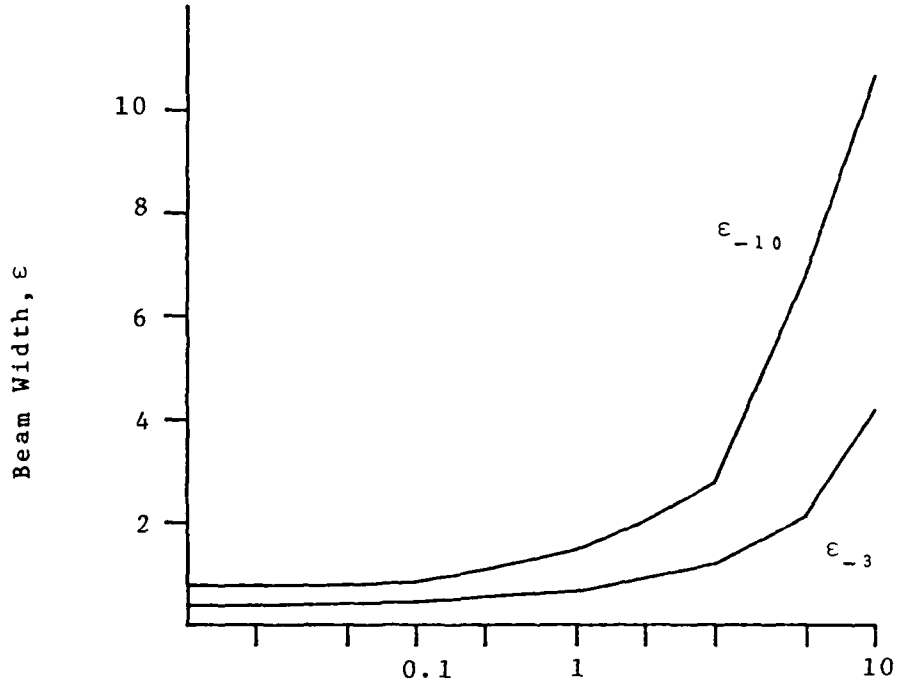

Figure 28. Numerical Simulation of the Experiment of Muir and Willette: Beam Widths of the Difference Frequency as a Function of Range.

tude solution is computationally more efficient.

The experiment performed by Eller (1974) used a projector 0.02 m in diameter, operating at a mean carrier frequency of 1435 kHz in fresh water. The numerical simulation used $N_1 = 29$, $N_2 = 28$, and $N_- = 1$, with a reference frequency of 50 kHz, equal in this case to the difference frequency. Figure 29 shows the difference-frequency level on axis as a function of range, as measured by Eller and as predicted by the numerical and weak-finite-amplitude solutions. Figure 30 shows the beam widths to the -10 dB point as a function of range, as predicted and as measured.

Numerical Simulations at Strong Finite Amplitudes

The fundamental assumption of the weak-finite-amplitude solution is that the carriers are not subject to finite-amplitude losses. As the scaled source level is increased, finite-amplitude losses in the carriers become significant. The reduced carrier levels in turn reduce the amount of energy which may be downshifted to the difference frequency. As the scaled source level becomes very large, the nonlinear interaction is restricted to the plane-wave collimation zone within the Rayleigh distance.

The fundamental parameters of the scaled nonlinear propagation problem are the scaled source level σ_o, the attenuation within the Rayleigh distance of the reference

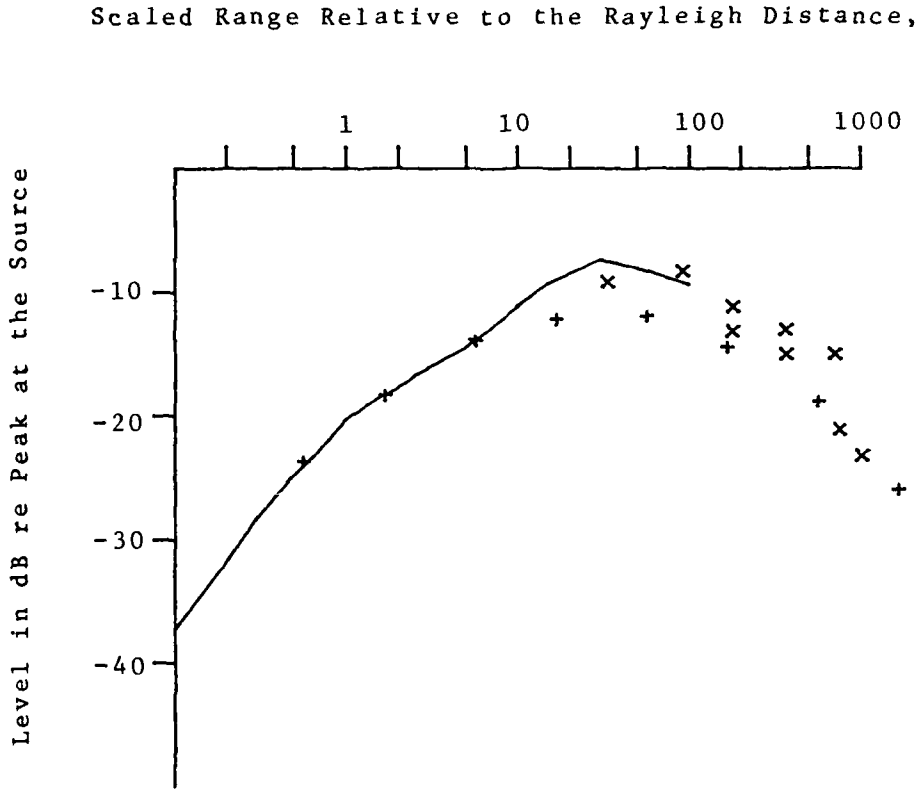

Figure 29. Numerical Simulation of the Experiment of Eller: Difference-Frequency Level On Axis as a Function of Range. Numerical Results are Shown as a Solid Curve; Experimental Data as 'x'; and Weak-Finite-Amplitude Theory as '+'.

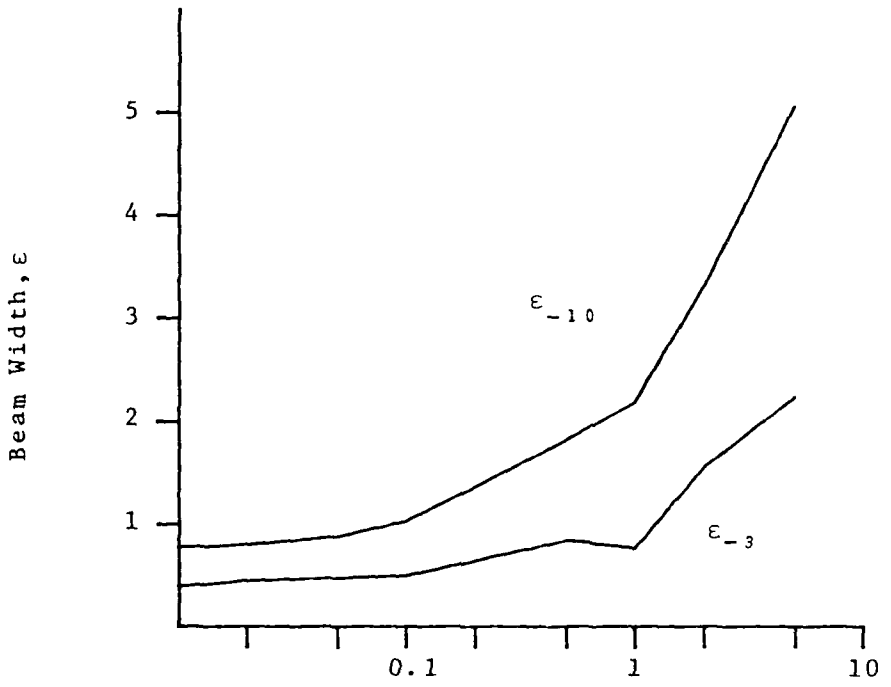

Figure 30. Numerical Simulation of the Experiment of Eller: Beam Widths of the Difference Frequency as a Function of Range.

frequency a_o, and the nature of the signal and projector. A bifrequency pair may be characterized by its frequency downshift ratio γ_o.

The following numerical simulations are of two types: numerical simulations of previously published research, and simulations of experiments with scaled parameters chosen so as to emphasize the effect of one, or to combine the effects of several.

The scaled source level indicates the strength of the nonlinear interaction relative to other effects of propagation. The choice of scaled source level values at approximately half-decade increments, or powers of $10^{1/2}$, as 10, 3, 1, 0.3, 0.1, and so on, permits a reasonable view of the continuum of scaled source levels. The attenuation coefficients a_T are chosen in decimal increments to represent high attenuation, which dominates the nonlinearity, and lower attenuation, which is dominated by nonlinearity. As the Fourier harmonics are have integer ratios, integer pairs are chosen to represent a bifrequency signal, e. g. $N_1=6$ and $N_2=5$ for a frequency downshift ratio of 5.5. Thus, frequency downshift ratios of 5.5 and 10.5 are used in the following simulations.

Figure 31 shows the difference-frequency level on axis as a function of range, as predicted by the numerical solution for various scaled source levels and as given by the weak-finite-amplitude solution for a frequency downshift ratio of 5.5. Figure 32 shows the same functions for a fre-

AD-A103 148 PENNSYLVANIA STATE UNIV UNIVERSITY PARK APPLIED RESE--ETC F/G 20/1
A NUMERICAL SOLUTION OF THE SECOND-ORDER-NONLINEAR ACOUSTIC WAV--ETC(U)
JAN 81 F S MCKENDREE N00024-79-C-6043
UNCLASSIFIED ARL/PSU/TM-81-44 NL

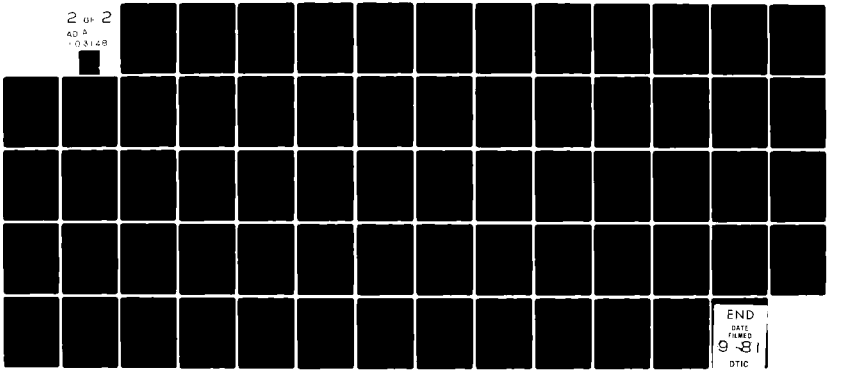

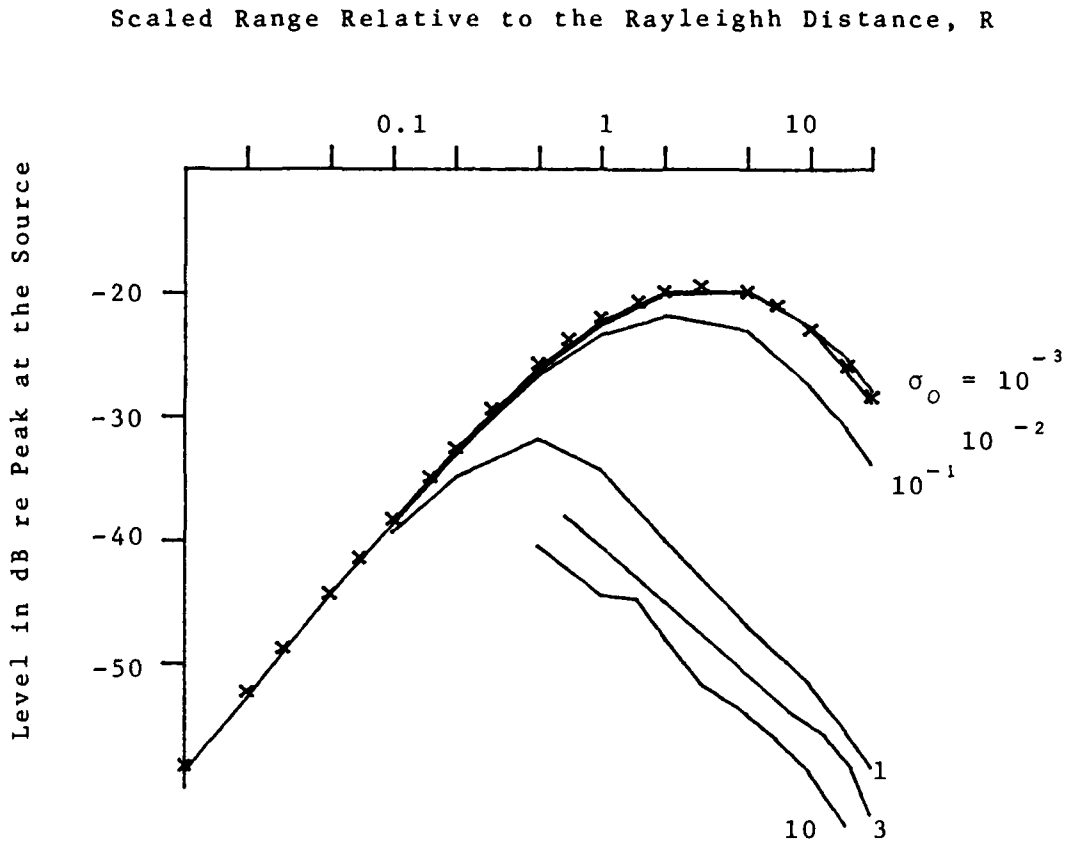

Figure 31. Difference-Frequency Level On Axis as a Function of Range, With a Frequency Downshift Ratio of 5.5 and a_T=0.1, for Selected Scaled Source Levels. Weak-Finite-Amplitude Results are Shown as Discrete Points, and Numerical Results as Solid Curves.

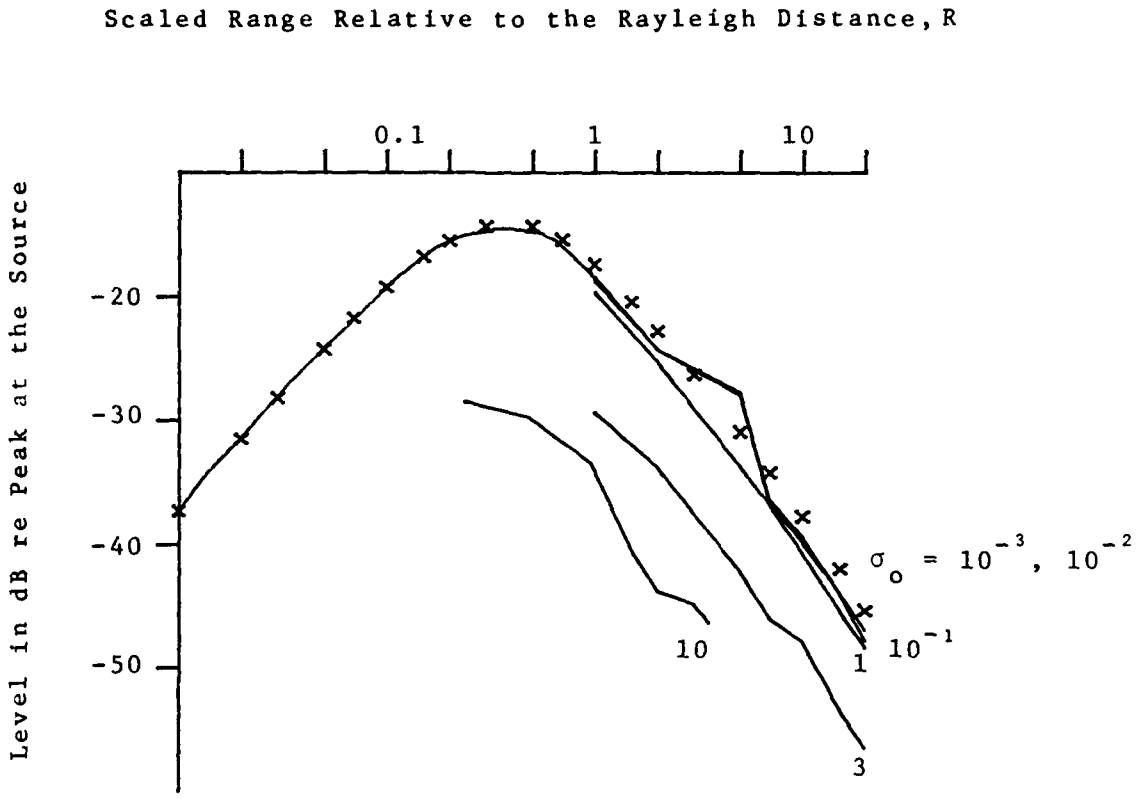

Figure 32. Difference-Frequency Level On Axis as a Function of Range, With a Frequency Downshift Ratio of 10.5 and a_T=4.0, for Selected Scaled Source Levels. Weak-Finite-Amplitude Results are Shown as Discrete Points, and Numerical Results as Solid Curves.

quency downshift ratio of 10.5. For each value of the scaled source level, the difference-frequency level is the same as the weak-finite-amplitude solution at small ranges. As the range increases, saturation of the carriers causes the difference frequency level to decrease. The greater the scaled source level, the sooner the departure occurs. For a scaled source level of 1 or greater, the increased source level is almost entirely canceled by finite-amplitude losses; the nonlinear interaction is saturated within the Rayleigh distance.

Figure 33 shows the difference-frequency level on axis as a function of range, as predicted by the numerical solution and as given by the weak-finite-amplitude solution, at various scaled source levels for a frequency downshift ratio of 5.5 and a reference combined-primary-wave attenuation coefficient of 1.0. In this instance thermoviscous losses are large enough to reduce the carrier levels to a large extent within the critical range.

The on-axis pressure in a Gaussian beam propagating in a linear manner obeys the following function of range:

$$|p_\omega(R)| = \left[|p_\omega(0)|/(1+R^2)^{1/2}\right] e^{-a_\omega R}. \qquad (4.23)$$

If the amplitude of the relative difference-frequency level derived from numerical results is divided by the right-hand side of Equation (4.23) the effects of thermoviscous and spreading losses are canceled in that region of the far field wherein only the linear loss mechanisms represented

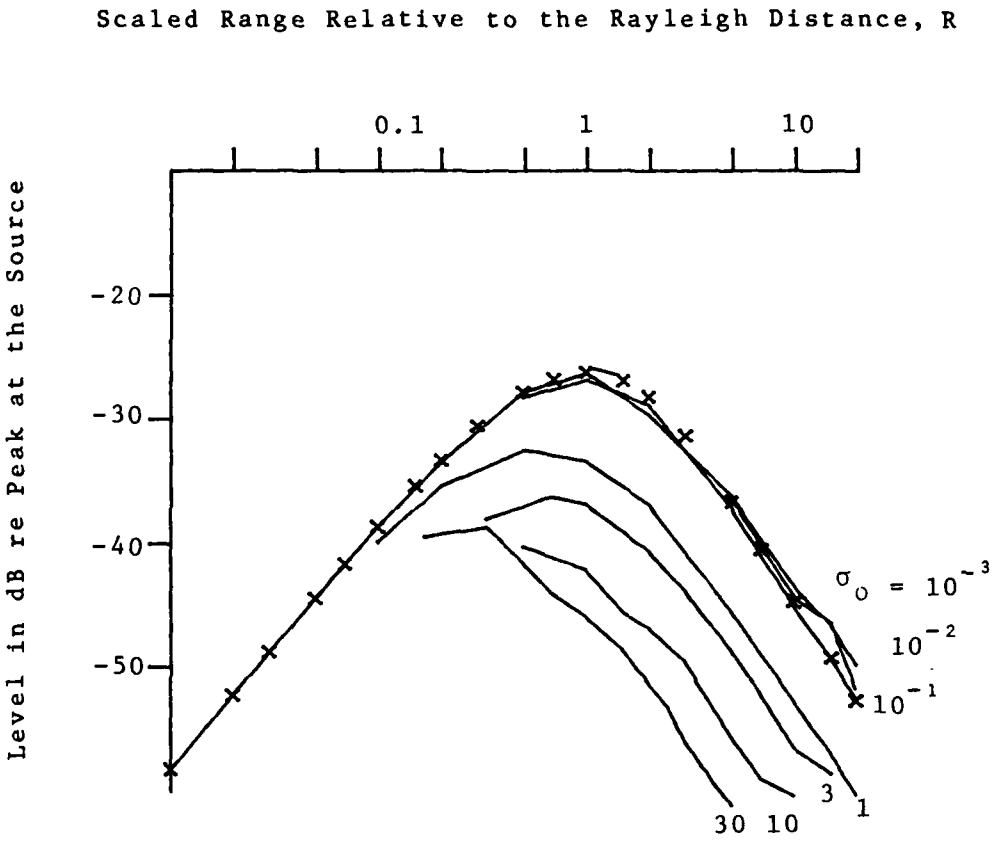

Figure 33. Difference-Frequency Level On Axis as a Function of Range, With a Frequency Downshift Ratio of 5.5 and a_T=1.0, for Selected Scaled Source Levels. Weak-Finite-Amplitude Results are Shown as Discrete Points, and Numerical Results as Solid Curves.

in Equation (4.23) remain. Figures 34, 35, and 36 each show the difference-frequency level adjusted for thermoviscous and spreading losses as a function of range, for various frequency downshift ratios and selected values of reference attenuation coefficient. These may be called saturation curves, as the saturation of the nonlinear interactions is reflected in their each attaining a constant value. From such curves, the extrapolated source level may be deduced by finding the saturation level and referring it back to the source.

The modified Bessel-Fubini solution derived by Fenlon (1972) provides a good model of bifrequency interaction in lossless media near the source. Figures 37 and 38 show predicted pressures in a bifrequency plane wave due to the source terms of the Bessel-Fubini solution, and as derived from the numerical solution. The spherically-spreading results for a scaled source level σ_o=20 are also shown. These are very similar to the plane-wave results.

The numerical work of Bakhvalov et al. (1978,1979), concerning initially monotonic waves in thermoviscous media at strong finite amplitudes, has been simulated numerically. Figure 39 shows the waveforms at R=0.09 and several values of the radial coordinate, for a scaled source level of 20 and a reference attenuation coefficient of 0.05. The corresponding figure from Bakhvalov's results is included for purposes of comparison. Figure 40 shows the waveform on axis at several ranges, for a scaled source level of 10,

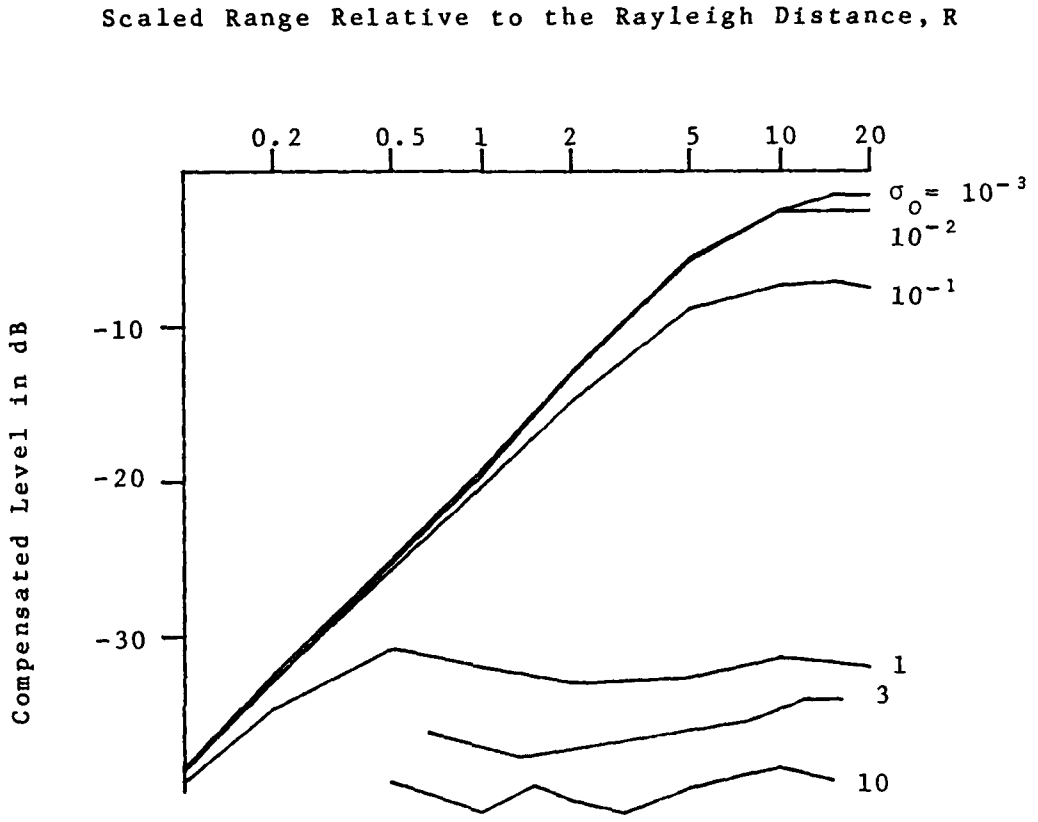

Figure 34. Difference-Frequency Level On Axis Compensated for Spherical Spreading and Thermoviscous Losses, With a Frequency Downshift Ratio of 5.5 and a_T=0.1, for Selected Scaled Source Levels.

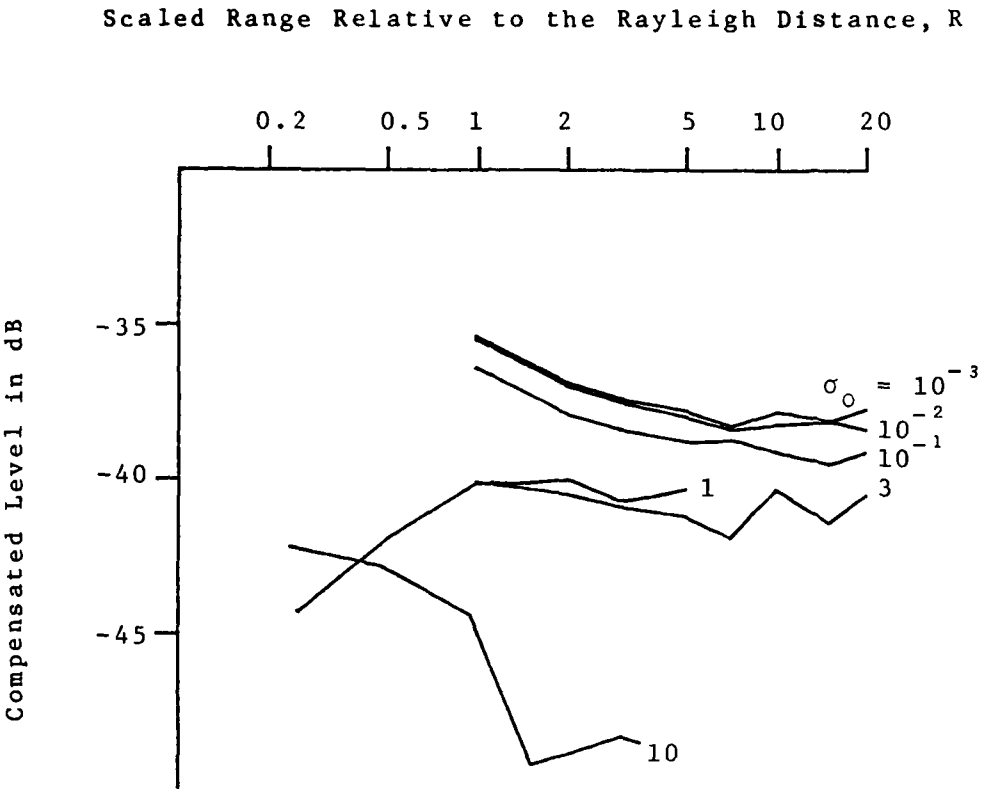

Figure 35. Difference-Frequency Level On Axis Compensated for Spherical Spreading and Thermoviscous Losses, With a Frequency Downshift Ratio of 10.5 and $a_T = 4.0$, for Selected Scaled Source Levels.

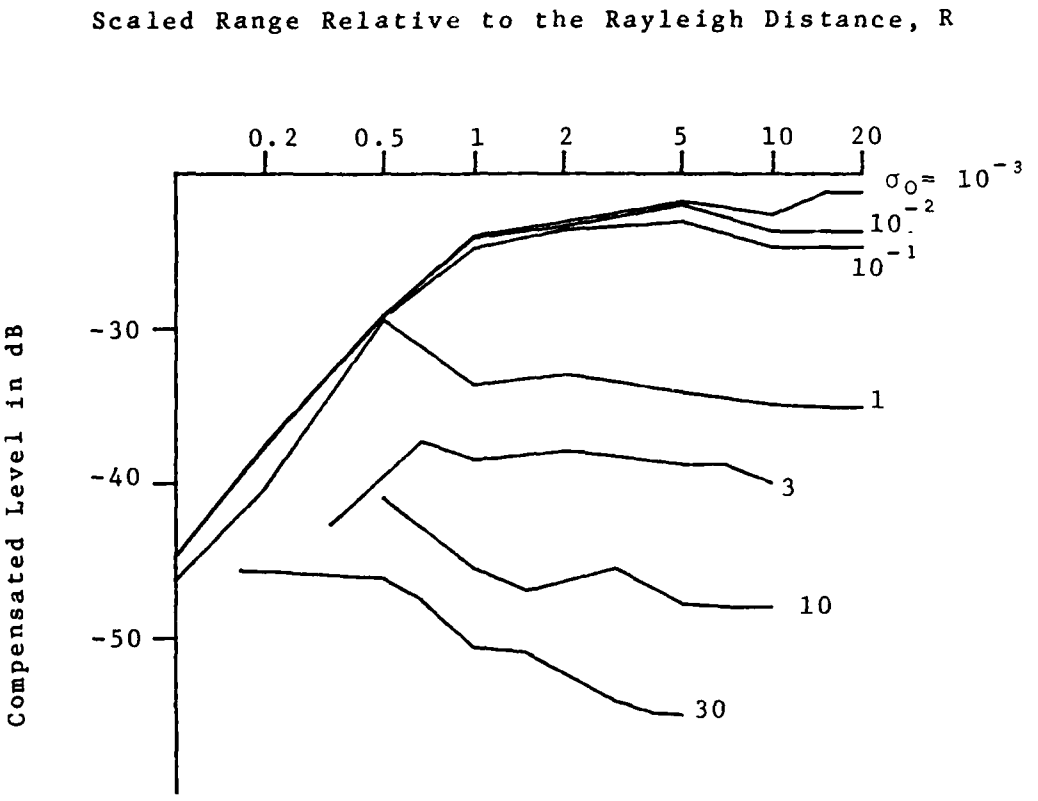

Figure 36. Difference-Frequency Level On Axis Compensated for Spherical Spreading and Thermoviscous Losses, With a Frequency Downshift Ratio of 5.5 and a_T=1.0, for Selected Scaled Source Levels.

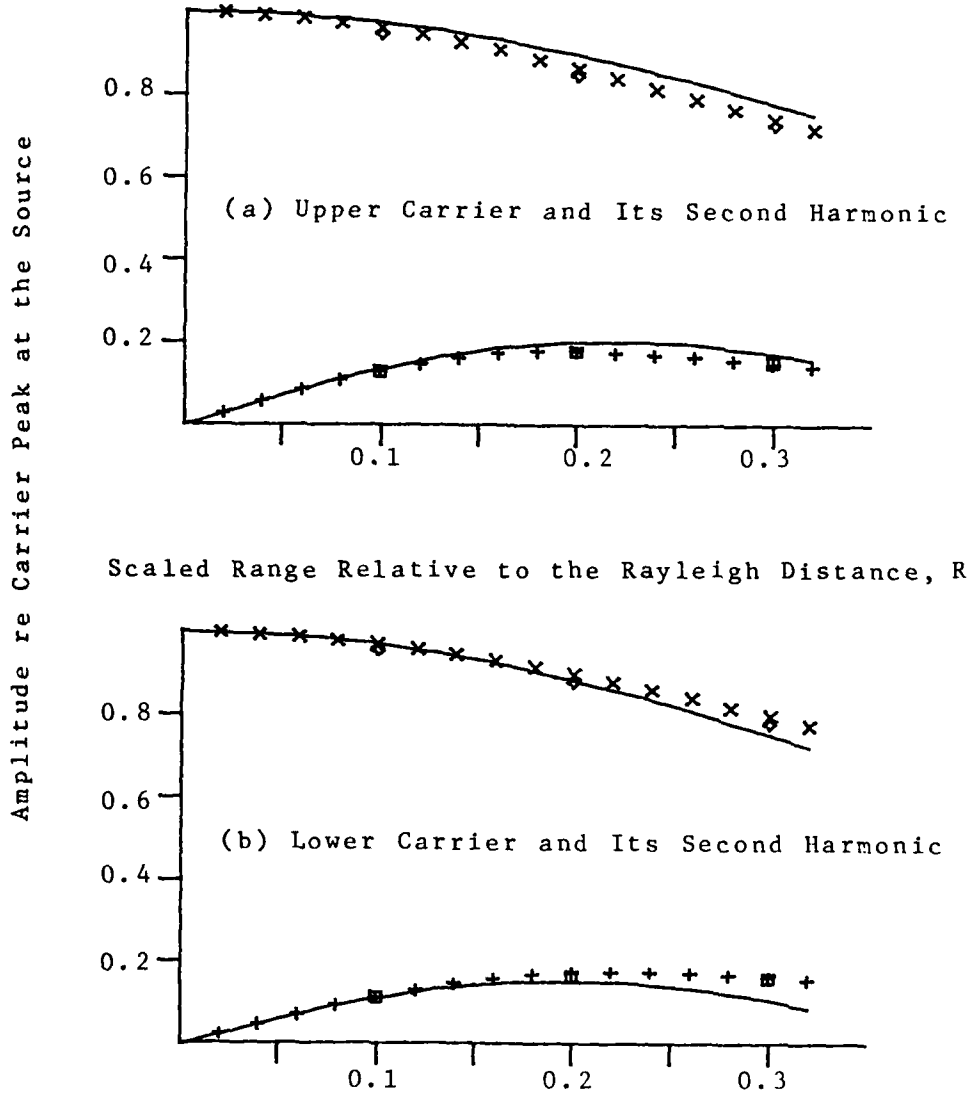

Figure 37. Lossless Plane-Wave Harmonic Levels as a Function of Range, Modeled By the Source Terms of the Modified Bessel-Fubini Series of Fenlon and by the Numerical Solution.

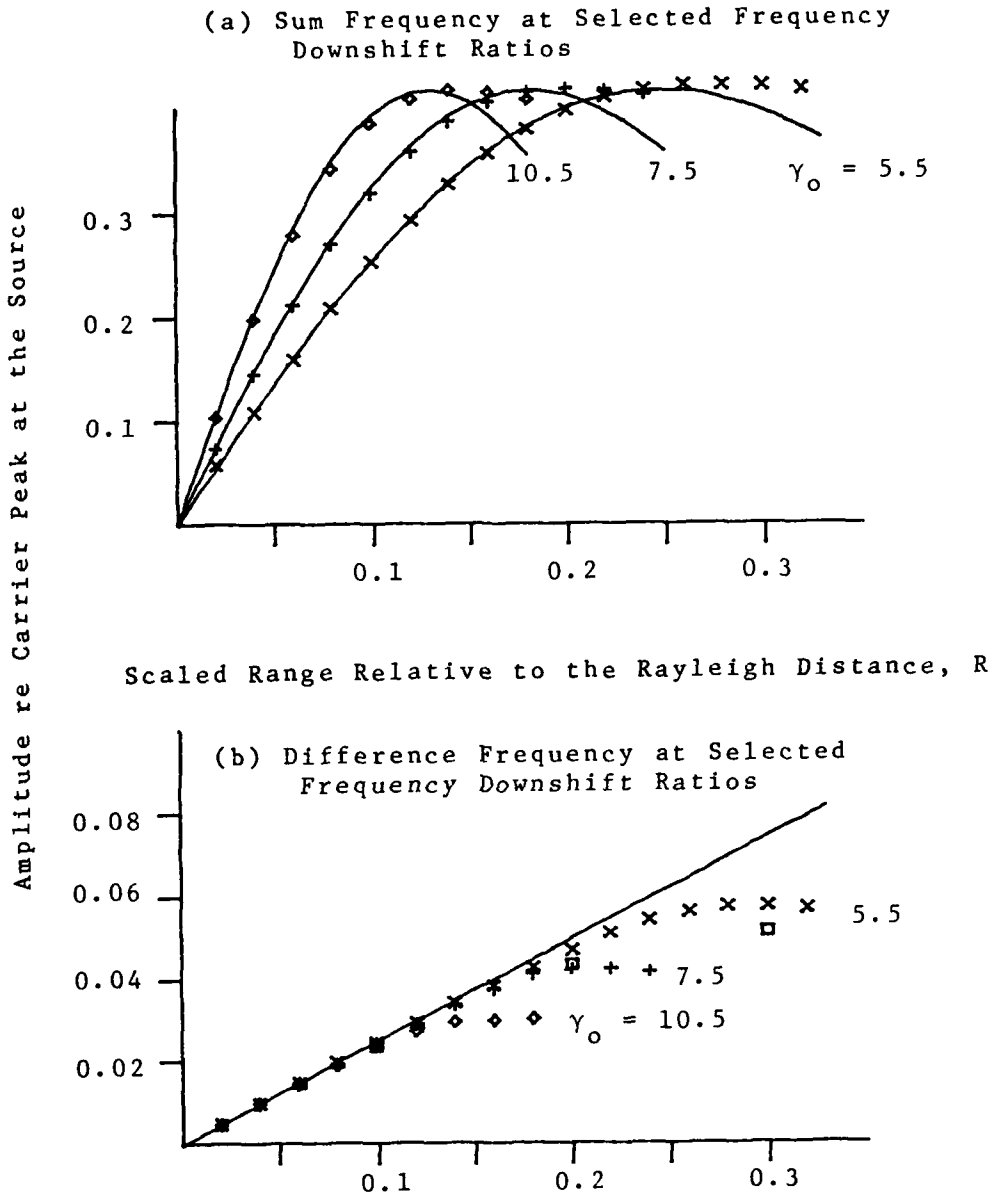

Figure 38. Lossless Plane-Wave Harmonic Levels as a Function of Range, Modeled by the Source Terms of the Modified Bessel-Fubini Series of Fenlon and by the Numerical Solution.

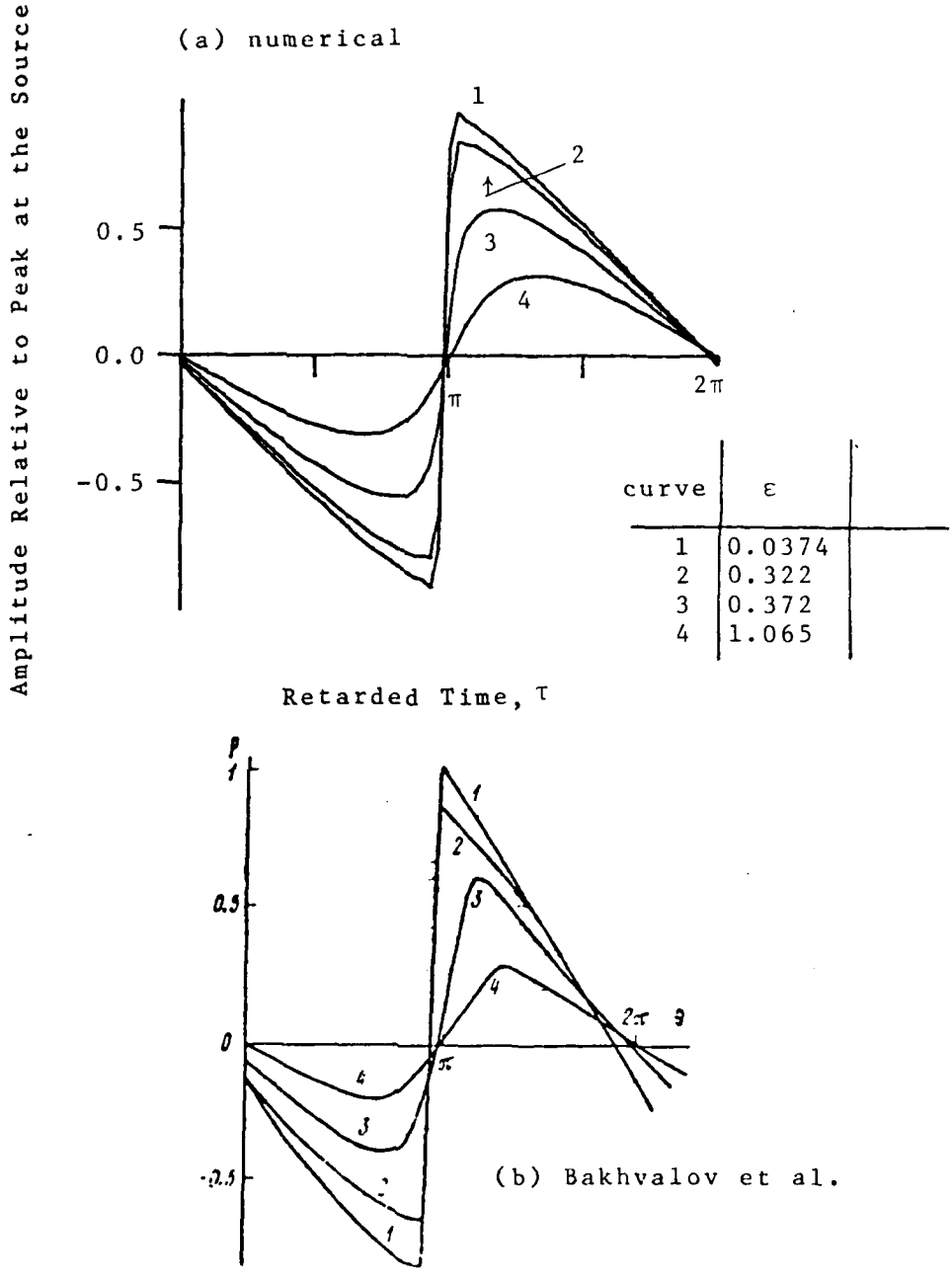

Figure 39. Waveforms in Three-Dimensional Propagation at R=0.09 and Selected Radial Distances, with a Scaled Source Level of 20 and Γ=200, for a Gaussian Beam Input.

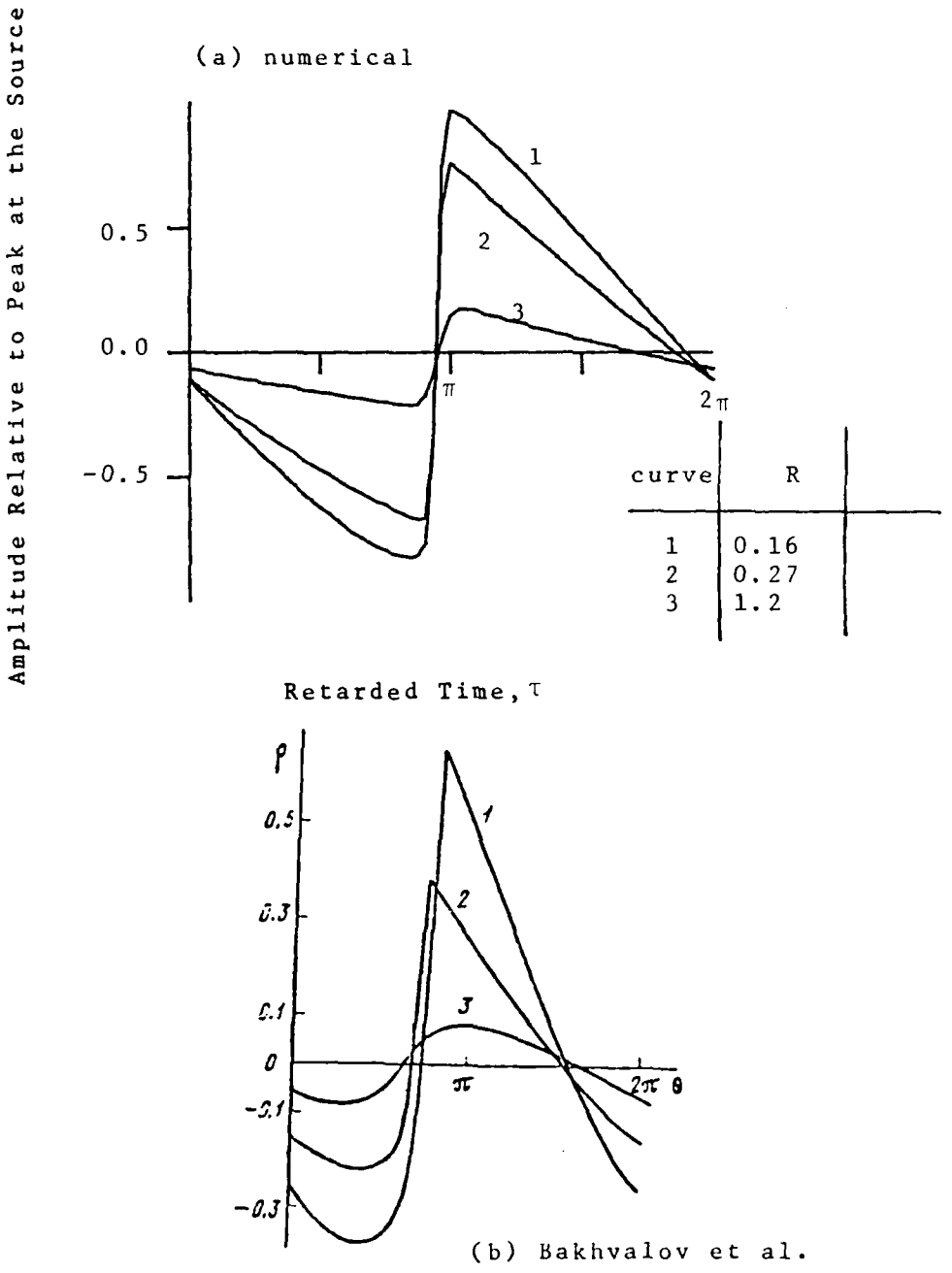

Figure 40. Waveforms in Three-Dimensional Propagation at Selected Ranges On Axis, with a Scaled Source Level of 10 and Γ=100, for a Fourth-Order Beam Input.

an attenuation coefficient of 0.05, and a beam shape at the source defined by $1-\varepsilon^4$ to $\varepsilon=1$ and zero beyond $\varepsilon=1$. Here also a comparison figure is included.

Bakhvalov et al. included in their results figures illustrating the region of shock formation, specified as a "quasi-discontinuous wave", as a function of range and radial distance for various scaled source levels and amounts of absorption. Figure 41 shows regions of shock formation, defined as that region in which the harmonics equal or exceed threshold values given on the figure. The corresponding figure from Bakhvalov's results is included for comparison. The numerical results are based upon the attainment of specified harmonic levels, rather than on the slope of the discontinuity as was used by Bakhvalov et al.; therefore the appearance of the former and latter is not precisely the same. A waveform having 50 percent second harmonic, 33 percent third harmonic, and so on in the correct relative phase, will have a discontinuity extending from the positive peak to the negative peak of the waveform.

(a) Numerical Simulation Results Using Relative Harmonic Levels as a Criterion.

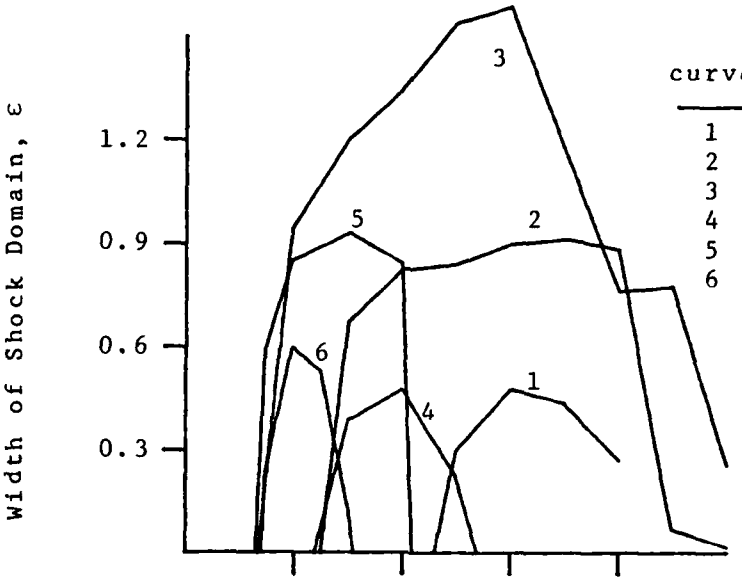

curve	σ_o	a_o
1	6.5	0.1
2	10	0.1
3	20	0.1
4	10	0.25
5	20	0.25
6	20	0.5

Scaled Range Relative to Rayleigh Distance, R

(b) Results of Bakhvalov et al., Using Shock Slope as a Criterion.

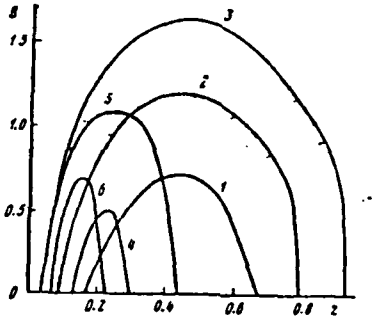

Figure 41. Shock Wave Domains of Existence as a Function of Range and Radial Distance, for Various Scaled Source Levels and Acoustic Reynold's Numbers.

Chapter 5

CONCLUSIONS

The first section of the conclusions deals with the results of tests of the numerical solution to determine the accuracy which is exhibited in these results. In the next section, the limits of applicability of the weak-finite-amplitude theory are discussed. The topic of near-field calibration of parametric sources is then considered. The conversion efficiencies which may be expected of parametric arrays is indicated by analysis of the results of numerical simulations. Finally, suggestions are given for further research in the numerical solutions of nonlinear wave equations.

Tests of the Numerical Solution

Table 5.1 shows the comparison between the matched asymptotic lossless initially monotonic plane-wave solution due to Blackstock and the results of numerical solution of the lossless Burger's equation. At each of several ranges and frequencies, the difference between the numerical solution and Blackstock's solution is presented as a percentage of the latter. The harmonic levels of the numerical solution are within a few percent of Blackstock's solution throughout the range. This degree of accuracy

Table 5.1. Numerical Harmonic Levels of the First Three Harmonics of a Monofrequency Signal at Selected Ranges, and the Values of the Matched Asymptotic Solution due to Blackstock (1966).

SIGMA	NUMERICAL	ANALYTIC	ERROR IN PERCENT
	(a) $B_1(\sigma)$		
0.5	.9649	.9691	-0.4
1.0	.8747	.8801	-0.6
2.0	.6435	.6484	-0.8
3.0	.4891	.4937	-0.9
5.0	.3274	.3333	-1.7
	(b) $B_2(\sigma)$		
0.5	.2274	.2298	-1.0
1.0	.3483	.3528	-1.3
2.0	.3102	.3134	-1.0
3.0	.2444	.2428	0.7
5.0	.1682	.1667	0.9
	(c) $B_3(\sigma)$		
0.5	.0791	.0813	-2.7
1.0	.2102	.2060	2.0
2.0	.2025	.2070	-2.2
3.0	.1581	.1610	-1.8
5.0	.1055	.1111	-5.0

confirms the validity of the numerical solution of the lossless Burger's equation.

Tables 5.2a, b, and c show the far-field difference-frequency level times $\exp(\sigma / \Gamma)$, as predicted by the solution of Fenlon (1972) and as derived from the numerical solution of the lossy Burger's equation. The agreement between analytic and numerical results is fairly good. For some of these simulations, as many as 4000 iterations of the nonlinear operator were required. The presence of bias in the results is therefore to be expected, though the largest error does not exceed 12 percent.

The numerical simulation of bifrequency propagation in a lossy medium requires the numerical solution to apply the nonlinear operator simultaneously at several frequencies, so as to simulate self-convolution of the input signal, and to apply the correct thermoviscous losses to each of the resulting frequency components. In fact, the analytic far-field difference-frequency levels are reproduced by the numerical solution with an amount of error not much larger than may be expected due to the bias of the lossless nonlinear operator itself. It is evident that the number of waveform samples and the number of steps per unit range will not significantly affect the results, so long as each is large enough. The ability of the numerical solution to simulate bifrequency propagation in a lossy medium indicates that both nonlinearity and viscous losses are properly modeled.

Table 5.2. Difference-Frequency Level in the Far Field Times $\exp(\sigma/\Gamma)$ As Predicted by the Numerical Solution and by the Solution due to Fenlon (1972), for Selected Frequency Downshift Ratios and Values of Γ.

GAMMA	ANALYTIC (Fenlon,1972)	NUMERICAL	ERROR IN PERCENT
	(a) frequency downshift ratio 5.5		
11	.0428	.043	-0.5
16	.0583	.057	-2.2
22	.0724	.070	-3.3
31	.0847	.081	-4.3
44	.0885	.085	-3.9
62	.0817	.077	-5.7
88	.0678	.065	-4.1
124	.0530	.051	-3.8
	(b) frequency downshift ratio 7.5		
15	.0314	.031	-1.3
21	.0415	.040	-3.6
30	.0531	.051	-4.0
42	.0620	.060	-3.2
60	.0649	.060	-7.6
85	.0598	.056	-6.4
120	.0497	.047	-5.4
170	.0387	.038	-1.8
	(c) frequency downshift ratio 10.5		
21	.0224	.022	-1.8
30	.0301	.029	-3.7
42	.0380	.036	-5.3
59	.0443	.040	-9.7
84	.0464	.041	-11.6
119	.0427	.041	-11.0
168	.0355	.032	-9.8
238	.0276	.025	-9.4

Simulated propagation in a lossless, dispersive medium is a severe test of the numerical solution. Since reasonably accurate simulations of dispersive propagation result from the use of the numerical solution, it may be assumed that the method of solution is valid.

The preceding tests apply to plane-wave propagation, for which the pertinent equation is equation 4.23. In order to accommodate spreading as in equation 4.22, the diffraction term must be handled by the method of diffusion-in-frequency. The present numerical implementation works well out to R on the order of 20; spherical spreading may be assumed to prevail beyond this range. The numerical solution is designed to allow the user to choose a value of R beyond which spherical spreading is assumed. If this value is chosen carefully, the resulting error is not intolerable.

The ability of the numerical solution to produce correct results when a combination of factors is present, such as nonlinearity and attenuation or nonlinearity and dispersion, indicates that the implementation which was used, regarding each of these effects as independent over small distances, is sufficiently accurate. There exist certain areas in which the computational efficiency could be improved. These are discussed in the suggestions for further research. The remaining computational problems are also discussed in the last section.

Limits of Applicability of the Weak-Finite-Amplitude Theory

The results of numerical analysis confirm that the weak-finite-amplitude solution is invalidated by finite-amplitude losses in the carriers. For relatively lossless cases, a simple constraint suffices to ensure the applicability of the weak-finite-amplitude theory: the maximum range of interest must be considerably less than the critical range of either of the carriers, so that they do not lose a significant amount of energy in generating harmonics or modulation frequencies.

The limiting case as the scaled source level becomes infinite, physically the case for very high frequencies or very large apertures, is that of collimated plane-wave propagation; the nonlinear interaction is confined to the very near field of the source. The largest scaled source levels actually used in computation, on the order of 20, are virtually indistinguishable from plane-wave propagation in the near field. In these cases, the carriers of a bifrequency signal do not go into shock, but attain second harmonic levels of 20 to 25 percent at most. The greatest amount of energy is transferred to the sum frequency and its harmonics, which will attain a shock profile in a relatively lossless medium.

In very lossy media, the weak-finite-amplitude solution is applicable at higher scaled source levels than in

less lossy media. The linear losses reduce the carrier amplitudes within the near field, thus suppressing part of the nonlinear interaction. For example, with a frequency downshift ratio of 5.5 and a scaled source level of 0.1, the numerical and weak-finite-amplitude results differ by 8 dB at R=20 if the combined-primary-wave attenuation coefficient is 0.001; whereas if it is increased to 1.0, the numerical and weak-finite-amplitude results are virtually the same out to R=30.

Near-Field Behavior and Calibration of Parametric Sources

The numerical solution provides a means of modeling the operation of parametric arrays in both the unsaturated and saturated regimes. The pressure waveform or spectrum may be obtained from the numerical solution at any point within the Fresnel zone, as the solution of the diffraction term is based upon a Fresnel approximation. Zemanek (1971) published a paper which investigates the near-field behavior of the beam from an axisymmetric vibrating piston of finite extent. His method has been implemented with excellent results, but as it is vastly slower than the diffusion-in-frequency technique, it is not suited for iterative computations.

The effective length of a parametric source operating in a relatively lossless medium may be much longer than the

Rayleigh distance of the projector at the difference frequency, which in many practical cases may be too long to allow calibration of the difference-frequency signal in an anechoic facility of practical size. The weak-finite-amplitude theory is capable of predicting the near-field behavior in the Fresnel zone of unsaturated arrays. The numerical solution as presently implemented is also restricted to the Fresnel zone, but will accommodate saturated parametric arrays. Thus calibration of the difference-frequency characteristics of a saturated parametric source is possible within its near field by comparison with the results of the numerical solution.

Conversion Efficiencies of Parametric Arrays

The amplitudes of carriers from a parametric source are reduced by finite-amplitude losses, by spreading, and by thermoviscous losses. Eventually, they will be reduced to a point where they no longer transfer a significant amount of energy to the difference-frequency signal. The difference frequency will propagate thereafter under the influence of spreading and thermoviscous losses. From the difference-frequency level in this region, an extrapolated source level may be deduced. A difference-frequency signal radiated from the source position at this level would give rise to the pressure observed in the far field as a result of the

parametric interaction.

It is of interest to determine what may be the extrapolated source level of the difference frequency relative to the level of the carriers. This may be done by analysis of the numerical results. Values of absorption, scaled source level, frequency downshift ratio or modulation type, and beam shape are chosen. The signal is allowed to propagate until nonlinear energization of the difference frequency is seen to have ended. The far-field difference-frequency pressure is converted to a pressure at the source by application of Equation (4.12), or its appropriate analogue for other beam types, and this equivalent source pressure is expressed in dB relative to the peak pressure which was actually transmitted.

The numerical solution requires the peak pressure at the source to be unity to account for the correct scaling of the nonlinear operator. Thus, the numerical value obtained from the program at any frequency, range, and radial distance is that which would be produced by a unit peak source. The Rayleigh distance does not appear explicitly in this calculation. The following figures show the extrapolated source levels of the difference frequency as a function of scaled source level of the carriers for selected combined-primary-wave attenuation coefficients.

Figure 42 shows the difference-frequency extrapolated source levels for a bifrequency signal having a frequency

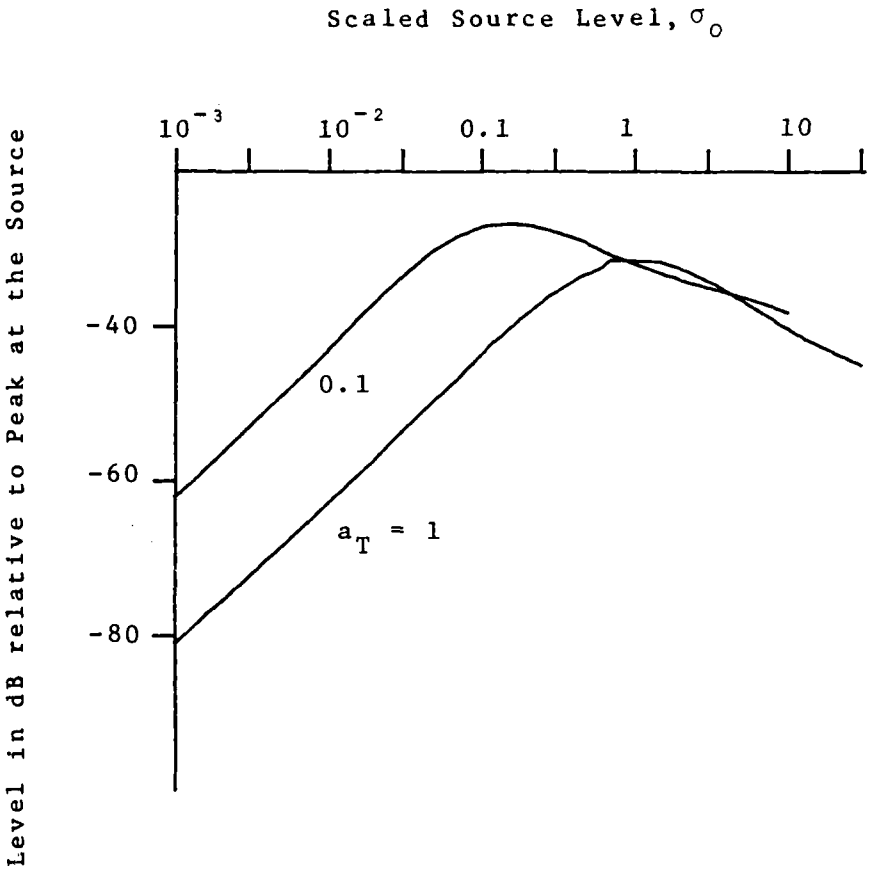

Figure 42. Difference-Frequency Extrapolated Source Level in dB Relative to the Peak of the Carriers at the Source for a Frequency Downshift Ratio of 5.5 and Selected Combined-Primary-Wave Attenuation Coefficients, a_T.

downshift ratio of 5.5, and Figure 43 for a frequency downshift ratio of 10.5. As an example of their use, consider a bifrequency signal having a frequency downshift ratio, γ_o, of 5.5, a scaled source level, σ_o, of 0.3, and a combined-primary-wave attenuation coefficient, a_T, of 1.0. By reference to Figure 42 it may be determined that the extrapolated source level of the difference frequency is 38 dB below the peak level of either of the carriers at the source. The numerical solution may be used as shown above to generate families of curves of this kind for any modulation type and range of source levels, limited only by the amount of space available for storage of waveform samples, and the amount of time available for computation.

Suggestions for Further Research

The method of numerical solution employed in this thesis produces good results in most cases. The validity of the basic approach to the problem is confirmed by the quality of its results. The method is subject to failure in certain respects, and as these impose the major restrictions on the usefulness of the numerical solution, it is the purpose of this section to discuss the causes of the computational problems and the benefits which may be expected from alleviating them.

The simple linear interpolator used in the solution of the lossless Burger's equation is highly satisfactory, but

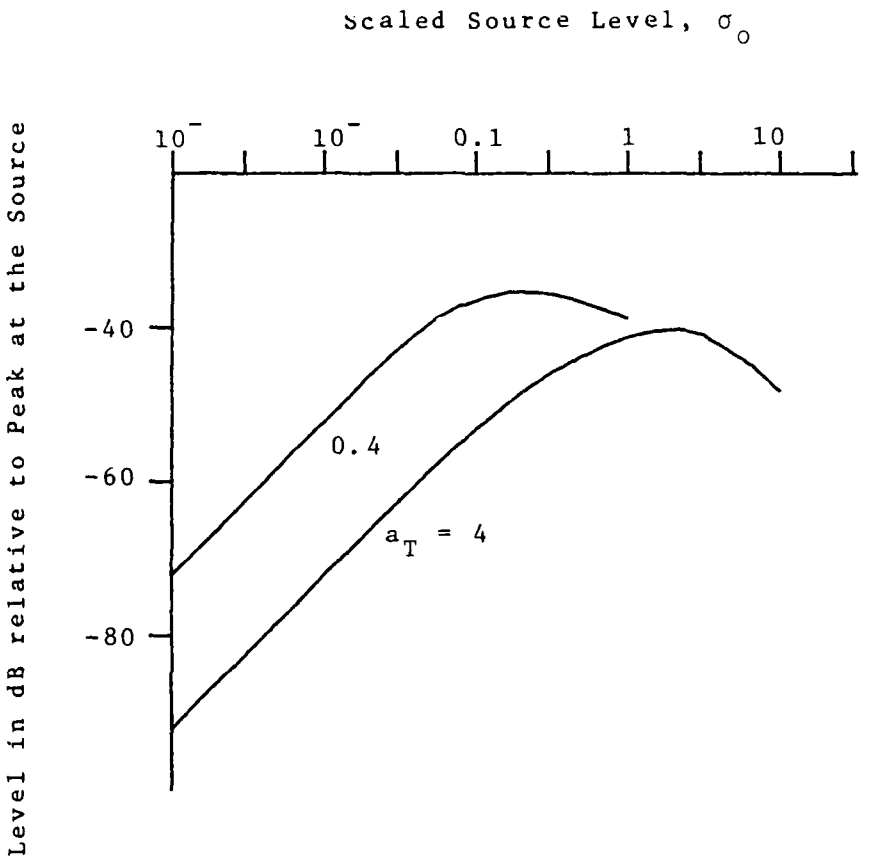

Figure 43. Difference-Frequency Extrapolated Source Level in dB Relative to the Peak of the Carriers at the Source for a Frequency Downshift Ratio of 10.5 and Selected Combined-Primary-Wave Attenuation Coefficients, a_T.

it requires a very small step size, $\Delta\sigma$, if the highest input frequency is a large multiple of the reference frequency or Fourier fundamental. If in addition the scaled source level, σ_o, is large, the number of iterations needed to reach the far field, $R>>1$, can become very large. The higher-quality interpolators which were tried in solutions to the lossless Burger's equation provided the same accuracy as the linear interpolator with a much larger step size until a discontinuity was formed, at which point instabilities would develop in the vicinity of the discontinuity. A method using a high-quality interpolator in regions where a discontinuity will not cause difficulties could improve the efficiency of the numerical solution.

The diffusion-in-frequency technique is implemented by means of an implicit Crank-Nicholson formula. This method is stable and efficient, and works well out to R on the order of 20, at which point the error in the level on axis is 0.3 dB and the largest errors in beamwidth are about 10 percent. The reason for the errors, which become very large at larger values of R, has been found to be the way in which the beam profile is sampled rather than the Crank-Nicholson formula itself. Other methods of solution, which are less efficient than the Crank-Nicholson technique but used the same beam sampling technique, have been tried and found subject to the same sampling problem. This problem is associated with the spreading of the radial coordinate system as it follows the beam propagating away from the source.

Spreading is characteristic of propagation from a source of finite extent. In the far field of a linear projector, the radial beamwidth is proportional to the range in the direction of propagation, and the angular beamwidth is constant. Therefore, if a given number of beam samples at a given spacing suffices near the source, then either the number of samples or the radial distance increment must be increased at larger distances if the edges of the beam are to remain visible as it propagates. The latter option, to increase the radial sample spacing when necessary, has been chosen for two reasons. First, the amount of storage available is fixed, and thus the number of samples cannot be allowed to grow without limit, and second, the time required for calculation increases rapidly as the number of radial samples increases.

The expansion of the radial sample spacing is done in the following way. The beam samples at the larger spacing are interpolated or selected from among those presently existing, which represent samples at a smaller sample spacing. The samples at expanded coordinates outside the domain previously defined are all assumed to be zero. This technique leads to progressive deterioration of the results beyond $R=20$, with considerable distortion of the beam shape by $R=50$.

Spherical spreading may be assumed to apply at large ranges. The manner in which this option is implemented in the numerical solution, although it works very well in

modeling linear diffraction, leads to difficulties in the nonlinear cases, as the phase distribution of the nonlinearly generated frequencies cannot be predicted a priori. In this thesis, the Crank-Nicholson formula is used exclusively for results confined to R less than about 30, and for longer ranges a transition zone, e. g., from R=10 to R=20, is defined and the Crank-Nicholson and imposed-spherical-spreading results are matched at the limits of the transition zone.

Advances in the nonlinear operator and in the expanding-grid diffraction technique should allow rapid and convenient numerical solution of many problems which are described by the second-order-nonlinear wave equation, more quickly and more accurately than the present implementation. The techniques of Zemanek (1971) and of Sziklas and Siegman (1974) should be useful points of departure in improving the numerical solution of the diffraction term. Zemanek demonstrated the usefulness of direct numerical integration of the diffraction integral. Although this method is not fast enough to be used in an iterative numerical solution, it might be used in performing the radial coordinate expansion which is required from time to time, without the errors associated with the present sampling technique. Sziklas and Siegman show a method for evaluating the diffraction integral in spherical coordinates by the use of weighted Fourier transforms, in a modified system of coordinates. These coordinates are such that a spherically

spreading beam will not change its shape or its relative size as it propagates.

REFERENCES

Bakhvalov, N.S., Ya. M. Zhileikin, E. A. Zablotskaya, and R. V. Kokhlov. Propagation of Finite-Amplitude Sound Beams in a Dissipative Medium.
Sov. Phys. Acoust., 1978, 24, Pp. 271-275.

_____, vide supra. Harmonic Generation in Sound Beams.
Sov. Phys. Acoust., 1979, 25, Pp. 101-106.

Banta, E. Lossless Propagation of One-Dimensional, Finite-Amplitude Sound Waves.
J. Math. Anal. Appl., 1965, 10, Pp. 166-173.

Bellman, R., S. P. Azen, and J. M. Richardson. On New and Direct Computational Approaches to Some Mathematical Models of Turbulence.
Quart. Appl. Math., 1965, 23, Pp. 55-67.

Beyer, R. T. Parameter of Nonlinearity in Fluids.
J. Acoust. Soc. Amer., 1960, 32, Pp. 719-721.

Blackstock, D. T. Connection Between the Fay and Fubini Solutions for Plane Sound Waves of Finite Amplitude.
J. Acoust. Soc. Amer., 1966, 39, Pp. 1019-1026.

Burgers, P. M. Advances in Applied Mechanics I.
Academic Press, New York, 1948, Pp. 171-199.

Cary, B. B. Nonlinear Losses Induced in Spherical Waves.
J. Acoust. Soc. Amer., 1967, 42, Pp. 88-92.

_____. Prediction of Finite-Amplitude Waveform Distortion with Dissipation and Spreading Loss.
J. Acoust. Soc. Amer., 1968, 43, Pp. 1364-1372.

_____. An Exact Shock Wave Solution to Burger's Equation for Parametric Excitation of the Boundary.
J. Sound Vib., 1973, 30, Pp. 455-464.

Cole, J.D. On a Quasi-Linear Parabolic Equation Occurring in Aerodynamics.
Quart. Appl. Math., 1951, 9, P. 225.

Cook, B. D. New Procedure for Computing Finite-Amplitude Distortion.
J. Acoust. Soc. Amer., 1962, 33, Pp. 941-946.

Earnshaw, S. On the Mathematical Theory of Sound.
Trans. Roy. Soc. (London), 1860, 150, Pp. 133-148.

REFERENCES (continued)

Eller, A. I. Application of the USRD Type E8 Transducer as an Acoustic Parametric Source.
J. Acoust. Soc. Amer., 1974, 56, Pp. 1735-1739.

Fay, R. D. Plane Sound Waves of Finite Amplitudes.
J. Acoust. Soc. Amer., 1931, 3, Pp. 222-241.

Fenlon, F. H. A Recursive Procedure for Computing the Nonlinear Spectral Interactions of Progressive Finite-Amplitude Waves in Nondispersive Fluids.
J. Acoust. Soc. Amer., 1971, 50, Pp. 1299-1312.

_____. An Extension of the Bessel-Fubini Series for a Multiple-Frequency CW Acoustic Source of Finite Amplitude.
J. Acoust. Soc. Amer., 1972, 51, Pp. 284-289.

_____ and F. S. McKendree. Axisymmetric Parametric Radiation -- A Weak Interaction Model.
J. Acoust. Soc. Amer., 1979, 66, Pp. 534-547.

Fox, F. E. and W. A. Wallace. Absorption of Finite-Amplitude Sound Waves.
J. Acoust. Soc. Amer., 1954, 26, Pp. 994-1006.

Fubini, E. Anomalies in the Propagation of Waves of Great Amplitude.
Alta Frequenza, 1935, 4, Pp. 530-581.

Goldstein, S. Lectures on Fluid Mechanics.
Wiley-Interscience, New York, 1960, Ch. 4.

Hopf, E. The Partial Differential Equation $u_t + uu_x = \mu_{xx}$.
Commun. Pure and Appl. Math., 1950, 3, P. 201.

Kokhlov, R. V. The Theory of Radio Shocks in Nonlinear Transmission Lines.
Radio Electronika, 1961, 6, Pp. 817-824

Kuznetsov, V. P. Equations of Nonlinear Acoustics.
Sov. Phys. Acoust., 1971, 16, Pp. 467-470.

Lamb, J. Thermal Relaxation in Liquids, in Physical Acoustics, Vol. 1 Part A, W. P. Mason, Ed.
Academic Press, New York, 1965.

Landau, L. D. and Lifshitz, E. M. Fluid Mechanics.
Addison-Wesley, New York, 1959.

REFERENCES (continued)

Lighthill, M. J. in Surveys in Mechanics, G. K. Batchelor and R. Davis, Eds.
Cambridge Univ. Press, 1956, Pp. 250-351.

Muir, T. G. and J. G. Willette. Parametric Acoustic Transmitting Arrays.
J. Acoust. Soc. Amer., 1972, 52, Pp. 1481-1486.

Naugolnyk'h, K., S. Soluyan, and R. V. Kokhlov. Spherical Waves of Finite Amplitude in a Viscous Thermally Conducting Medium.
Sov. Phys Acoust., 1963, 9, Pp. 42-46.

Pestorius, F. M. and D. T. Blackstock. Experimental and Theoretical Study of Propagation of Finite-Amplitude Sound in a Pipe.
Paper presented at the 85th meeting of the Acoustical Society of America, 11 April 1973, in Boston, Mass.
J. Acoust. Soc. Amer., 1973, 54, P. 302.

Riemann, B. Abhandlungen Göttingen, 1860, in Collected Works, Dover, New York, 1953, P. 156.

Rosen, G. B. Approximate Computation Solution of Nonlinear Parabolic Differential Equations, in Numerical Solutions of Nonlinear Partial Differential Equations, D. Greenspan Ed. Wiley, New York, 1966, Pp. 265-296.

Romanenko, E. Experimental Investigation of the Propagation of Finite-Amplitude Spherical Waves.
Sov. Phys. Acoust., 1959, 5, Pp. 100-104.

Sadchev, P. L. and P. Seebass. Propagation of Spherical and Cylindrical N-Waves.
J. Fluid Mech., 1973, 58, Pp. 179-205.

Shooter, J. A., T. G. Muir, and D. T. Blackstock. Acoustic Saturation of Spherical Waves in Water.
J. Acoust. Soc. Amer., 1974, 55, Pp. 54-62.

Sziklas, E. A. and A. E. Siegman. Diffraction Calculations Using Fast Fourier Transform Methods.
Proc. Inst. Elect. and Electronic Eng., 1974, 3, Pp. 410-412.

Westervelt, P. J. Parametric Acoustic Array.
J. Acoust. Soc. Amer., 1963, 35, Pp. 535-537.

Whitham, G. B. Linear and Nonlinear Waves.
Wiley, New York, 1974, Pp. 174-176.

REFERENCES (continued)

Zablotskaya, E. A., and R. V. Kokhlov. Quasiplane Waves in the Nonlinear Acoustics of Confined Beams. Sov. Phys. Acoust., 1969, 15, Pp. 35-40.

Zabusky, N. J. A Synergetic Approach to Problems of Nonlinear Wave Propagation and Interaction, in Proc. Symp. Nonlinear Partial Diff. Equations, W. Ames, Ed. Academic Press, New York, 1967, Pp. 223-258.

_____ and M. D. Kruskal. Interaction of Solitons in a Collisionless Plasma and the Recurrence of Initial States. Phys. Rev. Lett., 1965, 15, Pp. 240-243.

Zemanek, J. Beam Behavior within the Nearfield of a Vibrating Piston. J. Acoust. Soc. Amer., 1971, 49, Pp. 181-191.

APPENDIX

LARGE-FINITE-AMPLITUDE COMPUTER PROGRAM SOURCE LISTINGS

The following source listings give the code for the two programs used in deriving the numerical results presented in this thesis. Other versions differ only in slight details of the coding, usually in the format of output. The program named PRPGT2 is the main program which solves the plane-wave nonlinear propagation problem. The program named PRPGT8 solves the case of axisymmetric three-dimensional propagation. Both of these programs use the solution to Burger's equation expressed in Equation (3.4), as this was the formulation used to derive most of the results presented in this thesis.

```
C     PRPGT8 RELEASE 13.0 -- 8 MARCH     1981 --  F S MCKENDREE
C
C     FOR FURTHER INFORMATION CONTACT-----
C
C      FRANCIS S MCKENDREE
C      APPLIED RESEARCH LABORATORY
C      ROOM 123A
C      P O BOX 30
C      STATE COLLEGE, PA  16801
C
C      PPPPPP    RRRRRR    PPPPPP     GGGGG    TTTTTTT    88888
C      P     P   R     R   P     P   G     G      T      8     8
C      P     P   R     R   P     P   G            T      8     8
C      PPPPPP    RRRRRR    PPPPPP    G    GG      T       88888
C      P         R   R     P         G     G      T      8     8
C      P         R    R    P         G     G      T      8     8
C      P         R     R   P          GGGGG       T       88888
C
C     THIS PROGRAM SOLVES THE SECOND-ORDER-NONLINEAR PARABOLIC WAVE
C     EQUATION.
C
C     REVISION 4 FEBRUARY 1981 -- WAVEFORM PRINTOUT CAPABILITY ADDED
C     AT RANGES CALLED FOR IN 'SMAX' AND RADIAL COORDINATES GIVEN IN
C     ARRAY 'EPRNT'.  MAXIMUM 8 RADIAL VALUES AT EACH DISPLAY CYCLE;
C     SPECIFY RADIAL VALUE LESS THAN ZERO TO END DISPLAY AT GIVEN
C     RANGE, OR SMAX LESS THAN ZERO TO END ITERATIONS.
C
C     REVISION 8 MARCH 1981 -- (1) DELTA SIGMA MAY BE CHANGED AT THE
C     BEHEST OF THE USER TO THE NEW VALUE 'DSIGN' AT THE RANGE
C     'SIGCH'; (2) AN AXIAL BEAM LEVEL IS DEFINED AS THE MAXIMUM
C     FOUND WITHIN THE 1/2 DB WIDTH OF A LINEAR GAUSSIAN BEAM AT EACH
C     RANGE, AND IS DISPLAYED AND USED AS THE ZERO-DB LEVEL FOR THE
C     BEAM WIDTH CALCULATIONS.
C
      COMPLEX U0(256), UZ(256), W(256), CF, CFC, SPMD(129), AD, AF, SPI
      REAL ROOTV(3)/0.7071068,0.5,0.3162278/, BW(3,129), EPSV(41)
      REAL U(258,40), ATTF(129), DMAG(256), UR(256)
      REAL QLL/1.000/, RSPH/10.0/, RDIFF/0.300/
      INTEGER*4 TITLE(16)/'PROG','RAM ','PRPG','T8 R','ELEA','SE  ',
     1 '13.0','  8 ','MARC','H   ','198','1   ','    ','    ','  ','  '/
      INTEGER IDAT(2), JDAT(2)
      INTEGER IDIFFR(16), ISQ(256)
      LOGICAL NOLOSS, NORECD, NODIFF, NODISP, NOPRNT, NOSPM
      LOGICAL SW, S12, S11, S10, S09, NONONL, SW2
      REAL EPRNT(8), AXISLV(129)
C
C     SENSE SWITCH OPTIONS:
C        SWITCH 11 ON TO LIST INITIAL VARIABLES.
C        SWITCH 10 ON TO SUPPRESS DIFFRACTION.
C        SWITCH 9 ON TO ENABLE RECORDING OF DATA.
C        SWITCH 8 ON TO SUPPRESS LOSSES.
C        SWITCH 7 ON TO SUPPRESS DISPERSION.
C        SWITCH 6 ON TO SUPPRESS NONLINEAR OPERATOR.
C        SWITCH 5 ON TO READ QLL, RSPH, AND RDIFF
C        SWITCH 4 ON TO PRINT INITIAL WAVEFORMS.
C
C     SETUP.
C        FILE 'ICARD' IS USED FOR ALL SUBSEQUENT CONTROL INPUT.
C
      READ(5,8000) ICARD
      CALL SSWTCH(5,SW2)
      IF (SW2) READ(5,8020) QLL, RSPH, RDIFF
100   SW=.FALSE.
200   CALL SSWTCH(7,NODISP)
      CALL SSWTCH(8,NOLOSS)
      NOSPM=.FALSE.
      IF (NOLOSS .AND. NODISP) NOSPM=.TRUE.
      CALL SSWTCH(10,NODIFF)
      CALL SSWTCH(6,NONONL)
      CALL DATE(IDAT)
```

```
      CALL LINETT ( TITLE )
C
C     ZERO ATTF, DSP, AND SPMD ARRAYS
C
      CF=CMPLX(.0,0.)
      DO 150 I=1,129
      ATTF(I)=0.
      SPMD(I)=CF
150   CONTINUE
C
C     INPUT CONTROL VARIABLES:
C        INL - NUMBER OF WAVEFORM/RADIAN FREQUENCY SAMPLES; NUMBER OF
C              POINTS IN THE NON LINEAR OPERATOR.
C        IFB - NUMBER OF RADIAL SAMPLE POINTS
C        ICASE - CASE NUMBER FOR REFERENCE PURPOSES
C        NCOMP - NUMBER OF FOURIER COMPONENTS WHICH ARE TO BE ASSUMED TO
C        EXIST IN THE INPUT SIGNAL, FOR PURPOSES OF NORMALIZATION; IF
C        ZERO, NO NORMALIZATION IS PERFORMED.
C
      READ(ICARD,8000,END=7200) INL, IFB, ICASE, NCOMP
C
C        IDIFFR - ARRAY STORING THE DFT FREQUENCIES AT WHICH THE
C             NEED FOR RADIAL EXPANSION IS TO BE TESTED
C        DETERMINE THE NUMBER OF FREQUENCIES SELECTED IN 'ISF'.
C
      READ(ICARD,8000) IDIFFR
      K=1
      DO 300 I=1,16
      IF (IDIFFR(I) .LT. 0) GO TO 400
      K=I
300   CONTINUE
      K=16
400   ISF=K
C
C     REAL COEFFICIENTS -- SIGNAL DEPENDENT PARAMETERS:
C         SZER - SIGMA SUB ZERO, THE SACLED SOURCE LEVEL
C              (OR SCALED RAYLEIGH DISTANCE)
C         AZER - A SUB ZERO, THE ATTENUATION OF THE FUNDAMENTAL WITHIN
C              THE RAYLEIGH DISTANCE
C         B - WIDTH OF RADIAL SAMPLE SAPCE RELATIVE TO RHO SUB ZERO
C              NOTE: THE PROGRAM USES THE SIGNAL PARAMETERS TO DEDUCE
C              RHO SUB ZERO.
C
C     ALL REFERENCES TO THE 'FUNDAMENTAL' REFER TO THE SIGNAL WHICH
C     EXECUTES ONE CYCLE IN THE SAMPLE WINDOW AND WHICH HAS AN AMPLITUDE
C     EQUAL TO THE PEAK AMPLITUDE OF THE COMPOSITE SIGNAL.
C
C                    -- MEDIUM DEPENDENT PARAMETERS:
C         EMM - DISPERSION PARAMETER
C         TSUBC - RELAXATION TIME
C
C                    -- PROGRAM OPERATIONAL PARAMETERS:
C         SMAX - MAXIMUM SCALED RANGE OF INTEREST
C         DSIG - DELTA SIGMA, THE RANGE INCREMENT
C         DBLV - LEVEL OF THE BEAM EDGE RELATIVE TO THE CENTER WHICH WILL
C              TRIGGER RADIAL EXAPNSION OF COORDINATES
C         SIGCH - IF GREATER THAN ZERO, THE RANGE AT WHICH DELTA SIGMA
C              WILL BE CHANGED
C         DSIGN - NEW VALUE FOR DELTA SIGMA IF A CHANGE IS DESIRED
C         EPRNT - RADIAL DISTANCE(S) OF INTEREST FOR PRINTOUT
C
      READ(ICARD,8020) SZER, AZER, B
      READ(ICARD,8020) EMM, TSUBC
      READ(ICARD,8020) SMAX, DSIG, DBLV, SIGCH, DSIGN
      READ(ICARD,8020) (EPRNT(K),K=1,8)
C
      CALL LINENW( ICASE, IDAT )
C
C     GAMMA - SCALED ATTENUATION COEFFICIENT.
C     IRF - NUMBER OF RADIAN FREQUENCY COMPONENTS IN THE DFT.
```

```
C     DE - NORMALIZED RADIAL DISTANCE STEP, DELTA EPSILON.
C     DEPS - DELTA EPSILON, USED IN THE DIFFRA SUBROUTINE. THIS PARAMETER
C         FOLLOWS THE RADIAL EXPANSION OF THE COORDINATE SYSTEM.
C     STST - TEST SIGMA MAXIMUM; DECREMENTED TO ALLOW FOR ROUNDOFF ERROR
C     SLEVEL - SPECTRUM LEVEL NORMALIZATION FACTOR.
C     TESTCH - SIGMA VALUE FOR TEST PURPOSES AT WHICH DELTA SIGMA IS TO
C         BE CHANGED.  IF NO CHANGE IS DESIRED, IT IS TWICE THE MAXIMUM
C         RANGE OF INTEREST, WHICH IS NEVER ATTAINED.
C
      GAMMA = SZER/AZER
      IRF=INL/2
      JRF=IRF+1
      DE=B/FLOAT(IFB-1)
      DEPS=DE
      STST=SMAX-0.5*DSIG
      SLEVEL=1.
      IF (NCOMP .NE. 0.) SLEVEL=0.5*SQRT(FLOAT(INL))/FLOAT(NCOMP)
      TESTCH=2.*SMAX
      IF (SIGCH .GT. 0.) TESTCH=SIGCH-0.5*DSIG
C
C     IFILE - DSRN FOR PERMANENT RECORD
C     NZP - NUMBER OF RANGE STEPS BETWEEN OUTPUT CYCLES.
C     IFBO - NUMBER OF RADIAL DISTANCE STEPS BETWEEN PRINTOUT
C            CYCLES
C
      READ(ICARD,8000) IFILE, NZP, IFBO
      MZP=0
C
C     TITLE PAGE INFORMATION.
C
      WRITE(6,9010) INL, IFB, ISF
      WRITE(6,9170) (IDIFFR(KK),KK=1,ISF)
      WRITE(6,9020) SZER, AZER, SMAX, DSIG
      WRITE(6,9030) B, DE, GAMMA
      WRITE(6,9110) EMM, TSUBC
      WRITE(6,9330) DBLV, QLL, RSPH
      IF (NOLOSS) WRITE(6,9040)
      IF (NODISP) WRITE(6,9050)
      IF (NODIFF) WRITE(6,9210)
      IF (NOSPM) WRITE(6,9220)
      IF (NONONL) WRITE(6,9260)
      IF (SIGCH .GT. 0.) WRITE(6,9600) SIGCH, DSIGN
600   CALL LINENW(ICASE,IDAT)
C
C        SET UP THE INITIAL SIGNAL WAVEFORMS.
C
      CALL UNIT2D( U, 258, 40, INL, IFB, B, DMAG, DE, ICARD )
C
C     FILL IN THE EPSILON VALUE ARRAY
C
      FF=-DE
      DO 700 I=1,IFB
      FF=FF+DE
      EPSV(I)=FF
700   CONTINUE
C
C        COMPUTE THE ATTENUATION FACTORS
C
      CALL RALPHA(ATTF,INL,JRF,DSIG,GAMMA)
C                              NOTE: PURGE ATTF ARRAY OF VALUES LESS THAN
C                              1.E-8; THEY WOULD NOT CONTRIBUTE ANYWAY.
C
      DO 800 I=2,JRF
      IF (ATTF(I) .LT. 1.E-8) ATTF(I)=0.
800   CONTINUE
C
C        COMPUTE THE DISPERSION FACTORS.
C
      CALL CDISP( SPMD, JRF, DSIG, EMM, TSUBC )
C
```

```
C     CREATE SPECTRAL MODIFICATION ARRAY SPMD IF NECESSARY.
C
      DO 1000 I=1,JRF
      CFC=1.
      IF (NODISP) GO TO 900
      CFC=SPMD(I)
900   IF (NOLOSS) GO TO 1000
      CFC=CFC*ATTF(I)
1000  SPMD(I)=CFC
C
C    OUTPUT THE HEADER INFORMATION IF REQUESTED -- KREC COUNTS THE
C    RECORDS.
C
      CALL SSWTCH(9,NORECD)
      NORECD=.NOT.NORECD
      IF (NORECD) GO TO 1100
      KREC=1
      DF=DSIG*SZER
      WRITE(IFILE,8510) KREC,INL,IFB,ISF,ICASE,IRF,NZP,IFBO,IDIFFR
      WRITE(IFILE,8520) IDAT, NODISP, NOLOSS, NODIFF
      WRITE(IFILE,8500) SZER,AZER,SMAX,DSIG,B,EMM,TSUBC,DBLV,
     1                  GAMMA, DF, ATTF, SPMD
C
C     DISPLAY INITIAL FUNCTION IF REQUESTED.
C
1100  CALL SSWTCH(11,S11)
      IF (.NOT.S11) GO TO 1400
      CALL SSWTCH(4,SW)
      IF (.NOT.SW) GO TO 1300
      IDUM=3+(INL/10)
      DO 1200 I=1,IFB
      CALL LINECK(IDUM,ICASE,IDAT)
      WRITE(6,9070) I
      WRITE(6,9080) (U(KK,I),KK=1,INL)
1200  CONTINUE
      CALL LINENW(ICASE,IDAT)
1300  IDUM=3+(IRF/5)
      CALL LINECK(IDUM,ICASE,IDAT)
      WRITE(6,9120)
      WRITE(6,9130) (SPMD(KK),KK=1,IRF)
      CALL LINENW(ICASE,IDAT)
C
C     INITIALIZE FOR RANGE STEP PROCESSING.
C        DS - PARAMETER FOR NONLINEAR OPERATOR.
C        NSTEP - ITERATION COUNTER.
C        SIGMA - SCALED RANGE.
C        BFAC - BEAM WIDTH NORMALIZATION FACTOR.
C        EFAC - ENERGY NORMALIZATION FACTOR.
C
1400  DS=FLOAT(INL)*DSIG/6.2831853
      NSTEP=0
      SIGMA=0.
      BFAC=1.
      EFAC=1.
      FIF=FLOAT(INL)
C
C    INCREMENT SIGMA, THE SCALED RANGE.
C
1500  SIGMA=SIGMA+DSIG
C
C    SEE IF DELTA SIGMA MUST BE CHANGED -- IF SO, DO SO.
C
      IF (SIGMA .LT. TESTCH) GO TO 1550
      RSIGCH=DSIGN/DSIG
      DO 1520 J=1,JRF
      SPI=SPMD(I)
      SPMA=CABS(SPI)**RSIGCH
      SPMP=RSIGCH*ATAN2(AIMAG(SPI),REAL(SPI))
      SPMD(I)=SPMA*CMPLX(COS(SPMP),SIN(SPMP))
1520  CONTINUE
```

```
      TESTCH=2.*SMAX
      DSIG=DSIGN
      STST=SMAX-0.5*DSIG
C
C     AFTER (OR WITHOUT) CHANGE OF DELTA SIGMA, INCREMENT COUNTERS.
C
1550  NSTEP=NSTEP+1
      MZP=MZP+1
C
C     APPLY THE NONLINEAR OPERATOR WITHIN THIS LOOP TO EACH SET OF
C     WAVEFORMS SAMPLES AT THE RADIAL DISTANCE INCREMENT COUNTED BY J.
C
      DO 2400 J=1,IFB
C
C     MOVE THE J-TH RADIAL WAVEFORM SAMPLE INTO UR ARRAY.
C
      DO 1600 K=1,INL
      UR(K)=U(K,J)
1600  CONTINUE
      IF (NONONL) GO TO 1800
C
C     NON-LINEAR OPERATOR ON UR INTO UZ.
C
      DX=0.
      DO 1700 II=1,INL
      DX=DX+1.
      DL=DS*UR(II)
      XT=DX+DL
      IF (XT .LT. 0.) XT=XT+FIF
      M0=XT
      M1=M0+1
      DL=XT-FLOAT(M0)
      IF (M0 .LT. 1) M0=M0+INL
      IF (M0 .GT. INL) M0=M0-INL
      IF (M1 .LT. 1) M1=M1+INL
      IF (M1 .GT. INL) M1=M1-INL
      UZ(II)=UR(M0)*(1.-DL) + UR(M1)*DL
1700  CONTINUE
      GO TO 2000
C
C     BYPASS NONLINEAR OPERATOR.
C
1800  DO 1900 II=1,INL
      UZ(II)=CMPLX(UR(II),0.)
1900  CONTINUE
C
C     DIRECT FOURIER TRANSFORM -- TIME TO FREQUENCY DOMAIN.
C
2000  CALL DFT ( UZ, W, ISQ, INL, 2 )
C
C     APPLY ATTENUATION (DISPERSION).
C
      IF (NOSPM) GO TO 2200
      DO 2100 K=2,IRF
      UZ(K)=UZ(K)*SPMD(K)
2100  CONTINUE
      UZ(JRF)=UZ(JRF)*CABS(SPMD(JRF))
C
C     RESTORE RADIAN FREQUENCY SAMPLES TO U ARRAY.
C
2200  MM=0
      DO 2300 K=1,JRF
      MM=MM+1
      U(MM,J)=REAL(UZ(K))
      MM=MM+1
      U(MM,J)=AIMAG(UZ(K))
2300  CONTINUE
2400  CONTINUE
C
C     SEE IF DIFFRACTION IS TO BE BYPASSED.
```

```
C
      IF (NODIFF) GO TO 3100
C
C     PERFORM THE ZERO-FREQUENCY 'DIFFRACTION'
C     FIRST PICK UP THE ZERO-FREQUENCY (DFT CELL NUMBER 1) COMPONENTS;
C     THEN 'DIFFRACT' THEM USING SUBROUTINE DIFFRO.
C
      DO 2500 I=1,IFB
      UO(I)=CMPLX(U(1,I),U(2,I))
2500  CONTINUE
      CALL DIFFRO(UO,IFB,SIGMA,DSIG,SZER)
      DO 2550 I=1,IFB
      U(1,I)=REAL(UO(I))
      U(2,I)=AIMAG(UO(I))
2550  CONTINUE
C
C     PERFORM THE DIFFRACTION CALCULATION
C        FOR EACH OF THE RADIAN FREQUENCIES, SAMPLES AT EACH RADIAL
C        DISTANCE ARE MOVED INTO ARRAY UO.
C
      FI=0.
      LL=1
      MM=2
      DO 3000 I=2,JRF
      LL=LL+2
      MM=MM+2
      FI=FI+1.
C
C     SELECT THE RADIAL SAMPLES AT FREQUENCY I, MOVE INTO UO ARRAY.
C
      DO 2600 J=1,IFB
      UO(J)=CMPLX(U(LL,J),U(MM,J))
2600  CONTINUE
C
C     PERFORM THE DIFFRACTION.
C
      CALL DIFFRA ( UO, IFB, DSIG, DEPS, SZER, FI, QLL, SIGMA, RSPH )
C
C     RESTORE THE DIFFRACTED SPECTRAL SAMPLES TO THE U ARRAY.
C
      DO 2700 J=1,IFB
      U(LL,J)=REAL(UO(J))
      U(MM,J)=AIMAG(UO(J))
2700  CONTINUE
3000  CONTINUE
C
C     OUTPUT THE SPECTRUM IF REQUESTED.
C
3100  IF (MZP .NE. NZP) GO TO 3900
      IF (NORECD) GO TO 3300
      KREC=KREC+1
      WRITE(IFILE,8530) KREC,ICASE,DEPS,SIGMA
      DO 3200 JJ=1,IFB
      WRITE (IFILE,8540) (U(KK,JJ),KK=1,INL)
3200  CONTINUE
C
C     DETERMINE THE AXIAL LEVELS AND THE BEAM WIDTHS.
C
3300  LL=-1
      MM=0
      SST=SIGMA*0.2399/(SZER*DEPS)
      FRS=1.
      DO 3340 I=1,JRF
      LL=LL+2
      MM=MM+2
      IF (I .GT. 1) FRS=FLOAT(I-1)
      NAXIS=1+IFIX(SST/FRS)
      DO 3320 J=1,IFB
      DMAG(J)=SQRT(U(LL,J)**2+U(MM,J)**2)/SLEVEL
3320  CONTINUE
```

```
      FMAX=DMAG(1)
      IF (NAXIS .LT. 2) GO TO 3330
      CALL MAXFCN(DMAG,NAXIS,FMAX,INDEX)
3330  AXISLV(I)=FMAX
3340  CONTINUE
      LL=-1
      MM=0
      DO 3600 I=1,JRF
      LL=LL+2
      MM=MM+2
      DO 3400 J=1,IFB
      DMAG(J)=SQRT(U(LL,J)**2+U(MM,J)**2)/SLEVEL
3400  CONTINUE
      DO 3500 J=1,3
      TEST=AXISLV(I)*ROOTV(J)
      CALL FINDI(1,IFB,EPSV,DMAG,TEST,POINT,IDUM)
      BW(J,I)=0.
      IF (IDUM .EQ. 1) BW(J,I)=POINT*BFAC
3500  CONTINUE
3600  CONTINUE
      CALL LINECK(2,ICASE,IDAT)
      WRITE(6,9300) BFAC
C
C     BYPASS/FINISH SPECTRUM OUTPUT.
C
3900  KFBO=1
      JDUM=2+((IRF+9)/10)
C
C     SEE IF RADIAL COORDINATE EXPANSION IS REQUIRED.  EACH OF THE
C     NON-ZERO FREQUENCIES IN ARRAY IDIFFR IS TESTED TO SEE IF THE BEAM
C     HAS BROADENED SUFFICIENTLY TO REQUIRE RADIAL EXPANSION.
C
      IF ((SIGMA/SZER) .LT. RDIFF) GO TO 4500
      SQM=-1.
      DO 4100 I=1,ISF
      IDI=2*IDIFFR(I)+1
      SQS=SQRT((U(IDI,IFB)**2+U(IDI+1,IFB)**2)/
     1 (U(IDI,1)**2+U(IDI+1,1)**2))
      IF (SQS .GT. SQM) SQM=SQS
4100  CONTINUE
      IF (SQM .LT. DBLV) GO TO 4500
C
C     EXPAND RADIAL COORDINATES.
C
      LL=-1
      MM=0
      DO 4400 J=1,JRF
      LL=LL+2
      MM=MM+2
      DO 4200 K=1,IFB
      UO(K)=CMPLX(U(LL,K),U(MM,K))
4200  CONTINUE
      CALL EXPAND(UO,IFB,XFAC)
      DO 4300 K=1,IFB
      U(LL,K)=REAL(UO(K))
      U(MM,K)=AIMAG(UO(K))
4300  CONTINUE
4400  CONTINUE
C
C     ADJUST BFAC, THE BEAM WIDTH NORMALIZATION, DEPS, THE RADIAL
C     DISTANCE INCREMENT, AND EFAC, THE BEAM ENERGY NORMALIZATION
C     FACTOR, TO REFLECT THE EXPANDED RADIAL COORDINATES.
C
      BFAC=BFAC*XFAC
      DEPS=DEPS*XFAC
      EFAC=EFAC*SQRT(XFAC)
      IDUM=2
      CALL LINECK(IDUM,ICASE,IDAT)
      WRITE(6,9290) SIGMA, BFAC, EFAC
C
```

```
C     SELECT EACH OF THE IFB RADIAL SAMPLE SPECTRA IN SUCCESSION
C     AT SPATIAL FREQUENCY J.
C
4500  DO 5100 J=1,IFB
C
C     SELECT RADIAN FREQUENCY SAMPLES AT FREQUENCY K.
C
      LL=-1
      MM=0
      DO 4600 K=1,JRF
      LL=LL+2
      MM=MM+2
      UO(K)=CMPLX(U(LL,J),U(MM,J))
4600  CONTINUE
      NE=JRF
      NB=JRF+1
      DO 4650 K=NB,INL
      NE=NE-1
      UO(K)=CONJG(UO(NE))
4650  CONTINUE
      IF (J .NE. KFBO) GO TO 4800
      IF (MZP .NE. NZP) GO TO 4800
C
C     PICK UP THE MAGNITUDE
C
      DO 4700 KK=1,IRF
      DMAG(KK)=CABS(UO(KK))/SLEVEL
4700  CONTINUE
C
C     DISPLAY SPECTRUM IF REQUESTED.
C
      KFBO=KFBO+IFBO
      CALL LINECK(JDUM,ICASE,IDAT)
      WRITE(6,9190) J, NSTEP
      WRITE(6,9080) (DMAG(KK),KK=1,IRF)
C
C     INVERSE FOURIER TRANSFORM THE DATA AT EACH RADIAL SAMPLE DISTANCE.
C     THIS SECTION CONVERTS THE NON-NEGATIVE FREQUENCY COMPONENTS
C     STORED IN 'U' INTO REAL WAVEFORMS AT EACH OF THE RADIAL DISTANCES.
C
4800  CALL DFT(UO, W, ISQ, INL, -2 )
C
C     RESTORE THE WAVEFORMS INTO THE U ARRAY.
C
4900  DO 5000 K=1,INL
      U(K,J)=REAL(UO(K))
5000  CONTINUE
5100  CONTINUE
C
C     OUTPUT THE AXIAL LEVELS AND THE BEAM WIDTHS.
C
      IF (MZP .NE. NZP) GO TO 5200
      IDUM=4+(JRF+9)/10
      CALL LINECK(IDUM,ICASE,IDAT)
      WRITE(6,9610) NSTEP, SIGMA
      WRITE(6,9080) (AXISLV(KK),KK=1,JRF)
      IDUM=2+(JRF+9)/10
      CALL LINECK(IDUM,ICASE,IDAT)
      WRITE(6,9140)
      WRITE(6,9080) (BW(1,KK),KK=1,JRF)
      CALL LINECK(IDUM,ICASE,IDAT)
      WRITE(6,9150)
      WRITE(6,9080) (BW(2,KK),KK=1,JRF)
      CALL LINECK(IDUM,ICASE,IDAT)
      WRITE(6,9160)
      WRITE(6,9080) (BW(3,KK),KK=1,JRF)
C
C     RETURN FOR NEXT RANGE STEP.
C
5200  R=SIGMA/SZER
```

```
      IF (SIGMA .GE. STST) GO TO 7000
      IF (MZP .GE. NZP) MZP=0
      CALL LINECK(1,ICASE,IDAT)
      WRITE(6,9060) NSTEP, SIGMA, R
      GO TO 1500
C
C     PRINT WAVEFORM(S) IF REQUESTED;  SEE IF TASK IS FINISHED.
C
7000  CALL LINENW ( ICASE, IDAT )
      BB=BFAC*B
      IDUM=(INL/10)+4
      DO 7080 I=1,8
      EPI=EPRNT(I)
      IF (EPI .LT. 0.) GO TO 7120
      IF (EPI .GT. BB) GO TO 7120
      EO=1.+(EPI/DEPS)
      LE=IFIX(EO)
      FEO=EO-FLOAT(LE)
      GEO=1.-FEO
      ME=LE+1
      DO 7040 J=1,INL
      DMAG(J)=U(J,LE)*GEO+U(J,ME)*FEO
7040  CONTINUE
      CALL LINECK ( IDUM, ICASE, IDAT )
      WRITE(6,9240) NSTEP, SIGMA, R, EPI
      WRITE(6,9080)
      WRITE(6,9080) (DMAG(K),K=1,INL)
7080  CONTINUE
7120  READ(ICARD,8020) SMAX
      IF (SMAX .LT. 0.) GO TO 7160
      READ(ICARD,8020) (EPRNT(K),K=1,8)
      STST=SMAX-0.5*DSIG
      GO TO 1500
7160  IF (NORECD) GO TO 100
      KREC=-1
      WRITE(IFILE,8530) KREC,ICASE,DEPS,SIGMA
      GO TO 100
7200  WRITE(6,9090)
      STOP
C
C     INPUT FORMATS.
C
8000  FORMAT(16I5)
8020  FORMAT(8F10.1)
C
C     OUTPUT FORMATS FOR DATA STORAGE FILE.
C
8500  FORMAT(1P8E10.3)
8510  FORMAT(10I8)
8520  FORMAT(2A4,3L1)
8530  FORMAT(2I10,1P6E10.3)
8540  FORMAT(1P32E10.3)
C
C     OUTPUT FORMATS FOR PRINTED RECORD.
C
9010  FORMAT('0INL',I4,'     IFB',I3,'     ISF',I3)
9020  FORMAT('0  SZER',1PE12.3,'      AZER',E12.3,'      SMAX',E12.3,
     1       'DSIG',E12.3)
9030  FORMAT('0     B',1PE12.3,'        DE',E12.3,'     GAMMA',E12.3)
9040  FORMAT('0LINEAR LOSSES SUPPRESSED.')
9050  FORMAT('0DISPERSION SUPPRESSED.')
9060  FORMAT(' STEP',I5,'    SIGMA',1PE12.3,'    R',E12.3)
9070  FORMAT('0INITIAL FUNCTION AT RADIAL STEP',I4)
9080  FORMAT(' ',1P10E12.3)
9090  FORMAT('0PROGRAM REACHED NORMAL TERMINATION.')
9110  FORMAT('0   EMM',1PE12.3,'      TSUBC',E12.3)
9120  FORMAT('0 SPECTRUM MODIFICATION ARRAY (ATTENUATION/DISPERSION):')
9130  FORMAT(' ',1P10E13.4)
9140  FORMAT('0 3 DB BEAM WIDTHS:')
9150  FORMAT('0 6 DB BEAM WIDTHS:')
```

```
9160  FORMAT('010 DB BEAM WIDTHS:')
9170  FORMAT('0TEST FOR DIFFRACTION:',16I5)
9190  FORMAT('0 SPECTRUM SAMPLE',I4,' AFTER OPERATOR STEP',I5)
9210  FORMAT('0DIFFRACTION OPERATOR SUPPRESSED.')
9220  FORMAT('0RADIAN FREQUENCY SPECTRUM MODIFICATION SUPPRESSED.')
9240  FORMAT('0STEP',I5,'   SIGMA, R:',1P2E12.3,';   RADIUS:',
     1 E12.3)
9260  FORMAT('0NONLINEAR OPERATOR SUPPRESSED.')
9290  FORMAT('0AT SIGMA=',1PE9.2,' RADII EXPANDED TO',E9.2,' AND BEAM EN
     1ERGY TO',E9.2)
9300  FORMAT('0CURRENT BFAC',1PE12.4)
9330  FORMAT('0  DBLV',1PE12.3,'       QLL',E12.3,'      RSPH',E12.3)
9600  FORMAT('0AT SIGMA=',1PE12.4,' DELTA SIGMA BECOMES',E12.4)
9610  FORMAT('0AXIAL BEAM LEVELS AT STEP',I5,'  SIGMA',1PE12.4)
      END


      SUBROUTINE DIFFRO ( U0, N, SIGMA, DSIG, SZER )
C
C     THIS SUBROUTINE PERFORMS THE 'ZERO-FREQUENCY' DIFFRACTION FOR
C    THE PRPGT8 NONLINEAR WAVE EQUATION SOLUTION PROGRAM.
C
C              RATIONALE:
C    SPHERICAL OR 1/R SPREADING IS IMPOSED.  THE DIFFUSION-IN-FREQUENCY
C    ASSUMES THE FORM OF LAPLACE'S EQUATION (DEL SQUARED PHI = 0) IN THE
C    LIMIT AS FREQUENCY GOES TO ZERO.  A SOLUTION TO LAPLACE'S EQUATION
C    IS 1/R.
C
C     DEFINITIONS OF ARGUMENTS
C        U0 - COMPLEX DATA ARRAY TO BE 'DIFFRACTED'
C        N - NUMBER OF POINTS IN U0
C        SIGMA - SCALED RANGE ATTAINED
C        DSIG - SCALED STEP SIZE
C        SZER - SCALED DIFFRACTION PARAMETER (RAYLEIGH DISTANCE)
C
C        SOLI DEO GLORIA 5 XI 1979 -- F S MCKENDREE
C
      COMPLEX F, U0(N)
      COMPLEX UQ(50)
C
C    RN - NEW RANGE
C    RO - OLD RANGE
C    F - RANGE DECREMENT FACTOR
C
      RN=SIGMA/SZER
      RO=(SIGMA-DSIG)/SZER
      F=CSQRT(CMPLX(1.,-RO)/CMPLX(1.,-RN))
C
C    APPLY RANGE DECREMENT FACTOR TO THE DATA
C
      DO 1000 I=1,N
      UQ(I)=U0(I)*F
1000  CONTINUE
C
C    SPREAD THE DATA SPHERICALLY
C
      DG=(1.+SIGMA)/(1.+SIGMA+DSIG)
      EG=0.
      U0(1)=UQ(1)
      DO 2000 I=2,N
      EG=EG+DG
      J=IFIX(EG)+1
      K=J+1
      FG=EG-FLOAT(J-1)
      HG=1.-FG
      U0(I)=UQ(J)*HG+UQ(K)*FG
2000  CONTINUE
      RETURN
      END
```

```
      SUBROUTINE EXPAND ( P, N, XFAC )
C
C     100 PERCENT RADIAL EXPANSION -- INVOLVES NO INTERPOLATION.
C
      COMPLEX P(N), CF/(0.,0.)/
      M=1
      K=1
1000  M=M+2
      IF (M .GT. N) GO TO 2000
      K=K+1
      P(K)=P(M)
      GO TO 1000
2000  K=K+1
      IF (K .GT. N) GO TO 8888
      DO 3000 I=K,N
      P(I)=CF
3000  CONTINUE
8888  XFAC=2.
      RETURN
      END


      SUBROUTINE MAXFCN ( F, N, FMAX, INDEX )
C
C     F - REAL ARRAY TO BE SEARCH FOR MAXIMUM
C     N - LARGEST SAMPLE NUMBER TO BE SEARCHED
C     FMAX - RETURNED AS THE LARGEST VALUE IN F
C     INDEX - RETURNED  S THE LOCATION OF FMAX IN F
C
C               SOLI DEO GLORIA 8 III 1981 -- F S MCKENDREE
C
      REAL F(N)
      FMAX = F(1)
      INDEX=1
      IF (N .LT. 2) GO TO 8888
      DO 1000 I=2,N
      IF (F(I) .LE. FMAX) GO TO 1000
      FMAX=F(I)
      INDEX=I
1000  CONTINUE
8888  RETURN
      END


      SUBROUTINE UNIT2D ( U, IN, IF, INL, IFB, RHOZER, RHO, DR, ICARD )
C
C     THIS SUBROUTINE PROVIDES INITIALIZATION OF THE DATA ARRAY IN THE
C     TIME DOMAIN AS REQUIRED BY PRPGT8.  THREE BEAM TYPES ARES PROVIDED,
C     INCLUDING THOSE USED BY BAKHVALOV ET. AL.
C
C     SOLI DEO GLORIA 21 DECEMBER 1979 -- F S MCKENDREE
C
C     DEFINITIONS OF ARGUMENTS:
C         U - REAL ARRAY OF TWO DIMENSIONS IN BY IF, WHICH WILL CONTAIN
C               THE ORIGINAL TIME WAVEFORMS UPON RETURN.
C         IN,IF - DIMENSIONS OF THE U ARRAY.
C         INL - NUMBER OF SAMPLES OF THE WAVEFORM AT A GIVEN RADIAL
C               DISTANCE -- I. E., THE NUMBER OF SAMPLE ROWS ALONG THE
C               DIRECTION OF PROPAGATION.
C         IFB - NUMBER OF SAMPLES ACROSS THE WIDTH OF THE BEAM AT EACH
C               TIME SAMPLE -- I. E., THE NUMBER OF SAMPLE COLUMNS ACROSS
C               THE RADIAL DIRECTION.
C     RHOZER - RHO SUB ZERO, NO LONGER USED BUT INCLUDED FOR PURPOSES
C               OF COMPATABILITY WITH EARLIER ROUTINES.
C         RHO - REAL ARRAY USED FOR TEMPORARY STORAGE OF THE BEAM PROFILE
C               AMPLITUDE.
C         DR - RADIAL DISTANCE STEP SIZE.
C         ICARD - DSRN TO BE USED FOR CONTROL INPUT TO 'UNIT2D'.
C
      REAL RHO(IF), U(IN,IF)
```

```
C
C     ZERO THE U ARRAY.
C
      DO 500 I=1,IF
      DO 500 J=1,IN
      U(J,I)=0.
500   CONTINUE
C
C     READ A DATA 'CARD'.  THIS CARD SPECIFIES THE FREQUENCY, AMPLITUDE,
C     AND PHASE OF UP TO TWO COMPONENTS.
C         F1 LESS THAN ZERO CAUSES THE SUBROUTINE TO NORMALIZE THE
C     SAMPLE SET TO UNIT PEAK AMPLITUDE AND RETURN.
C         IF THE PHASE IS IN THE RANGE 0 TO 360 DEGREES, A GAUSSIAN BEAM
C     PROFILE IS USED; IF IN THE RANGE 360 TO 720 DEGREES, A BOXCAR PROFI
C     LE IS USED; AND IF IN THE RANGE 720 TO 1080 DEGREES, A FOURTH ORDER
C     POLYNOMIAL IS USED.
C
      WRITE(6,9100) ICARD
      WRITE(6,9000)
1000  READ(ICARD,8000) F1, A1, P1, F2, A2, P2
      IF (F1 .LT. 0.) GO TO 4000
      R=-DR
      IF (P1 .LT. 360.) GO TO 1200
      IF (P1 .LT. 720.) GO TO 1800
      IF (P1 .LT. 1080.) GO TO 2200
C
C     GAUSSIAN BEAM -- DEFAULT OR PHASE < 360
C
1200  WRITE(6,9020)
      DO 1500 I=1,IFB
      R=R+DR
      RHO(I)=EXP(-(R*R))
1500  CONTINUE
      GO TO 3000
C
C     UNIFORM EXCITATION TO R=1 -- PHASE < 720
C
1800  P1=P1-360.
      WRITE(6,9040)
      DO 2000 I=1,IFB
      R=R+DR
      RHO(I)=1.
      IF (R .GT. 1.) RHO(I)=0.
2000  CONTINUE
      GO TO 3000
C
C     FOURTH ORDER POLYNOMIAL BEAM
C
2200  P1=P1-720.
      WRITE(6,9060)
      DO 2500 I=1,IFB
      R=R+DR
      RHO(I)=1./((1.+R*R)**2)
2500  CONTINUE
C
C     HAVING THE BEAM PROFILE IN R, INSERT THE FREQUENCY COMPONENTS.
C
3000  TAU=6.2831853/FLOAT(INL)
      WRITE(6,9080) F1, A1, P1, F2, A2, P2
      P1=P1*0.01745329
      P2=P2*0.01745329
      T=-TAU
      DO 3500 I=1,INL
      T=T+TAU
      S=A1*COS(F1*T+P1)+A2*COS(F2*T+P2)
      DO 3200 J=1,IFB
      U(I,J)=U(I,J)+S*RHO(J)
3200  CONTINUE
3500  CONTINUE
      IF (F2 .LT. 0.) GO TO 4000
```

```
      GO TO 1000
C
C     NORMALIZE TO UNIT PEAK AMPLITUDE -- FIRST FIND THE MAXIMUM, THEN
C     ADJUST THE AMPLITUDES ACCORDINGLY.
C
4000  AMAX=-1.
      DO 4400 I=1,INL
      DO 4200 J=1,IFB
      A=ABS(U(I,J))
      IF (A .GT. AMAX) AMAX=A
4200  CONTINUE
4400  CONTINUE
      AMAX=1./AMAX
      DO 4800 I=1,INL
      DO 4600 J=1,IFB
      U(I,J)=U(I,J)*AMAX
4600  CONTINUE
4800  CONTINUE
      RETURN
8000  FORMAT(8F10.1)
9000  FORMAT('0UNIT2D       F1',10X,'A1',10X,'P1',10X,'F2',10X,'A2',10X,
     1 'P2')
9020  FORMAT('0GAUSSIAN')
9040  FORMAT('0UNIFORM')
9060  FORMAT('04TH ORDER')
9080  FORMAT('0',10X,1P6E12.3)
9100  FORMAT('0DATA TAKEN FROM FILE',I5)
      END


      SUBROUTINE FIND1 ( NB, NE, ORDI, ABSC, ROOT, POINT, ITEST )
C
C     'ROOT' FINDING SUBROUTINE.  THE ARRAY ABSC IS SEARCHED BETWEEN
C     ELEMENTS NB AND NE TO FIND THE VALUE ROOT.  POINT IS RETURNED
C     AS THE LINEARLY-INTERPOLATED VALUE, DETERMINED FROM ARRAY ORDI,
C     AT WHICH THE FUNCTION IN ABSC WILL ATTAIN THE VALUE ROOT.  ITEST
C     IS RETURNED AS ZERO IF NO SUCH VALUE IS FOUND AND AS 1 IF SUCH
C     A VALUE IS FOUND.
C
C     DESIGNED/CODED BY F S MCKENDREE, 31 V 1978.
C
      REAL ORDI(NE), ABSC(NE)
C
C     DETERMINE IF 'ROOT' IS ATTAINED.
C
      K=NB
      AOLD=ABSC(K)
 1000 K=K+1
      ANEW=ABSC(K)
      IF (AOLD .LE. ROOT .AND. ANEW .GE. ROOT) GO TO 2000
      IF (AOLD .GE. ROOT .AND. ANEW .LE. ROOT) GO TO 2000
      AOLD=ANEW
      IF (K .LT. NE) GO TO 1000
      POINT=0.
      ITEST=0
 8888 RETURN
C
C     FIX VALUE OF 'POINT' CORRESPONDING TO 'ROOT'.
C
 2000 ITEST=1
      IF (ANEW .EQ. AOLD) GO TO 3000
      ORDO=ORDI(K-1)
      ORDN=ORDI(K)
      POINT = ORDO + (((ROOT-AOLD)/(ANEW-AOLD))*(ORDN-ORDO))
      GO TO 8888
C
C     EQUAL AMPLITUDES BOTH EQUAL TO ROOT.
C     CHOOSE A VALUE FOR POINT MIDWAY IN THE CORRESPONDING ORDINATES.
C
 3000 POINT=(ORDI(K-1)+ORDI(K))*0.5
```

```
      GO TO 8888
      END


      SUBROUTINE LINECK ( LINES, ICASE, IDAT )
C
C     CLEAN PRINTER CONTROLLER.
C     REVISED 9 OCTOBER 1978 TO INCLUDE TITLE ARRAY.
C
C      LINECK(LINES,ICASE,IDAT) - DETERMINES IF 'LINES' MAY BE ADDED
C     TO THE CURRENT PAGE; IF NOT, INCREMENT PAGE COUNTER AND MOVE TO
C     HEAD OF NEXT PAGE, WRITING THE TITLE ARRAY, 'ICASE' AND THE DATE
C     FIELD 'IDAT'.
C
C      LINETT(DUMMY) - MOVE THE TITLE ARRAY POINTED TO BY 'DUMMY' INTO
C     THE 'TITLE' ARRAY.
C
C      LINENW(ICASE,IDAT) - PAGE IMMEDIATELY, DISPLAYING 'ICASE' AND
C     'IDAT'; LINE COUNTER 'LOCAL' BECOMES 2.
C
C     SOLI DEO GLORIA 5 OCTOBER 1978.
C
      INTEGER NPAGE/0/, LOCAL/60/, IDAT(2)
      INTEGER TITLE(16), DUMMY(16)
C
C                                SEE IF PAGING IS REQUIRED -- IF SO, PAGE
      LOCAL=LOCAL+LINES
      IF (LOCAL .LT. 60) GO TO 1000
      LOCAL=LINES+2
  700 NPAGE=NPAGE+1
      WRITE(6,9000) TITLE, ICASE, IDAT, NPAGE
 1000 RETURN
C                                SET UP THE TITLE FIELD
      ENTRY LINETT(DUMMY)
      DO 2000 I=1,16
      TITLE(I)=DUMMY(I)
 2000 CONTINUE
      GO TO 1000
C                                PAGE IMMEDIATELY
      ENTRY LINENW ( ICASE, IDAT )
      LOCAL=2
      GO TO 700
C                                THE TITLE'S FORMAT
C
 9000 FORMAT('1',16A4,' CASE',I8,'   DATE ',2A4,'   PAGE',I 4)
      END


      SUBROUTINE RALPHA(ATTF,INL,IRF,DSIGMA,GAMMA)
C
C     COMPUTE THE ATTENUATION FACTORS FOR SPECIFIED INPUT.
C
      REAL ATTF(IRF)
C
      ATTF(1)=1.
      K=0
      DSG=DSIGMA/GAMMA
      DO 1000 I=2,IRF
      K=K+1
      E=-FLOAT(K*K)*DSG
      IF (E .LT. -60.) E=-60.
      ATTF(I)=EXP(E)
 1000 CONTINUE
      RETURN
      END


      SUBROUTINE CDISP ( DSP, IRF, DSIG, EMM, TSUBC )
C
C     EVALUATE THE DISPERSION COEFFICIENT.
```

```
C        DSP - ARRAY TO STORE THE  COEFFICIENTS.
C        INL - NUMBER OF FOURIER COMPONENTS.
C        DSIG - RANGE STEP PARAMETER.
C        EMM - DISPERSION PARAMETER.
C        TSUBC - RELAXATION PARAMETER.
C
C     SOLI DEO GLORIA OCTOBER MCMLXXVIII.
C
      COMPLEX DSP(IRF), CA
C
      DSP(1)=1.
      FI=0.
      FT=0.
      DM=-DSIG*EMM
      DO 1000 I=2,IRF
      FI=FI+1.
      FT=FT+TSUBC
      CA=DM*(F I**2)/CMPLX(1.,FT)
      IF (CABS(CA) .LT. 1.E-6) GO TO 800
      DSP(I) = CEXP(CA)
      GO TO 1000
 800  DSP(I)=1.
1000  CONTINUE
      DSP(IRF)=REAL(DSP(IRF))
      RETURN
      END


      SUBROUTINE DIFFRA(W,N,DS,DEPS,SZER,FI,QLL,SIGMA,RSPH)
C
C     THIS SUBROUTINE PERFORMS THE DIFFUSION-IN-FREQUENCY CALCULATIONS
C     BY MEANS OF A GAUSS ELIMINATION SOLUTION OF THE IMPLICIT CRANK-
C     NICHOLSON FORMULATION OF THE PROBLEM.
C
C              SOLI DEO GLORIA 29 OCTOBER 1980 -- F S MCKENDREE
C
C     ADDITION 6 NOVEMBER 1980 -- CODE FOR SPHERICAL SPREADING ADDED
C         AFTER THE DESIGN OF THIS DATE.
C
      COMPLEX W(N), P(50), AJ(50), BJ(50), CJ(50), AF(50), SF(50), D(50)
      COMPLEX A1, A2, B1, B2, R1, A3, A4, A5
      COMPLEX CG
      REAL B/1./, C/2./
      REAL SS1/1.065/, SS2/7.000/, SS3/1.750/, SS4/2.000/
C
C     TEST RANGE FOR SPHERICAL SPREADING.
C
      RG=SIGMA/(SZER*FI)
      IF (RG .GT. RSPH) GO TO 5000
C
C     SET UP NUMBER OF ITERATIONS.
C
      T=C*DS*QLL/(0.5*FI*SZER*(DEPS**2))
      NT=IFIX(T)
      IF (NT .LT. 1) NT=1
      DSIG=0.25*DS/FLOAT(NT)
C
C     SET UP FOR ITERATION.
C
      A1=CMPLX(0.,DSIG/(2.*FI*SZER*(DEPS**2)))
      A2=CMPLX(0.,B*DSIG/(4.*SZER*FI*DEPS))
      A3=1.+2.*A1
      A4=2.*C*A1
      A5=1.+A4
      CJ(1)=-2.*C*A1
      BJ(1)=1.+CJ(1)
      B2=1.-2.*A1
      DO 1000 I=2,N
      BJ(I)=B2
      FJ=1.+B/(2.*FLOAT(I-1))
```

```
      CJ(I)=-A1*FJ
      AJ(I)=A1*(FJ-2.)
1000  CONTINUE
C
C     PERFORM THE FINITE-DIFFERENCE EVALUATION AS MANY TIMES AS IS
C     REQUIRED.
C
      DO 3500 II=1,NT
      DO 1500 I=1,N
      P(I)=W(I)
1500  CONTINUE
      P(N+1)=1.5*P(N)-0.5*P(N-1)
      D(1)=W(1)*A5-W(2)*A4
      EPS=0.
      DO 2000 I=2,N
      EPS=EPS+DEPS
      D(I)=P(I-1)*(-A1+A2/EPS)+P(I)*A3+P(I+1)*(-A1-A2/EPS)
2000  CONTINUE
      AF(1)=BJ(1)
      SF(1)=D(1)
      DO 2500 I=2,N
      R1=AJ(I)/AF(I-1)
      AF(I)=BJ(I)-R1*CJ(I-1)
      SF(I)=D(I)+R1*SF(I-1)
2500  CONTINUE
C
C     ON EVALUATING THE NEW TIME ROW, RESTORE THE SAMPLES TO THE W ARRAY.
C
      W(N)=SF(N)/AF(N)
      K=N
      DO 3000 I=2,N
      K=K-1
      W(K)=(SF(K)+CJ(K)*W(K+1))/AF(K)
3000  CONTINUE
3500  CONTINUE
      IF (RG .LT. 0.5*RSPH) GO TO 8888
8888  RETURN
C
C     SPHERICAL SPREADING BY IMPOSITION -- FIRST
C     APPLY THE RANGE DECREMENT CG, THEN INTERPOLATE TO ACCOUNT FOR
C     THE RECTANGULAR SAMPLE GRID.
C
5000  RI=DS/(SZER*FI)
      CG=CMPLX(1.,RG)/CMPLX(1.,RG+RI)
      DO 5200 I=1,N
      P(I)=W(I)*CG
5200  CONTINUE
      W(1)=P(1)
      DG=RG/(RG+RI)
      IF (RG .LE.  (SS3*RSPH)) DG=RG/(RG+SS4*RI)
      IF (RG .LE.  (SS1*RSPH)) DG=RG/(RG+SS2*RI)
      EG=0.
      DO 5500 I=2,N
      EG=EG+DG
      J=IFIX(EG)+1
      K=J+1
      FG=EG-FLOAT(J-1)
      HG=1.-FG
      W(I)=P(J)*HG+P(K)*FG
5500  CONTINUE
      GO TO 8888
      END


      SUBROUTINE SSWTCH(N,V)
      LOGICAL V,S(13)/.FALSE.,.FALSE.,.FALSE.,.FALSE.,.FALSE.,
     1                .TRUE., .FALSE.,.TRUE., .FALSE.,
     2                .FALSE.,.FALSE.,.TRUE., .FALSE./
      L=N+1
      V=.FALSE.
```

```
      IF ((L .GT. 13) .OR. (L .LT. 1)) GO TO 8888
      V=S(L)
8888  RETURN
      END


      SUBROUTINE DFT ( Z, W, ISQ, N, NC )
C
C        DISCRETE FOURIER TRANSFORM SUBROUTINE WITH PASSED ARGUMENTS
C
C     THIS SUBROUTINE IS OPTIMIZED FOR RAPID SEQUENTIAL PERFORMANCE
C     OF SUCCESSIVE DIRECT AND INVERSE TRANSFORMS OF THE SAME SIZE.
C
C     DEFINITIONS OF  ARGUMENTS:
C        Z - ON CALL, INPUT COMPLEX SEQUENCE; ON RETURN, OUTPUT
C              COMPLEX SEQUENCE.
C        W - COMPLEX WORKING ARRAY; THESE VALUES MUST NOT BE CHANGED
C              BETWEEN CALLS TO THE SAME SIZE DFT.
C        ISQ - INTEGER ARRAY  USED TO STORE THE SEQUENCE NUMBERS
C              WHICH ARE EXCHANGED IN THE BIT REVERSAL.
C        N - NUMBER OF POINTS IN THE FOURIER TRANSFORM; MINIMUM
C              LENGTH OF THE Z, W, AND ISQ ARRAYS.
C        NC - CONTROL INTEGER VARIABLE; LESS  THAN ZERO FOR INVERSE
C              TRANSFORM, OTHERWISE DIRECT IS ASSUMED.
C
C     THE MINIMUM ALLOWABLE N IS 8 AND THE MAXIMUM IS 4096; THE VALUE
C     OF N MUST BE AN INTEGER POWER OF 2.
C
      COMPLEX C, D, Z(N), W(N)
      REAL*8 CO, SI, CD, SD, SS, ARG, SO
      INTEGER JU(12), JD(12), ISQ(N), OLDN/-9999/
C
C     DETERMINE IF THE VALUE OF N CALLED FOR IS CURRENT.
C     IF SO, CHOOSE DIRECT TRANSFORM (IOFS=0) OR INVERSE TRANSFORM.
C
      IF (OLDN .NE. N) GO TO 7000
1000  IOFS=0
      IF (NC .LT. 0) IOFS=N2
C
C     FIRST DFT LOOP; MULTIPLY BY AMPLITUDE FACTOR AND TAKE THE
C     SUM AND DIFFERENCE.  SINCE THE COMPLEX EXPONENTIAL SAMPLE
C     FOR THIS LOOP IS 1, COMPLEX MULTIPLICATION IS NOT REQUIRED.
C
3000  DO 3100 I=1,N2
      II=I+N2
      C=Z(I)
      D=Z(II)
      C=C*AMPL
      D=D*AMPL
      Z(I)=C+D
      Z(II)=C-D
 3100 CONTINUE
C
C     BIT-REVERSED RESEQUENCING OF THE Z ARRAY.  USE THE VALUES
C     STORED IN ISQ TO CONTROL THE SEQUENCING.
C
      IN2=N2+1
      DO 4500 I=2,N2
      IN2=IN2+1
      IF (ISQ(I) .LT. 0) GO TO  4500
      C=Z(ISQ(I))
      Z(ISQ(I))=Z(ISQ(IN2))
      Z(ISQ(IN2))=C
4500  CONTINUE
C
C     REMAINING ITERATIONS OF THE DFT.
C
      DO 5100 I=2,L2N
      K=JU(I)
      KK=JD(I)
```

```
      KI=K+K
      M=-KI
      DO 5100 II=1,KK
      M=M+KI
      J=1-KK
      DO 5100 III=1,K
      J=J+KK
      L=III+M
      LL=L+K
      C=Z(L)
      D=Z(LL)
      IF (J.EQ.1) GO TO 5000
      D=D*W(J+IOFS)
 5000 Z(L)=C+D
      Z(LL)=C-D
 5100 CONTINUE
C
C     RETURN AFTER TRANSFORM IS COMPLETED.
C
 9999 RETURN
C
C     EVALUATE THE COMPLEX EXPONENTIAL SAMPLES IN THE W ARRAY, THE
C     POWERS OF 2 IN ASCENDING AND DESCENDING ORDERS RESPECTIVELY
C     IN JU AND JD, AND THE BIT-REVERSE PAIRS FOR SWAPPING IN ISQ.
C
7000  OLDN=N
      SS=DFLOAT(N)
      ARG=-6.28318530718D0
      SS=ARG/SS
      SD=DSIN(SS)
      CD=DCOS(SS)
      CO=CD
      SI=SD
      N8=N/8
      N4=N8+N8
      N2=N4+N4
      N4P2=N4+2
      N2P2=N2+2
      W(1)=CMPLX(1.,0.)
      J=1
      OLDO=0
      W(N4+1)=CMPLX(0.,-1.)
7200  J=J+1
      COP=SNGL(CO)
      SIP=SNGL(SI)
      W(J)=CMPLX(COP,SIP)
      W(J+N4)=CMPLX(SIP,-COP)
      IF (J.GT.N8) GO TO 7300
      W(N2P2-J)=CMPLX(-COP,SIP)
      W(N4P2-J)=CMPLX(-SIP,-COP)
      SO=SI
      SI=SI*CD+CO*SD
      CO=CO*CD-SO*SD
      GO TO 7200
C
C     DETERMINE THE TRANSFORM NORMALIZATION FACTOR AMPL AND FILL IN
C     THE REMAINDER OF THE W ARRAY.
C
7300  AMPL=1./SQRT(FLOAT(N))
      K=N2
      DO 7400 I=1,N2
      K=K+1
      W(K)=CONJG(W(I))
7400  CONTINUE
C
C     DETERMINE THE LOG TO THE BASE 2 OF N, L2N, AND FILL IN THE JU
C     AND JD ARRAYS.
C
      KK=1
      A=ALOG10(FLOAT(N))*3.321928 + 0.5
```

```
      L2N=IFIX(A)
      LL=L2N
      DO 7500 L=1,L2N
      JU(L)=KK
      JD(LL)=KK
      LL=LL-1
      KK=KK+KK
7500  CONTINUE
C
C     FILL IN THE ISQ ARRAY WITH THE BIT-REVERSE PAIRS.
C
      DO 8100 I=1,N
      ISQ(I)=-1
8100  CONTINUE
      MM=1
      DO 8500 I=2,N
      K=I-1
      KK=0
      DO 8200 L=1,L2N
      JJ=K-JD(L)
      IF (JJ .LT. 0) GO TO 8200
      KK=KK+JU(L)
      K=JJ
      IF (K .LE. 0) GO TO 8300
8200  CONTINUE
8300  KK=KK+1
      JJ=KK-I
      IF (JJ .LE. 0) GO TO 8500
      MM=MM+1
      ISQ(MM)=I
      ISQ(MM+N2)=KK
8500  CONTINUE
      GO TO 1000
      END
```

```
C      PROGRAM PRPGT2
C     LARGE FINITE-AMPLITUDE WAVE PROPAGATION PROGRAM -- RELEASE SIX
C               AS REVISED IN FEBRUARY 1981.
C
C      DEFINITION OF MAJOR PROGRAM VARIABLES:
C         UZERO  - CONTAINS THE INITIAL OR BASE WAVEFORM, BEFORE THE
C                        NONLINEAR OPERATOR
C         USIGMA - CONTAINS THE WAVEFORM AFTER THE NONLINEAR OPERATOR
C         ALIST  - ARRAY FOR STORING LISTS OF REAL NUMBERS ON INPUT
C         Z      - COMPLEX ARRAY FOR THE SPECTRUM
C         W      - COMPLEX ARRAY FOR THE VALUES OF EXP(J2PI/N)
C         ISQ    - INTEGER ARRAY FOR THE BIT-REVERSAL PAIRS.
C         CALFA  - COMPLEX ARRAY FOR THE FACTORS DEFINING THE ATTENUATION
C                        AND/OR DISPERSION DURING PROPAGATION
C         ATTN   - .TRUE. IF ATTENUATION IS ENABLED
C         DISP   - .TRUE. IF DISPERSION IS ENABLED
C         RELX   - .TRUE. IF RELAXATION IS ENABLED
C         AMPLR  - .TRUE. IF THE OPERATOR IS NOT TO COMPENSATE FOR
C                        FINITE AMPLITUDE LOSSES -- THIS IS THE DEFAULT
C         ATRK   - ARRAY TO STORE SPECTRAL POINTS FOR PRINTED DISPLAY
C         ITRK   - ARRAY TO STORE FREQUENCIES OF THE SPECTRAL POINTS
C                        TO B5 PRINTED
C         ILIST  - ARRAY TO STORE DFT CELL NUMBERS OF SPECTRAL POINTS
C                        TO BE PRINTED
C
C     REVISION 11 JULY 1980 - AMPLITUDE NORMALIZATION TO A SPECIFIED NUMB
C              OF EQUAL INPUT COMPONENTS PROVIDED VIA INPUT VARIABLE
C               'IDUM'.
C
      REAL UZERO(2048), USIGMA(2048), ALIST(10), ATRK(11), RALFA(2048),
     1 RZ(4096)
      COMPLEX Z(2048), W(2048), CALFA(1024), CF
      LOGICAL ATTN, DISP, RELX, LV, AMPLR, S04, S05
      INTEGER IDAT(2), ITRK(11) , ILIST(11), ISQ(2048)
C
      EQUIVALENCE (Z(1),RZ(1)), (CALFA(1),RALFA(1))
C
C     READY TO RUN.
C
800   LPPAGE=0
      FMUL=1.
      CALL DATE(IDAT)
      READ(5,8020,END=7000) ICARD
C
C     INPUT CASE NUMBER ICASE, NUMBER OF FOURIER SAMPLES IFOUR, AND
C     SCALED FOURIER FUNDAMENTAL FSUBF.
C
1000  READ(ICARD,8020,END=7000) ICASE, IFOUR, FSUBF
      IMAXF=IFOUR/2
C
C     INPUT MEDIUM PARAMETERS:
C         ADELTA - ATTENUATION COEFFICENT;
C         CZERO - SMALL-SIGNAL SPEED OF SOUND;
C         BETA - PARAMETER OF NONLINEARITY;
C         EMM - SIMPLE DISPERSION PARAMETER;
C         TSUBC - RELAXATION TIME OF MEDIUM, TIMES SCALING FREQUENCY.
C
      READ(ICARD,8000,END=7000) ADELTA, CZERO, BETA, EMM, TSUBR
C
C     SENSE SWITCH OPTIONS:
C         12 - ON TO ENABLE DISPERSION
C         11 - ON TO ENABLE RELAXATION
C         10 - ON TO ENABLE ATTENUATION
C          9 - ON TO INPUT SIGNAL PARAMETERS, OFF FOR SCALED PARAMETERS
C                EPSLON - SIGNAL MACH NUMBER
C                FREQ   - SIGNAL FREQUENCY IN HERTZ
C                GAMMA  - SCALED ACOUSTIC REYNOLD'S NUMBER
C                CLAMBD - SCALED RELAXATION PARAMETER
C                SMALLD - SCALED SIMPLE DISPERSION PARAMETER
C                RSUBC  - PLANE-WAVE CRITICAL RANGE OR SHOCK
C                           FORMATION DISTANCE
```

```
C         8 - INVISCID OPERATOR DISABLED
C         7 - ON TO DISABLE NORMALIZATION OF INITIAL FUNCTION.
C
      CALL SSWTCH(12,DISP)
      CALL SSWTCH(11,RELX)
      CALL SSWTCH(10,ATTN)
      CALL SSWTCH(9,LV)
      IF (LV) GO TO 1500
C
C     ENTER SCALED PARAMETERS
C
      READ(ICARD,8000,END=7000) SMALLD, CLAMBD, GAMMA
C
C     COMPUTE THE CORRESPONDING SIGNAL PARAMETERS.
C
      EPSLON=EMM*CLAMBD/(2.*BETA)
      IF (GAMMA .NE. 0.) FREQ = 6.2831853*BETA*EPSLON / (CZERO*
     1 ADELTA*GAMMA)
      IF (FSUBF .LT. 0.) FSUBF = FREQ
      RSUBC = CZERO/(6.283185*FREQ*BETA*EPSLON)
      GO TO 1600
C
C     INPUT EPSLON AND FREQ.
C
1500  READ(ICARD,8020,END=7000) EPSLON, FREQ
C
C     COMPUTE CORRESPONDING SCALED PARAMETERS.
C
      IF (FSUBF .LT. 0.) FSUBF = FREQ
      CLAMBD =2.*BETA*EPSLON/EMM
      GAMMA=CLAMBD*EMM*3.141593/(CZERO*ADELTA*FSUBF)
      SMALLD = CLAMBD/(6.2831853*TSUBR*FSUBF)
      RSUBC=CZERO/(6.2831853*FREQ*BETA*EPSLON)
C
C     SET UP FOR ITERATION
C        ISC - INDEX AT WHICH SIGMA CHANGES; AT THIS STEP NUMBER THE
C                  RANGE STEP SIZE IS MULTIPLIED BY SIGST2 (OR BY 10 IF
C                  SIGST2 IS LESS THAN 0).
C        ISF - FILE TO WHICH SPECTRA ARE TO BE WRITTEN; LESS THAN ZERO
C                  TO SUPPRESS SPECTRAL OUTPUT.
C        IPR - NUMER OF RANGE STEPS PER PRINTOUT CYCLE.
C        IDUM - IF NOT ZERO, THE ASSUMED NUMBER OF EQUAL AMPLITUDE
C             INPUT COMPONENTS, USED FOR NORMALIZATION OF THE SPECTRAL
C           AMPLITUDE OUTPUT.  IF ZERO, NO NORMALIZATION IS PERFORMED.
C        SIGSTP - INITIAL NUMBER OF RANGE STEPS PER UNIT SIGMA.
C        SIGST2 - IF GREATER THAN ZERO, MULTIPLE OF RANGE STEP TO BE
C                  USED AFTER STEP ISC.
C        SMAX - MAXIMUM SCALED RANGE OF INTEREST.
C
1600  READ(ICARD,8060) ISC, ISF, IPR, IDUM, SIGSTP, SIGST2, SMAX
      AMPNRM=1.
      IF (IDUM .GT. 0) AMPNRM=FLOAT(IDUM)/SQRT(FLOAT(IFOUR/4))
      CALL SSWTCH(8,AMPLR)
      AMPLR=.NOT.AMPLR
      ATTF=0.
      ATT2=0.
      DSPF=0.
      TF2=(TSUBR*FSUBF)**2
      STEPI=1./SIGSTP
      IF (ATTN .AND. GAMMA .NE. 0.) ATTF=STEPI/GAMMA
      IF (RELX) GO TO 1700
      IF (DISP .AND. SMALLD .NE. 0.) DSPF=-STEPI/SMALLD
      GO TO 1800
1700  IF (CLAMBD .EQ. 0.) GO TO 1800
      DSPF = STEPI*TF2/CLAMBD
      IF (ATTN) ATT2 = TSUBR*FSUBF*GAMMA/CLAMBD
1800  READ(ICARD,8040) LI, ILIST
      NTRK=-1
      IF (LI .LT. 1) GO TO 2000
      IF (LI .GT. 11) LI=11
```

```
      NTRK=LI
      DO 1900 I=1,LI
      ITRK(I)=ILIST(I)+1
1900  CONTINUE
C
C     GET INITIAL WAVEFORM
C
2000  LPPAGE=LPPAGE+1
      WRITE(6,9090) ICASE, IDAT, LPPAGE
      WRITE(6,9010) ICARD
      CALL UNIT(IFOUR,UZERO,FSUBF,FREQ,FMUL,GAMMA,CLAMBD,EPSLON,SMALLD,
     1          ICARD)
      IF (UZERO(1) .LE. 1.) GO TO 2100
      WRITE(6,9180)
      GO TO 6000
C
C     SET UP ITERATION VARIABLES
C
2100  SIGMA = 0.
      KOUNT=0
      DSIG=1./SIGSTP
      DS=FLOAT(IFOUR)*DSIG/6.2831853
      IFH = IFOUR/2
      IF2 = IFH+1
      IF21 = IFOUR+2
      KPR=0
C
C     GET THE COMPLEX FACTORS ACCOUNTING FOR ATTENUATION, DISPERSION,
C     AND RELAXATION.
C
      CALL CMPFAC(CALFA,IFOUR,ATTF,ATT2,DSPF,TF2,RELX,IMAXF,ICARD)
C
C     DISPLAY RUN PARAMETERS
C
      WRITE(6,9100) DISP, ATTN, RELX, AMPLR
      WRITE(6,9110) GAMMA, CLAMBD, SMALLD
      WRITE(6,9120) EPSLON, FREQ, FSUBF
      WRITE(6,9130) DSPF, ATTF, ATT2
      WRITE(6,9140) IFOUR, DS, SIGSTP
      WRITE(6,9150) BETA, EMM, CZERO
      WRITE(6,9160) ADELTA, TSUBR
      IF (ISC .GT. 0) WRITE(6,9190) SIGST2, ISC
      IF (ISF .GE. 0) WRITE(6,9040) ISF
      IF (IPR .GT. 1) WRITE(6,9050) IPR
      LPPAGE=LPPAGE+1
      WRITE(6,9090) ICASE, IDAT, LPPAGE
      KLINPR=1
      WRITE(6,9080)
      IF (NTRK .GT. 0) WRITE(6,9200) (ILIST(KK),KK=1,NTRK)
C
C     COMPUTATION OF U(SIGMA) GIVEN U(ZERO)
C
2300  IF (KOUNT .NE. ISC) GO TO 2400
      WRITE(6,9210) KOUNT, SIGST2
      DS  =DS  *SIGST2
      ATTF=ATTF*SIGST2
      DSIG=DSIG*SIGST2
      DSPF=DSPF*SIGST2
      CALL CMPFAC(CALFA,IFOUR,ATTF,ATT2,DSPF,TF2,RELX,IMAXF,ICARD)
2400  KOUNT=KOUNT+1
      SIGMA = SIGMA + DSIG
      KPR=KPR+1
      IF (AMPLR) GO TO 2600
C
C     GET RMS AMPLITUDE BEFORE NON LINEAR OPERATOR
C
      RMSBEF = 0.
      DO 2500 I=1,IFOUR
      RMSBEF = RMSBEF + UZERO(I)**2
2500  CONTINUE
```

```
      RMSBEF=SQRT(RMSBEF/FLOAT(IFOUR))
C
C     FINITE DIFFERENCE INTERPOLATOR
C
2600  DX=0.
      DO 2800 I=1,IFOUR
      DX=DX+1.
      DL=UZERO(I)*DS
      XT=DX+DL
      M=XT
      XT=XT-FLOAT(M)
      M0=M
      IF(M0 .LT. 1) M0=M0+IFOUR
      IF (M0 .GT. IFOUR) M0=M0-IFOUR
      M1=M+1
      IF(XT .LT. 0.) M1=M-1
      IF (M1 .LT. 1) M1=M1+IFOUR
      IF (M1 .GT. IFOUR) M1=M1-IFOUR
      IF (XT .LT. 0.) XT=-XT
      USIGMA(I) = UZERO(M0)*(1.-XT) + UZERO(M1)*XT
2800  CONTINUE
C
C     END OF THE F.D.I. LOOP.
C
      IF (AMPLR) GO TO 3100
C
C     GET RMS AMPLITUDE AFTER NON LINEAR OPERATOR
C
      RMSAFT = 0.
      DO 2900 I=1,IFOUR
      RMSAFT=RMSAFT + USIGMA(I)**2
2900  CONTINUE
      RMSAFT = SQRT(RMSAFT/FLOAT(IFOUR))
C
C     FIX UP THE DIFFERENCE
C
      FACTOR = RMSBEF/RMSAFT
      DO 3000 I=1,IFOUR
      USIGMA(I) = USIGMA(I) * FACTOR
3000  CONTINUE
C
C     DISPERSION AND/OR ATTENUATION, IF EITHER, ARE APPLIED IN THE
C     FREQUENCY DOMAIN.
C        IF EITHER ATTENUATION OR DISPERSION IS ENABLED, THEN THE
C    SPECTRUM MODIFICATION MUST BE PERFORMED-- IF NIETHER IS ENABLED,
C    TRANSFORM INTO THE SPECTRAL DOMAIN ONLY IF SPECTRAL INFORMATION
C    IS TO BE OUTPUT.
C
3100  IF (ATTN .OR. DISP) GO TO 3200
      IF (NTRK .LT. 1) GO TO 5200
      IF (KPR .NE. IPR) GO TO 5200
C
C     UNPACK THE REAL DATA INTO THE REAL PARTS OF A COMPLEX ARRAY.
C
3200  DO 3300 I=1,IFOUR
      Z(I) = CMPLX(USIGMA(I),0.)
3300  CONTINUE
      CALL DFT ( Z, W, ISQ, IFOUR, 2 )
C
C     BYPASS THIS SECTION IF ONLY THE SPECTRAL RECORD IS DESIRED-- NO
C     ATTENUATION OR DISPERSION.
C
      IF (.NOT. (ATTN .OR. DISP) ) GO TO 4000
      K=IFOUR
      IF (DISP) GO TO 3500
C
C     APPLY ATTENUATION ONLY.
C
      N=1
      DO 3400 I=2,IMAXF
```

```
      N=N+2
      RN = RALFA(N)
      RZ(N) = RZ(N) * RN
      RZ(N+1) = RZ(N+1) * RN
      Z(K) = CONJG(Z(I))
      K=K-1
3400  CONTINUE
      GO TO 3700
C
C     APPLY DISPERSION AND POSSIBLY ATTENUATION.
C
3500  DO 3600 I=2,IMAXF
      Z(I) = Z(I)*CALFA(I)
      Z(K) = CONJG(Z(I))
      K=K-1
3600  CONTINUE
C
C     DELETE H-F PART OF SPECTRUM
C
3700  CF=CMPLX(0.,0.)
      N=IMAXF+1
      M=IFOUR+2-N
      DO 3800 I=N,M
      Z(I)=CF
3800  CONTINUE
C
C     OUTPUT SPECTRUM IF DESIRED
C
 4000 IF (ISF .LT. 0) GO TO 4100
      MMU= -1
      WRITE (ISF) KOUNT, SIGMA, IFOUR, ICASE, (IDAT(KKK),KKK=1,2), MM U
      WRITE(ISF) (Z(KK),KK=1,IF2)
C
C     PRINT TRACKED SPECTRUM IF DESIRED
C
4100  IF (NTRK .LT. 0) GO TO 4300
      DO 4200 I=1,NTRK
      ATRK(I) = CABS(Z(ITRK(I)))*AMPNRM
4200  CONTINUE
C
C     INVERSE FOURIER TRANSFORM AND RESTORE REAL FUNCTION TO THE
C     UZERO ARRAY.
C
4300  CALL DFT ( Z, W, ISQ, IFOUR, -2 )
      J=IFOUR
      DO 4400 I=1,IFOUR
      CF=Z(J)
      F=CABS(CF)
      IF (REAL(CF) .LT. 0.) F=-F
      UZERO(J) = F
      J=J-1
4400  CONTINUE
C
C    SEE IF A PRINTED DATA RECORD IS DESIRED -- IF SO, OUTPUT IT AFTER
C    CHECKING WHETHER THE PAGE IS FULL.
C
4500  IF (KPR .LT. IPR) GO TO 4800
      KPR=0
      KLINPR=KLINPR+1
      IF (KLINPR .LE. 50) GO TO 4600
      KLINPR=1
      LPPAGE=LPPAGE+1
      WRITE(6,9090) ICASE, IDAT, LPPAGE
      WRITE(6,9080)
      IF (NTRK .GT. 0) WRITE(6,9200) (ILIST(KK),KK=1,NTRK)
      WRITE(6,9170)
C
C     COMPUTE RMS, FIND MAX AND MIN, AND ANYTHING ELSE TO BE PRINTED.
C
4600  URMS=UZERO(1)**2
```

```
      UMIN=UZERO(1)
      UMAX=UMIN
      DO 4700 I=2,IFOUR
      UI=UZERO(I)
      URMS=URMS + UI**2
      IF (UI .GT. UMAX) UMAX=UI
      IF (UI .LT. UMIN) UMIN=UI
4700  CONTINUE
      URMS=SQRT(URMS/FLOAT(IFOUR))
      IF (NTRK .LT. 1) WRITE(6,9000) KOUNT, SIGMA, URMS, UMAX, UMIN
      IF (NTRK .GT. 0) WRITE(6,9000) KOUNT, SIGMA, URMS, UMAX, UMIN,
     1 (ATRK(KK),KK=1,NTRK)
C
C     SEE IF DESIRED RANGE IS ATTAINED.
C
4800  IF (SIGMA .GE. SMAX) GO TO 5000
      GO TO 2300
C
C     END-OF-SEQUENCE HANDLER
C
5000  WRITE(6,9340) KOUNT, SIGMA
      KOUNT=-1
      IF (ISF .GE. 0) WRITE (ISF) KOUNT, SIGMA, IFOUR, ICASE, (IDAT(KKK)
     1,KKK=1,2), MMU
      GO TO 1000
C
C     PUT NEW WAVEFORM BACK IN OLD ARRAY
C
5200  DO 5300 I=1,IFOUR
      UZERO(I) = USIGMA(I)
5300  CONTINUE
      GO TO 4500
C
C     END-OF-STEP HANDLER
C
6000  KOUNT=-1
      IF (ISF .GE. 0) WRITE (ISF) KOUNT, SIGMA, IFOUR, ICASE, (IDAT(KKK)
     1,KKK=1,2), MMU
      STOP
C
C    ERROR HANDLER
C
7000  KOUNT=-1
      IF (ISF .GE. 0) WRITE (ISF) KOUNT, SIGMA, IFOUR, ICASE, (IDAT(KKK)
     1,KKK=1,2), MMU
      STOP
C
C     FORMAT STATEMENTS
C
8000  FORMAT(8F10.1)
8020  FORMAT(2I5,7F10.1)
8040  FORMAT(16I5)
8060  FORMAT(4I5,6F10.1)
9000  FORMAT(' ',I5,F8.3,F10.4,2F10.3,11F8.4)
9010  FORMAT('0CARD-IMAGE CONTROL INPUT FROM DEVICE',I3)
9040  FORMAT('0RECORD SPECTRA ON',I3)
9050  FORMAT('0DISPLAY PRINTED RECORD EVERY',I3,' RANGE STEPS.')
9080  FORMAT('0 STEP   SIGMA    U(RMS)     (MAX)     (MIN)')
9090  FORMAT('1 B E L L M A N S   M E T H O D   -   RELEASE FIVE, 7 AUGU
     1ST 1980 - CASE',I10,4X,2A4,5X,'PAGE',I4)
9100  FORMAT('0 DISPERSION ',L1,' ; ATTENUATION ',L1,'; RELAXATION ',L1,
     1 '; INVISCID OPERATOR ',L1)
9110  FORMAT('0GAMMA    ',1PE13.3,'    CLAMBDA ',E13.3,'    SMALL D ',
     1E13.3)
9120  FORMAT('0EPSLON  ',1PE13.3,'    FREQ    ',E13.3,'    F SUB F ',
     1E13.3)
9130  FORMAT('0DSPF    ',1PE13.3,'    ATTF    ',E13.3,'    ATT2    ',
     1E13.3)
9140  FORMAT('0IFOUR   ',I13,'    DS      ',1PE13.3,'    SIGSTP  ',E13.3
     1)
```

```
9150  FORMAT('0BETA    ',1PE13.3,'    EMM     ',E13.3,'    CZERO   ',
     1E13.3)
9160  FORMAT('0DELTA   ',1PE13.3,'    T SUB R ',E13.3)
9170  FORMAT(' ')
9180  FORMAT('0*** BEWARE *** UNSPECIFIED INITIAL WAVEFORM.')
9190  FORMAT('0NOTE; DELTA SIGMA WILL BE MULTIPLIED BY',1PE11.3,
     1  ' AFTER',I6,' STEPS.')
9200  FORMAT('+',40X,11I8)
9210  FORMAT('0AFTER STEP',I4,' MULTIPLY DELTA SIGMA BY',F8.1)
9340  FORMAT('0END OF TASK AT STEP',I5,' SIGMA',1PE12.3)
      END


      SUBROUTINE CMPFAC ( CALFA, IFOUR, ATTF, ATT2, DSPF, TF2, RELX,
     1                    IMAXF, ICARD )
C
C     ATTENUATION, RELAXATION, AND DISPERSION FACTORS.  SEE 19 X '77 AND
C     24 VI '80 NOTES FOR DETAILS.
C
C     REVISION 8 VII 1980 -- PROGRAM MODIFIED TO LIST STYLE OF
C     ATTENUATION, RELAXATION, AND DISPERSION ON PRINTED LISTING.
C
C     REVISION 30 JULY 1980 -- INPUT TAKEN FROM CARD-IMAGE FILE 'IFILE'.
C
      COMPLEX CALFA(IFOUR), CF
      LOGICAL RELX
C
      WRITE(6,9000)
      CALFA(1)=1.
      ENN=0.
      CF=CMPLX(0.,0.)
      N1=IFOUR/2 + 1
      DO 1000 I=2,N1
      ENN=ENN+1.
      EN2=ENN**2
      DEN=1.+EN2*TF2
      EF=EXP(-EN2*ATTF*(1.+ATT2/DEN))
      IF (EF .LT. 1.E-10) GO TO 800
      PF=ENN**3*DSPF
      IF (RELX) PF=PF/DEN
      CALFA(I)=CMPLX(EF*COS(PF),EF*SIN(PF))
      GO TO 1000
800   CALFA(I)=CF
1000  CONTINUE
8888  RETURN
9000  FORMAT('0COMPLEX ATTENUATION, DISPERSION, AND ATTENUATION; SEE NOT
     1ES OF 24 JUNE 1980 FOR DETAILS.')
      END


      SUBROUTINE UNIT ( IFOUR, UZERO, FSUBF, FREQ, FMUL, GAMMA,
     1 CLAMBD, EPSLON, SMALLD , ICARD )
C
C     WAVEFORM INITIALIZATION SUBROUTINE.
C     DESIGNED/CODED 24 VI 1980.
C
C     SOLI DEO GLORIA 24 VI 1980 -- F S MCKENDREE.
C
C     REVISION 30 JULY 1980 -- INPUT TAKEN FROM CARD-IMAGE FILE 'IFILE'.
C
C     REVISION 5 AUGUST 1980 - ABILITY TO DISABLE INITIAL FUNCTION
C         NORMALIZATION ADDED; USE SWITCH 7 ON TO DISABLE.
C
      REAL UZERO(IFOUR)
      LOGICAL S07
C
C     SET UP AND ZERO DATA ARRAY.
C
      DO 500 I=1,IFOUR
      UZERO(I)=0.
500   CONTINUE
```

```
      DP=6.2831853*FMUL/FLOAT(IFOUR)
      WRITE(6,9000) IFOUR, FSUBF, FMUL
C
C     READ FREQUENCY, AMPLITUDE, AND PHASE OF EACH COMPONENT, AND
C     ACCUMULATE IN UZERO ARRAY.
C
1000  READ(ICARD,8000,END=2000) F1, A1, P1, F2, A2, P2
      WRITE(6,9020) F1, A1, P1, F2, A2, P2
      R1=P1*0.01745329
      R2=P2*0.01745329
      P=-DP
      DO 1500 I=1,IFOUR
      P=P+DP
      UZERO(I)=UZERO(I)+A1*COS(F1*P+R1)+A2*COS(F2*P+R2)
1500  CONTINUE
      IF (F1 .GT. 0. .AND. F2 .GT. 0.) GO TO 1000
C
C     NORMALIZE TO UNITY PEAK AMPLITUDE.
C
2000  CALL SSWTCH(7,S07)
      IF (S07) WRITE(6,9040)
      IF (S07) GO TO 8888
      AMAX=ABS(UZERO(1))
      DO 2500 I=2,IFOUR
      AM=ABS(UZERO(I))
      IF (AM .GT. AMAX) AMAX=AM
2500  CONTINUE
      AM=1./AMAX
      DO 3000 I=1,IFOUR
      UZERO(I)=UZERO(I)*AM
3000  CONTINUE
8888  RETURN
8000  FORMAT(8F10.1)
9000  FORMAT('0UNIT SUBROUTINE: IFOUR',I5,' FSUBF, FMUL',1P2E12.3)
9020  FORMAT('0F1, A1, P1:',1P3E12.3,'; F2, A2, P2:',3E12.3)
9040  FORMAT('0INITIAL FUNCTION WILL NOT BE NORMALIZED TO UNITY PEAK AMP
     1LITUDE.')
      END


      SUBROUTINE DFT ( Z, W, ISQ, N, NC )
C
C        DISCRETE FOURIER TRANSFORM SUBROUTINE WITH PASSED ARGUMENTS
C
C     THIS SUBROUTINE IS OPTIMIZED FOR RAPID SEQUENTIAL PERFORMANCE
C     OF SUCCESSIVE DIRECT AND INVERSE TRANSFORMS OF THE SAME SIZE.
C
C     DEFINITIONS OF  ARGUMENTS:
C         Z - ON CALL, INPUT COMPLEX SEQUENCE; ON RETURN, OUTPUT
C                COMPLEX SEQUENCE.
C         W - COMPLEX WORKING ARRAY; THESE VALUES MUST NOT BE CHANGED
C                BETWEEN CALLS TO THE SAME SIZE DFT.
C         ISQ - INTEGER ARRAY  USED TO STORE THE SEQUENCE NUMBERS
C                WHICH ARE EXCHANGED IN THE BIT REVERSAL.
C         N - NUMBER OF POINTS IN THE FOURIER TRANSFORM; MINIMUM
C                LENGTH OF THE Z, W, AND ISQ ARRAYS.
C         NC - CONTROL INTEGER VARIABLE; LESS  THAN ZERO FOR INVERSE
C                TRANSFORM, OTHERWISE DIRECT IS ASSUMED.
C
C     THE MINIMUM ALLOWABLE N IS 8 AND THE MAXIMUM IS 4096; THE VALUE
C     OF N MUST BE AN INTEGER POWER OF 2.
C
      COMPLEX C, D, Z(N), W(N)
      REAL*8 CO, SI, CD, SD, SS, ARG, SO
      INTEGER JU(12), JD(12), ISQ(N), OLDN/-9999/
C
C     DETERMINE IF THE VALUE OF N CALLED FOR IS CURRENT.
C     IF SO, CHOOSE DIRECT TRANSFORM (IOFS=0) OR INVERSE TRANSFORM.
C
      IF (OLDN .NE. N) GO TO 7000
1000  IOFS=0
      IF (NC .LT. 0) IOFS=N2
```

```
C
C     FIRST DFT LOOP; MULTIPLY BY AMPLITUDE FACTOR AND TAKE THE
C     SUM AND DIFFERENCE.  SINCE THE COMPLEX EXPONENTIAL SAMPLE
C     FOR THIS LOOP IS 1, COMPLEX MULTIPLICATION IS NOT REQUIRED.
C
3000  DO 3100 I=1,N2
      II=I+N2
      C=Z(I)
      D=Z(II)
      C=C*AMPL
      D=D*AMPL
      Z(I)=C+D
      Z(II)=C-D
 3100 CONTINUE
C
C     BIT-REVERSED RESEQUENCING OF THE Z ARRAY.  USE THE VALUES
C     STORED IN ISQ TO CONTROL THE SEQUENCING.
C
      IN2=N2+1
      DO 4500 I=2,N2
      IN2=IN2+1
      IF (ISQ(I) .LT. 0) GO TO  4500
      C=Z(ISQ(I))
      Z(ISQ(I))=Z(ISQ(IN2))
      Z(ISQ(IN2))=C
4500  CONTINUE
C
C     REMAINING ITERATIONS OF THE DFT.
C
      DO 5100 I=2,L2N
      K=JU(I)
      KK=JD(I)
      KI=K+K
      M=-KI
      DO 5100 II=1,KK
      M=M+KI
      J=1-KK
      DO 5100 III=1,K
      J=J+KK
      L=III+M
      LL=L+K
      C=Z(L)
      D=Z(LL)
      IF (J.EQ.1) GO TO 5000
      D=D*W(J+IOFS)
 5000 Z(L)=C+D
      Z(LL)=C-D
 5100 CONTINUE
C
C     RETURN AFTER TRANSFORM IS COMPLETED.
C
 9999 RETURN
C
C     EVALUATE THE COMPLEX EXPONENTIAL SAMPLES IN THE W ARRAY, THE
C     POWERS OF 2 IN ASCENDING AND DESCENDING ORDERS RESPECTIVELY
C     IN JU AND JD, AND THE BIT-REVERSE PAIRS FOR SWAPPING IN ISQ.
C
7000  OLDN=N
      SS=DFLOAT(N)
      ARG=-6.283185307180
      SS=ARG/SS
      SD=DSIN(SS)
      CD=DCOS(SS)
      CO=CD
      SI=SD
      N8=N/8
      N4=N8+N8
      N2=N4+N4
      N4P2=N4+2
      N2P2=N2+2
```

```
      W(1)=CMPLX(1.,0.)
      J=1
      OLDO=0
      W(N4+1)=CMPLX(0.,-1.)
7200  J=J+1
      COP=SNGL(CO)
      SIP=SNGL(SI)
      W(J)=CMPLX(COP,SIP)
      W(J+N4)=CMPLX(SIP,-COP)
      IF (J.GT.N8) GO TO 7300
      W(N2P2-J)=CMPLX(-COP,SIP)
      W(N4P2-J)=CMPLX(-SIP,-COP)
      SO=SI
      SI=SI*CD+CO*SD
      CO=CO*CD-SO*SD
      GO TO 7200
C
C     DETERMINE THE TRANSFORM NORMALIZATION FACTOR AMPL AND FILL IN
C     THE REMAINDER OF THE W ARRAY.
C
7300  AMPL=1./SQRT(FLOAT(N))
      K=N2
      DO 7400 I=1,N2
      K=K+1
      W(K)=CONJG(W(I))
7400  CONTINUE
C
C     DETERMINE THE LOG TO THE BASE 2 OF N, L2N, AND FILL IN THE JU
C     AND JD ARRAYS.
C
      KK=1
      A=ALOG10(FLOAT(N))*3.321928 + 0.5
      L2N=IFIX(A)
      LL=L2N
      DO 7500 L=1,L2N
      JU(L)=KK
      JD(LL)=KK
      LL=LL-1
      KK=KK+KK
7500  CONTINUE
C
C     FILL IN THE ISQ ARRAY WITH THE BIT-REVERSE PAIRS.
C
      DO 8100 I=1,N
      ISQ(I)=-1
8100  CONTINUE
      MM=1
      DO 8500 I=2,N
      K=I-1
      KK=0
      DO 8200 L=1,L2N
      JJ=K-JD(L)
      IF (JJ .LT. 0) GO TO 8200
      KK=KK+JU(L)
      K=JJ
      IF (K .LE. 0) GO TO 8300
8200  CONTINUE
8300  KK=KK+1
      JJ=KK-I
      IF (JJ .LE. 0) GO TO 8500
      MM=MM+1
      ISQ(MM)=I
      ISQ(MM+N2)=KK
8500  CONTINUE
      GO TO 1000
      END


      SUBROUTINE SSWTCH(N,V)
      LOGICAL V,S(13)/.FALSE.,.FALSE.,.FALSE.,.FALSE.,.FALSE.,
     1                .FALSE.,.FALSE.,.FALSE.,.FALSE.,
     2                .FALSE.,.TRUE. ,.FALSE.,.FALSE./
```

```
      L=N+1
      V=.FALSE.
      IF ((L .GT. 13) .OR. (L .LT. 1)) GO TO 8888
      V=S(L)
8888  RETURN
      END
```

DISTRIBUTION LIST FOR TM 81-44

Commander (NSEA 0342)
Naval Sea Systems Command
Department of the Navy
Washington, DC 20362 — Copies 1 and 2

Commander (NSEA 9961)
Naval Sea Systems Command
Department of the Navy
Washington, DC 20362 — Copies 3 and 4

Defense Technical Information Center
5010 Duke Street
Cameron Station
Alexandria, VA 22314 — Copies 5 through 10


DATE
ILME